

Colloquium: Spin-orbit effects in superconducting hybrid structures

Morten Amundsen

Nordita, KTH Royal Institute of Technology and Stockholm University, Roslagstullsbacken 23, SE-106 91 Stockholm, Sweden

Jacob Linder

*Center for Quantum Spintronics, Department of Physics, Norwegian University of Science & Technology, NO-7491 Trondheim, Norway**

Jason W. A. Robinson

Department of Materials Science and Metallurgy, University of Cambridge, 27 Charles Babbage Road, Cambridge CB3 0FS, United Kingdom

Igor Žutić

Department of Physics, University at Buffalo, State University of New York, Buffalo, New York 14260, USA†

Niladri Banerjee

*Department of Physics, Loughborough University, Loughborough, LE11 3TU, United Kingdom
The Blackett Laboratory, Imperial College London, London SW7 2AZ, United Kingdom‡*

Spin-orbit coupling (SOC) describes the interaction between an electron's motion and its spin, and is ubiquitous in condensed matter systems. The interplay of SOC with superconductivity has attracted significant interest over the past decade and understanding has substantially progressed, both experimentally and theoretically. Even with well-understood materials, conventional *s*-wave superconducting hybrid structures with SOC provide a platform for realizing exotic phenomena and counterparts in the normal state. Understanding the emergent phenomena in such systems is an important aim in condensed matter physics. One such area relates to the generation and interplay of spin-polarized spin-triplet Cooper pairs in superconducting structures with magnetic interfaces. It is established that certain forms of magnetic inhomogeneity at an *s*-wave superconductor interface with a ferromagnet can transform spin-singlet Cooper pairs into a spin-polarized spin-triplet Cooper pairs, enabling transformative concepts for cryogenic computing. Recently, theory and experiments have demonstrated singlet-to-triplet pair conversion via SOC in *s*-wave superconducting structures with or without magnetic layers. Moreover, the spin-dependent properties of quasiparticles and their non-equilibrium behavior also change in the presence of SOC. These breakthroughs create the potential for energy-efficient control of static and dynamic spin phenomena in superconducting structures and devices. This article reviews progress in superconducting spintronics with a focus on the coupling of superconductivity and SOC in hybrid structures and devices, and outlines directions that are critical for future device development and fundamental understanding.

CONTENTS

I. Introduction	1	C. Magnetization dynamics	12
II. Background	3	D. Spectroscopic techniques	12
A. Spin-orbit coupling	3	IV. Recent developments	13
B. Validity of Rashba and Dresselhaus models	4	A. Majorana zero modes	13
C. Triplet superconductivity	4	B. Superconducting critical temperature	15
D. Theoretical frameworks	5	C. Modification of magnetic anisotropy	16
1. General considerations of spin-dependent fields	6	D. Interfacial magnetoanisotropy	16
2. Superconducting proximity effect	7	E. Josephson junctions	18
3. The Ginzburg-Landau formalism	9	F. Supercurrent diodes	22
4. Bogoliubov-de Gennes method	9	G. Spin-pumping	23
5. Quasiclassical theory	10	H. Spin-Hall phenomena with superconductors	23
III. Experimental techniques	11	V. Open questions and future directions	25
A. Transition temperature measurements	11	Acknowledgments	26
B. Josephson junctions	12	References	26

* Corresponding author: jacob.linder@ntnu.no

† Corresponding author: zigor@buffalo.edu

‡ Corresponding author: n.banerjee@lboro.ac.uk

I. INTRODUCTION

Spin-orbit coupling (SOC) has a relativistic origin: from the viewpoint of a moving electron, it is the positively charged

lattice that is moving, creating a magnetic field which couples to the electron spin. Additional SOC effects arise in crystals which lack an inversion center, and also in thin-film materials and structures, or at interfaces, making this interaction prevalent in condensed matter.

Superconductivity is one of the most quintessential manifestations of quantum behaviour in materials. Its involvement is critical in the development of condensed matter physics, from extremely sensitive magnetometers to the discovery of exotic phases of matter and emergent particles.

The interplay of superconductivity with spin-dependent properties such as SOC in hybrid structures is attracting increasing attention, stimulated by discoveries relating to superconducting spin transport, the supercurrent diode effect, and enhanced spin Hall phenomena, as well as Majorana fermions and topological transport. Remarkably, some of the most fundamental phenomena associated with this interplay may also enable emerging applications in energy-efficient cryogenic computing and quantum technologies.

With the push to meet the rapidly growing demands in information communication technologies (ICTs), beyond the Moore's law of scaling down semiconductor transistors, there is an urgency to identify alternative materials and device concepts that can deliver high performance with a lower-energy consumption. The main source of power dissipation, through Joule heating due to electrical resistance, is increasingly related to communicating, rather than processing, information. Just large data centers alone are predicted to require 8% of the global energy use by 2030 (Jones, 2018).

Superconducting electronics is an emerging alternative technology for large-scale applications in ICT since supercurrents flow without dissipation and could greatly reduce the energy consumption of data centers, even taking into account the cooling overhead for cryogenic operation (Holmes *et al.*, 2013; Tafuri, 2019). Superconducting components, such as Josephson junctions (JJs), are key elements in quantum computers (Krantz *et al.*, 2019; Wendin, 2017), where quantum supremacy has already been reported (Arute *et al.*, 2019).

Spintronics is also making technological gains (Hirohata *et al.*, 2020; Tsymbal and Žutić, 2019; Žutić *et al.*, 2004) by utilizing electron spin as information carriers in addition to or instead of, the electron charge. Discoveries in spintronics have been adopted by industry, leading to performance improvements in memory using giant (Baibich *et al.*, 1988; Binasch *et al.*, 1989) and tunneling (Julliere, 1975; Miyazaki and Tezuka, 1995; Moodera *et al.*, 1995; Parkin *et al.*, 2004; Yuasa *et al.*, 2004) magnetoresistance. More recent developments include spin-transfer and spin-orbit torque magnetic random access memories (Bhatti *et al.*, 2017; Kent and Worledge, 2015; Tsymbal and Žutić, 2019). Although there are examples of pure spin currents which involve a net flow of spin in the absence of a net charge transfer (Kajiwara *et al.*, 2010; Lebrun *et al.*, 2018; Vaidya *et al.*, 2020), practical spintronic applications still rely on a charge current accompanying the spin transport, and hence suffer from the same heating problems as semiconductor-based electronics.

A potential solution to the heating problem in large data centers and high-performance computing is to combine superconducting electronics with spintronics to seamlessly integrate logic and memory (Birge and Houzet, 2019) and thereby overcome the von Neumann bottleneck (Dery *et al.*, 2012). In fact, some of the earliest experiments in spintronics to investigate the spin-dependent density of states in transition metal ferromagnets involved tunneling across a superconductor/ferromagnet (S/F) interface (Meservey and Tedrow, 1994; Tedrow and Meservey, 1971) and have subsequently inspired a widely-used concept of spin injection (Aronov, 1976; Johnson and Silsbee, 1985; Žutić *et al.*, 2004).

A major step in this direction came from a series of pioneering experiments over the past two decades which have demonstrated singlet-to-triplet pair conversion at S/F interfaces with certain forms of inhomogeneous magnetism (Keizer *et al.*, 2006; Khaire *et al.*, 2010; Robinson *et al.*, 2010). These triplet Cooper pairs can have spins aligned parallel to the F layer magnetization, \mathbf{M} , and establish a proximity effect over a length scale of the order $\sqrt{D/2\pi T}$ in the diffusive limit, where D is the diffusion coefficient of the F and T is temperature. These discoveries built a foundation for superconducting spintronics (Eschrig, 2015; Linder and Robinson, 2015; Ohnishi *et al.*, 2020; Yang *et al.*, 2021) which, through the transport of superconducting spin currents, aims to establish energy-efficient cryogenic technology. Moreover, the introduction of superconducting correlations brings unique features absent in the normal state, including superconducting phase coherence which could enable new device concepts for quantum computing.

Initially, the transformation of singlet pairs to triplet pairs focused on inhomogeneous magnetism at s -wave superconductor interfaces with magnetically noncollinear rare earth ferromagnets (Robinson *et al.*, 2012, 2010; Usman *et al.*, 2011), misaligned transition metal ferromagnetic layers (Banerjee *et al.*, 2014; Khaire *et al.*, 2010), magnetic domain walls (Robinson *et al.*, 2012), or spin active interfaces (Halperin and Valls, 2009; Linder *et al.*, 2009; Žutić and Das Sarma, 1999). Less than a decade ago a series of theoretical papers (Bergeret and Tokatly, 2013, 2014; Jacobsen *et al.*, 2015) showed that SOC in diffusive S/F hybrids can promote singlet-to-triplet pair conversion (Feng *et al.*, 2008; Högl *et al.*, 2015; Yokoyama *et al.*, 2006). Unlike the anisotropic-in-momentum triplet condensate (Edelstein, 2003; Gor'kov and Rashba, 2001), triplet pairs created in S/F hybrids with or without SOC, can survive in diffusive systems.

In the last few years, several experiments (Banerjee *et al.*, 2018; Cai *et al.*, 2021; González-Ruano *et al.*, 2021, 2020; Jeon *et al.*, 2018, 2019b, 2020; Martínez *et al.*, 2020) have demonstrated evidence for singlet-to-triplet pair conversion via SOC, placing superconducting spintronics in a much more generalised framework with connections to other areas of research including Majorana zero modes. Importantly, not only does the behavior of Cooper pairs in superconductors change in the presence of SOC, but so does the behaviour of quasi-particle excitations which leads to, for instance, renormalized

and enhanced spin-Hall phenomena.

In this review, we summarize recent advances in the field following a brief introduction on the adaptation of superconductivity in the presence of spin-dependent interactions such as SOC in hybrid structures and devices. We also address open questions and highlight promising research directions.

II. BACKGROUND

This section reviews basic concepts which build a basis for the results outlined in the following sections. We start by describing SOC, specifically Rashba and Dresselhaus types in bulk materials and structures with inversion asymmetry. We then introduce s -wave spin-triplet superconductivity in hybrid proximity structures and include a discussion on theory methods that incorporate SOC in such systems.

A. Spin-orbit coupling

SOC is an interaction between the motion of an electron and its spin, and stems from the fact that in the reference frame of the electron, it is the positively charged lattice that moves. Moving charges create a magnetic field, which may couple to the electron spin. Hence, in a Lorentz-invariant formulation, a SOC term emerges, as shown in the Dirac equation (Dirac, 1928)

$$\begin{pmatrix} mc^2 + V(\mathbf{r}) & -i\hbar c \boldsymbol{\sigma} \cdot \nabla \\ -i\hbar c \boldsymbol{\sigma} \cdot \nabla & -mc^2 + V(\mathbf{r}) \end{pmatrix} \begin{pmatrix} \psi_e \\ \psi_h \end{pmatrix} = (\varepsilon + mc^2) \begin{pmatrix} \psi_e \\ \psi_h \end{pmatrix}, \quad (1)$$

and taking the nonrelativistic limit, $\varepsilon, V \ll mc^2$, where ε is the particle energy without its rest mass. Here, $V(\mathbf{r})$ is the lattice potential and m is the free electron mass. One then derives a Hamiltonian for the electron wavefunction ψ_e ,

$$H = \frac{\mathbf{p}^2}{2m} + V(\mathbf{r}) + \frac{\hbar}{4m^2 c^2} \boldsymbol{\sigma} \cdot (\nabla V \times \mathbf{p}), \quad (2)$$

where irrelevant terms are discarded. The last term represents SOC, and is large near a lattice site. For a spherically-symmetric V it can be written in a form similar to an isolated atom (Fabian *et al.*, 2007),

$$H_{so} = \frac{\hbar}{4m^2 c^2} \frac{1}{r} \frac{dV}{dr} \mathbf{L} \cdot \mathbf{S}, \quad (3)$$

where $\mathbf{L} = \mathbf{r} \times \mathbf{p}$ and \mathbf{S} , represent the orbital and the spin angular momentum operators, respectively. Alternatively, the second quantized form of the last term in Eq. (2) can be written as, in the basis of the Bloch functions (Samokhin, 2009),

$$H_{so} = \sum_k \sum_{m'} \sum_{s'} Q_{nm'}(\mathbf{k}) \cdot \boldsymbol{\sigma}_{ss'} c_{kns}^\dagger c_{kn's'}, \quad (4)$$

where $Q_{nm'}$ is a phenomenological model function which expresses the coupling between momentum and spin, with n

and n' band indices, and \mathbf{k} the crystal momentum. As discussed by (Samokhin, 2009), the behavior of $Q_{nm'}$ can be characterized by symmetry. For a centrosymmetric material, it can be deduced that the diagonal terms Q_{nn} vanish, meaning that SOC can only be described by models containing at least two bands. However, in a noncentrosymmetric material a one-band model is possible, allowing the simplification that $\sum_{nm'} Q_{nm'} \rightarrow Q$ in Eq. (4). Furthermore, Q must in such a case have odd parity, $Q(\mathbf{k}) = -Q(-\mathbf{k})$.

In a noncentrosymmetric material, it is helpful to distinguish bulk and structure inversion asymmetry (BIA, SIA), which lead to the spin splitting and SOC that can be expressed as

$$H_{so}(\mathbf{k}) = \frac{1}{2} \hbar \boldsymbol{\sigma} \cdot \boldsymbol{\Omega}(\mathbf{k}), \quad (5)$$

where $\boldsymbol{\Omega}(\mathbf{k})$ is the Larmor frequency for the electron spin precession in the conduction band (Žutić *et al.*, 2004) or, equivalently, SOC field. Here momentum scattering, $\boldsymbol{\Omega}(\mathbf{k})$ is responsible for spin dephasing. Related SOC manifestations in semiconductors are extensively studied and usually focus on effective models which capture the low-energy properties of the conduction and valence bands. A prominent example of BIA is the Dresselhaus SOC (Dresselhaus, 1955), given by

$$\boldsymbol{\Omega}_D = \frac{2\gamma}{\hbar} [k_x(k_y^2 - k_z^2), k_y(k_z^2 - k_x^2), k_z(k_x^2 - k_y^2)], \quad (6)$$

where γ is the SOC strength. In two-dimensional (2D) systems with quantum confinement along the unit vector \hat{n} , $\boldsymbol{\Omega}_D$ can be linearized,

$$\boldsymbol{\Omega}_D^{2D} \sim k_n^2 [2n_x(n_y k_y - n_z k_z) + k_x(n_y^2 - n_z^2) + c.p.], \quad (7)$$

where k_n^2 is the expectation value of the square of the wave number operator normal to the plane in the lowest subband state is the confinement unit vector of the quantum well, and c.p. denotes the cyclic index permutation. For a rectangular well of width a , $k_n^2 = (\pi/a)^2$. For a triangular well with a confining potential $V(z) = eEz$ when $z \geq 0$ and $V(z) = \infty$ when $z < 0$, $k_n^2 \approx 0.7794(2m^*E/\hbar^2)^{2/3}$, where E is the electric field and m^* is the conduction-band edge effective mass (de Sousa and Das Sarma, 2003). With a strong confinement, $k_{\parallel}^2 \ll k_n^2$, where \mathbf{k}_{\parallel} is the in-plane wave vector ($\perp \hat{n}$), cubic terms in $\boldsymbol{\Omega}_D$ from Eq. (7) can be neglected.

For commonly considered quantum well confinements, one obtains for [001]: $\boldsymbol{\Omega}_D^{2D} \sim k_n^2(-k_x, k_y, 0)$, for [111]: $\boldsymbol{\Omega}_D^{2D} \sim k_n^2(\mathbf{k} \times \mathbf{n})$, and for [110]: $\boldsymbol{\Omega}_D^{2D} \sim k_n^2 k_x(-1, 1, 0)$, as shown in Fig. 1. Several features can be readily seen, BIA [100] displays a "breathing" pattern, while BIA [110] $\boldsymbol{\Omega}(\mathbf{k})$ is perpendicular to the plane such that, within the linear in \mathbf{k} approximation, the perpendicular spins do not dephase.

An extensively studied SIA example is given by Bychkov-Rashba (or just Rashba) SOC (Bychkov E. I. and Rashba, 1984), which arises in asymmetric quantum wells or in deformed bulk systems, expressed by

$$\boldsymbol{\Omega}_R = 2\alpha(\mathbf{k} \times \mathbf{n}), \quad (8)$$

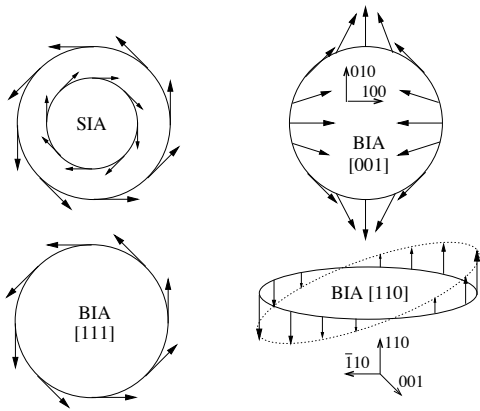


FIG. 1 Vector fields $\Omega(\mathbf{k})$ on a circular Fermi surface for structure (SIA) and bulk (BIA) inversion asymmetry. Since $\Omega(\mathbf{k})$ is the spin quantization axis, the vector pattern is also the pattern of the spin on the Fermi surface. As opposite spins have different energies, the Fermi circle splits into two concentric circles with opposite signs of spin; shown here only for the SIA case, but the analogy extends to all examples. The field for BIA [110] perpendicular to the plane, with the magnitude varying along the Fermi surface. All other cases have constant fields lying in the plane. From Žutić *et al.*, 2004.

where α parametrizes its strength and the inversion symmetry is broken along the \mathbf{n} -direction. We see in Fig. 1 that its functional form, Ω_R , coincides with BIA Ω_D^{2D} in [111] quantum wells. A desirable property of Rashba SOC is that α is tunable by an applied electric field.

The most popular SOC models are Rashba and Dresselhaus that are linearized in momentum, respectively given as,

$$H_R = \alpha \boldsymbol{\sigma} \cdot (\mathbf{p} \times \mathbf{n}), \quad (9)$$

$$H_D = \beta (\sigma_x p_x - \sigma_y p_y). \quad (10)$$

However, these forms are usually simply stated and given without any further assumptions about their validity. For example, in Rashba SOC there is a growing class of materials where cubic terms in \mathbf{p} can play an important role, or even be dominant (Alidoust *et al.*, 2021), while, from the above description, Eq. (10) with the Dresselhaus SOC strength β , is only relevant for a linearized BIA [001] quantum wells.

B. Validity of Rashba and Dresselhaus models

The validity of effective low-energy SIA and BIA SOC models, such as Rashba and Dresselhaus, can be examined from more complete electronic structure calculations, using first-principles, $\mathbf{k} \cdot \mathbf{p}$ method, or a tight-binding model. Going beyond Rashba and Dresselhaus model might be necessary for interfacial SOC in junctions which contains interface-induced symmetry reduction in the individual bulk constituents. This is exemplified in an Fe/GaAs junction, shown in Figs. 2(a) and (b), where the cubic and T_d symmetries of bulk Fe and GaAs, respectively, are reduced to C_{2v} in the heterostructure (Fabian *et al.*, 2007; Žutić *et al.*, 2019).

Since the interfacial SOC is present only in the vicinity of the interface, its effects can be controlled electrically by gate voltage or an applied external bias capable of pushing the carriers wave function into or away from the interface. Interfacial SOC can also be controlled magnetically, as it strongly depends on the orientation of \mathbf{M} in the Fe layer, as illustrated from the first-principles calculation in Figs. 2(c) and (d) (Gmitra *et al.*, 2013). The bias-dependence of the SOC can be inferred from the transport anisotropy in Figs. 2(f) and (g).

While the resulting interfacial SOC for Fe/GaAs junction corresponds neither to Rashba, nor Dresselhaus models, its existence can be probed through tunneling anisotropic magnetoresistance (TAMR). Such TAMR gives the dependence of the tunneling current in a tunnel junction with only *one* magnetic electrode on the spatial orientation of \mathbf{M} (Gould *et al.*, 2004). For an in-plane rotation of \mathbf{M} depicted in Fig. 2(e), we can define TAMR as the normalized resistance difference,

$$\text{TAMR} = (R(\phi) - R_{[110]})/R_{[110]}, \quad (11)$$

where $R(\phi = 0) \equiv R_{[110]}$ is the resistance along the [110] crystallographic axis. Analogously, one can also define TAMR resulting from the out-of-plane (OOP) rotation of \mathbf{M} . TAMR appears because the electronic structure depends on the \mathbf{M} orientation, due to SOC. The surface or an interface electronic structure can strongly deviate from its bulk counterparts and host pure or resonant bands. In the presence of SOC, the dispersion of these states depends on the \mathbf{M} orientation (Chantis *et al.*, 2007). As a result, the tunneling conductance, which, in a crystalline junction, is very sensitive to the transverse wave vector, develops both OOP and in-plane (IP) MR, shown in Figs. 2(f)-(h), whose angular dependence reflects the crystallographic symmetry of the interface. For example, the TAMR inherits the C_{4v} symmetry for the Fe (001) surface (Chantis *et al.*, 2007) and the reduced C_{2v} symmetry for the Fe(001)/GaAs interface (Moser *et al.*, 2007).

Our prior discussion of SOC and its manifestations in the normal-state properties have important superconducting counterparts as well as enable entirely new phenomena, absent in the normal state. As we will explain in subsequent sections, even when the SOC results in only a very small transport anisotropy in the normal state, as shown in Figs. 2(f) and (g), the superconducting analogs of such phenomena can lead to effects that are several orders of magnitude greater.

C. Triplet superconductivity

Conventional s -wave superconductors are well-described by the Bardeen-Cooper-Schrieffer (BCS) microscopic theory. The superconducting correlations consist of Cooper pairs in a spin singlet state, and thus carry no net spin. Proximity-induced spin-triplet superconducting correlations, in contrast, do carry a net spin, and thus have spin-dependent properties. There are materials believed to exhibit intrinsic triplet superconductivity such as Bechgaard salts (Sengupta *et al.*, 2001),

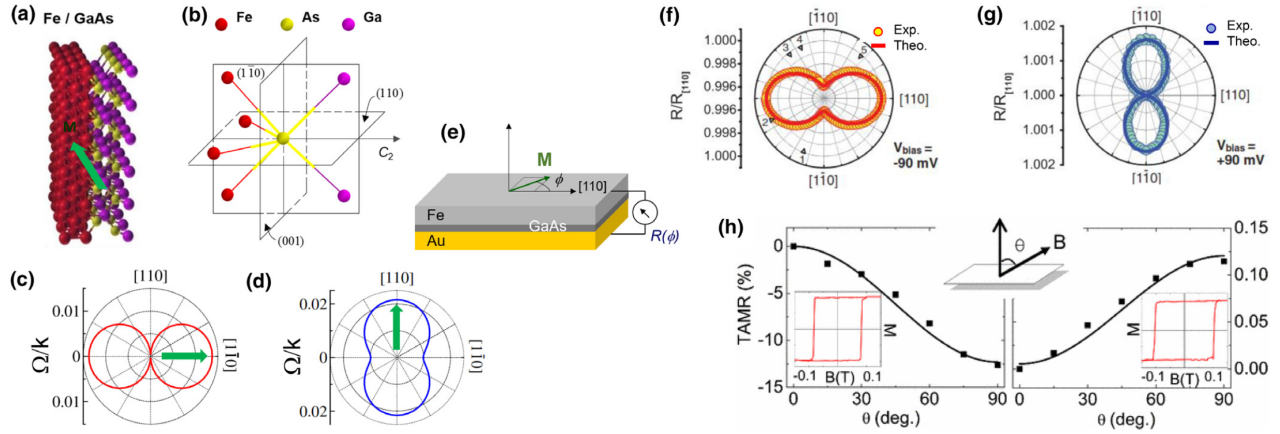


FIG. 2 (a) Schematic of a Fe/GaAs slab. (b) The nearest As neighbors at the Fe/GaAs interface with the point group C_{2v} symmetry, containing a C_2 rotation axis and mirror planes (110) and $(1\bar{1}0)$. (c) Angular \mathbf{k} -space dependence of the amplitude of the interfacial SOC field for \mathbf{M} along the GaAs $[1\bar{1}0]$ direction (green arrow). (d) Same as in (c) but for \mathbf{M} along the $[110]$ direction (Gmitra *et al.*, 2013). (e) Experimental setup for in-plane TAMR. \mathbf{M} , is rotated in the plane of the magnet, the tunneling resistance R is measured as a function of ϕ and normalized to its $\phi = 0$ value, $R_{|[110]}$. Results for bias voltages of -90 meV and 90 meV are shown in (f) and (g), respectively (Moser *et al.*, 2007). (h) Angular dependence of the TAMR in the out-of-plane configuration. Left (right) panels correspond to CoPt/AIO_x/Pt (Co/AIO_x/Pt) tunnel junctions. The presence of an extra Pt layer with strong SOC yields a TAMR in CoPt/AIO_x/Pt two orders of magnitude larger than in Co/AIO_x/Pt. The insets show \mathbf{M} measurements in out-of-plane magnetic fields (Park *et al.*, 2008). Adapted with permission from Žutić *et al.*, 2019.

UPT₃ (Joynt and Taillefer, 2002), as well as the ferromagnetic superconductors (Aoki *et al.*, 2011). A direct interaction between superconductivity and SOC is also found in the growing group of noncentrosymmetric superconductors, where electron pairing is a mixture of spin-singlet and spin-triplet (Smidman *et al.*, 2017).

An accessible means of generating triplet superconducting correlations using only conventional materials is to engineer it through the proximity effect. Indeed, it is well-known that in S/F bilayers, the spin splitting in the latter leads to oscillations in the pair correlation between the singlet and triplet spin configurations due to a process akin to the Fulde-Ferrell-Larkin-Ovchinnikov (FFLO) oscillations (Buzdin, 2005; Fulde and Ferrell, 1964; Larkin and Ovchinnikov, 1965). Nevertheless, such a coupling between S and homogeneous F is rapidly suppressed as one moves away from the interface region, leading to a proximity effect of short range. The situation is, however, different in F with an inhomogeneous \mathbf{M} direction. This is because the spin of the short-ranged triplet correlations is orthogonal to \mathbf{M} . If the orientation of \mathbf{M} changes, then the triplet spin will obtain a component parallel to \mathbf{M} . This component is not influenced by the spin splitting to the same degree as their short-ranged counterparts and may persist for long distances. It is therefore referred to as a long-ranged triplet component.

Engineering superconducting hybrid structures for generating spin-polarized triplets have been extensively studied. There are several ways to engineer the necessary inhomogeneous \mathbf{M} . One involves using magnets in which \mathbf{M} is intrinsically inhomogeneous which applies to several rare earth materials including holmium where evidence of triplet pair creation has been obtained in JJs (Robinson *et al.*, 2010; Sosnin *et al.*, 2006). Alternatively, noncollinear magnetic structures

can be engineered in magnetic multilayers (Banerjee *et al.*, 2014; Khaire *et al.*, 2010). Neither of these systems are without challenges, as magnets that are intrinsically inhomogeneous are rare, and controlling \mathbf{M} -misalignment in ferromagnetic multilayers can be difficult, especially in the barrier of a JJ due to magnetostatic interaction (Banerjee *et al.*, 2014).

An effective inhomogeneous \mathbf{M} is generated in a homogeneous F in the presence of SOC. This takes the form of a Dzyaloshinskii-Moriya exchange interaction (Dzyaloshinsky, 1958; Moriya, 1960), which cants \mathbf{M} creating magnetic structures such as helical spin textures (Ferriani *et al.*, 2008) and skyrmions (Heinze *et al.*, 2011; Rößler *et al.*, 2006). Such magnetic structures at S/F interface can generate spin-polarized triplets. Furthermore, SOC in S/F structures is an auspicious combination as the former is generated at interfaces due to broken inversion symmetry. The formation of triplets in S/F structure with SOC is new area of intense study (Banerjee *et al.*, 2018; Bergeret and Tokatly, 2013, 2014; Jacobsen *et al.*, 2016; Jeon *et al.*, 2018, 2019b, 2020; Mel’Nikov *et al.*, 2012; Satchell and Birge, 2018; Satchell *et al.*, 2019).

D. Theoretical frameworks

In the following we describe common theoretical models which describe SOC in superconducting hybrid structures with increasing realism and complexity. We start by highlighting basic features of the proximity effect in such systems.

1. General considerations of spin-dependent fields

To understand the response of a superconductor to magnetic interactions, we consider the BCS model in an infinite domain, with spin splitting of the type

$$H = \sum_{ks} \xi_k c_{ks}^\dagger c_{ks} - \sum_{ks} \left[s \Delta c_{ks}^\dagger c_{-k,-s}^\dagger + s \Delta^* c_{-k,-s} c_{ks} \right] - \sum_{kss'} \mathbf{h}(\mathbf{k}) \cdot \boldsymbol{\sigma}_{ss'} c_{ks}^\dagger c_{ks'}, \quad (12)$$

where $\xi_k = \hbar^2 \mathbf{k}^2 / 2m - \mu$, μ is the chemical potential, and m is the electron rest mass. Δ is the superconducting order parameter, and \mathbf{h} relates to the spin splitting. The operators c_{ks}^\dagger (c_{ks}) create (annihilate) an electron with momentum k and spin s . Consider the case where $\mathbf{h} = h_0 \hat{z}$ is independent of momentum, and therefore reduces to a Zeeman field. Insight into the superconducting behavior can be gained by inspecting the normal state dispersions ($\Delta = 0$) as shown in Fig. 3. The Zeeman field splits the energy bands of the two spin species—the spin-up band is slightly lowered in energy, and the spin-down band slightly raised. The corresponding gap induced in the band structure of the two spin species when superconductivity is introduced, E_g^\uparrow and E_g^\downarrow respectively, is $E_g^s = \Delta - sh$, and indicates a difference in the strength of the hybridization between electrons and holes for the two opposite spins. We can study the effect of superconductivity via the opposite-spin electron pair correlations, given as $F_{\uparrow\downarrow}(\mathbf{k}, t) = \langle c_{k\uparrow}^\dagger(t) c_{-k\downarrow}^\dagger(0) \rangle$. We note that this quantity can represent a scattering process between a spin-down hole and a spin-up electron, and therefore involves no exchange of spin. This is because $c_{-k\downarrow}^\dagger$ creates a spin-down electron, which is equivalent to the removal of a spin-up hole.

A similar analysis also applies to $F_{\downarrow\uparrow}(\mathbf{k}, t) = \langle c_{k\downarrow}^\dagger(t) c_{-k\uparrow}^\dagger(0) \rangle$, which now involves spin-down parti-

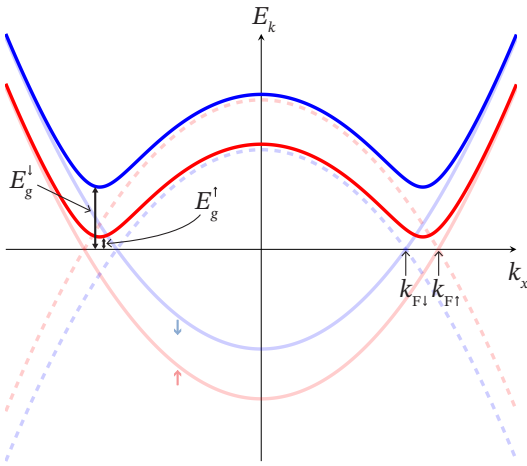


FIG. 3 The band structure of a superconductor in the presence of a Zeeman field. E_g^s indicates the superconducting gap of the two branches. The faded, full (dashed) lines show the normal-state electron (hole) band structures of the two spin species.

cles. The Zeeman field changes the relative size of the pair correlations. Furthermore, they have to obey certain symmetry constraints, which ultimately stem from fermion statistics that govern electrons. Indeed, the superconducting correlations have to be antisymmetric under the combined interchange of spin, momentum, band (for multiband systems) and time indices, a relationship known as the SPOT rule (Berezinskii, 1964; Linder and Balatsky, 2019). Singlet pairing (odd in spin index), $F_s \propto F_{\uparrow\downarrow} - F_{\downarrow\uparrow}$, is the most conventional form of superconductivity, and is typically s wave (even parity), single-band (even in band index), and even frequency (even in time index). However, since $F_{\uparrow\downarrow}$ and $F_{\downarrow\uparrow}$ now are different, one obtains a triplet component $F_t \propto F_{\uparrow\downarrow} + F_{\downarrow\uparrow}$. Since we have no k dependence in either the order parameter or the Zeeman field, we typically get s -wave correlations, meaning that the triplets must be odd frequency. Hence we derive

$$F_{\uparrow\downarrow} = - \frac{\Delta}{(i\omega + h)^2 - \xi_k^2 - |\Delta|^2}, \quad (13)$$

$$F_{\downarrow\uparrow} = + \frac{\Delta}{(i\omega - h)^2 - \xi_k^2 - |\Delta|^2}, \quad (14)$$

from which we see that $F_t \propto i\hbar\omega$, and odd when $\omega \rightarrow -\omega$.

In the model considered here, even frequency triplets require oppositely aligned spins with mismatched momenta so that an odd-parity component appears. This is possible in the presence of a Zeeman field with a spontaneous symmetry breaking, and the appearance of spatial modulations of the superconducting gap. This is the FFLO phase (Fulde and Ferrell, 1964; Larkin and Ovchinnikov, 1965), which has not been observed experimentally in the bulk. Such triplets are more visible by considering a spin splitting of the form $\mathbf{h} = h_0 k_x \hat{z}$, i.e., a form of SOC. The normal-state dispersions are shown in the upper panel of Fig. 4, plotted along k_x . In this case, there is a relative horizontal shift of the energy bands of the two spins meaning that spin-up particles on average have a positive momentum along k_x , while spin-down particles have a negative momentum. Hence, even in the absence of \mathbf{M} , there exists an equilibrium spin current – even in the normal state (Droghetti *et al.*, 2022; Rashba, 2003). The momentum shift of the normal-state dispersions leads to a similar, relative momentum-shift in the pair correlations $F_{\uparrow\downarrow}$ and $F_{\downarrow\uparrow}$,

$$F_{\uparrow\downarrow} = - \frac{\Delta}{(i\omega)^2 - (\xi_k - h_0 k_x)^2 - |\Delta|^2}, \quad (15)$$

$$F_{\downarrow\uparrow} = + \frac{\Delta}{(i\omega)^2 - (\xi_k + h_0 k_x)^2 - |\Delta|^2}, \quad (16)$$

which gives rise to p_x wave triplets, $F_t \propto h_0 k_x$.

When $F_{\uparrow\downarrow} \neq F_{\downarrow\uparrow}$ it means that one spin species has a greater hybridization with their corresponding hole branch than the other. In other words, we have spin-dependent scattering processes in the electron-hole sector, and hence might expect an observable \mathbf{M} to appear. However, there is a caveat. To obtain \mathbf{M} , it is a requirement that the relative phase difference

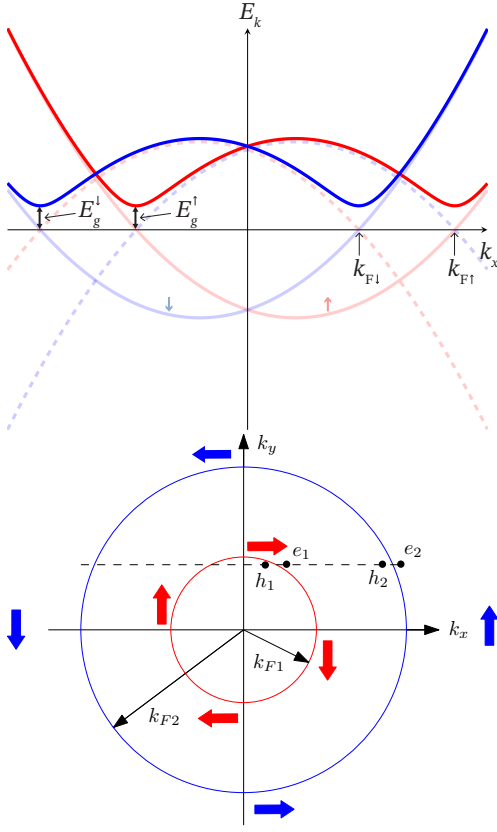


FIG. 4 *Upper panel*: Band structure of a superconductor in the presence of SOC of the form $\hat{H}_{\text{SOC}} = \alpha k_x \sigma_z$. The color and style of the bands matches the meaning in Fig. 3. *Lower panel*: Band structure in a 2D material with Rashba SOC [Eq. (17)]. The blue and red bands have opposite spins for a given angle in the $k_x - k_y$ plane. For an electron incident toward the interface with a direction away from the interface normal ($k_y \neq 0$), Andreev reflection is possible both via inter- and intraband scattering. Thus, the superconducting proximity becomes a mix of oscillatory and nonoscillatory terms inside the material with SOC. Made after Fig. 1(c) in Reeg and Maslov, 2015.

between the singlet and the triplet is *different from* $\pi/2$, otherwise $F_{\uparrow\downarrow} \propto |F_s| + i|F_t|$ and $F_{\downarrow\uparrow} \propto |F_s| - i|F_t|$ remain equal in magnitude (Linder *et al.*, 2017). For the Zeeman field, the odd-frequency triplets indeed incur such a phase shift of $\pi/2$, and therefore do not directly contribute to \mathbf{M} . On the other hand, the even frequency triplets are not phase shifted relative to the singlet correlations. Clearly, this produces a superconducting contribution to the spin currents, since $F_{\uparrow\downarrow} \propto |F_s| + |F_t|$ for $k_x > 0$, and $F_{\uparrow\downarrow} \propto |F_s| - |F_t|$ for $k_x < 0$, and vice versa for $F_{\downarrow\uparrow}$. In other words, there is preferential particle-hole scattering of one spin species for $k_x > 0$, and for the other spin species for $k_x < 0$.

2. Superconducting proximity effect

The superconducting proximity effect in a metallic material is enabled by the process of Andreev reflection (Buzdin, 2005; Deutscher, 2005; Žutić *et al.*, 2004). In this process,

an incoming electron from the metallic side enters the superconducting material, crosses quasiparticle branch when it has penetrated far enough so that its energy equals the local value of the superconducting gap, and then travels back as a hole-like excitation which enters the normal metal. In the process of the incident electron crossing branch, a total charge of $-2e$ is transferred to the superconducting condensate, resulting in the creation of a Cooper pair. On the normal-metal side, the incoming electron becomes correlated to the hole that tunnels back into the normal metal, creating a superconducting phase-coherence that extends a long distance in the normal metal.

Before discussing how SOC modifies the proximity effect, it is instructive to first briefly consider the case of a ferromagnetic material. As discussed in the previous section, the two spin-bands are, in such a case, split by an exchange field, modelled by a magnetic part of the Hamiltonian of the form $\hat{H} = \mathbf{h} \cdot \boldsymbol{\sigma}$ where \mathbf{h} is the exchange field and $\boldsymbol{\sigma}$ is a vector with Pauli matrices as components. This causes the superconducting proximity effect to behave qualitatively differently compared to a normal metal (Bergeret *et al.*, 2005; Buzdin, 2005). First of all, there will appear odd-frequency triplets due to the presence of superconducting correlations in a spin-split material. In addition, since the interface between the superconductor and the ferromagnet breaks translation invariance, momentum in the direction normal to the interface is not a good quantum number. This leads to mixing between odd and even parity pair correlations, and thus odd parity, even frequency triplets. Consider the wavevectors of an electron excitation with a given spin, such as spin up, and a hole excitation with opposite spin at a given energy ε . The electron will have momentum $\pm k_{\uparrow}$ whereas the hole will have momentum $\mp k_{\downarrow}$. In effect, there is a momentum mismatch $\Delta k = k_{\uparrow} - k_{\downarrow}$ between the electron and hole, which gives the Cooper pair wavefunction induced in the ferromagnet a finite center of mass momentum even in the absence of any net current through the system. Because of this, the superconducting correlations will not only decay as one moves deeper into the ferromagnetic region, but they will also oscillate in magnitude (Bergeret *et al.*, 2005; Buzdin, 2005). This is shown in Fig. 5.

We now discuss the superconductor proximity effect in hybrid structures with SOC, following a similar presentation to (Reeg and Maslov, 2015). An important point which distinguishes the magnetic and SOC case is that the dimensionality is important for the qualitative behavior of the proximity effect. Consider first the 1D case, *e.g.* a nanowire with SOC in contact with a superconductor. We can model an antisymmetric Rashba-like SOC by a Hamiltonian

$$\hat{H}_{\text{SOC}} = \alpha g_k \cdot \boldsymbol{\sigma}, \quad (17)$$

where α is the magnitude of the SOC and $\mathbf{g}_k = (0, 0, k_x)$ for a nanowire extending along the x -axis. We again consider an electron and hole with opposite spins at an energy ε in the upper panel of Fig. 4, as these are the excitations involved in the Andreev-reflection process inducing superconductivity

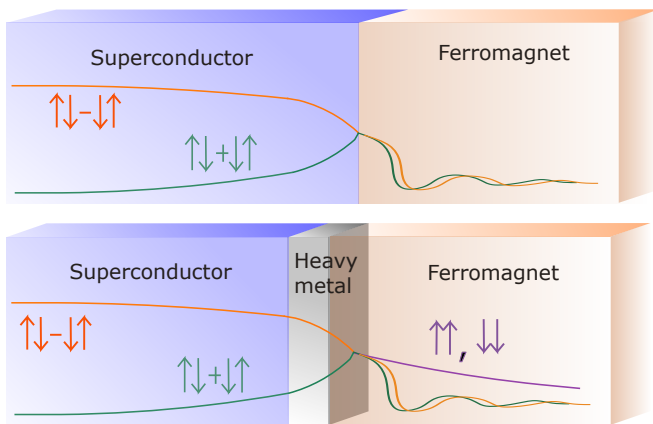


FIG. 5 Illustrations of the superconductor proximity effect at homogeneously magnetized S/F interfaces. The singlet pairing amplitude $\uparrow\downarrow - \downarrow\uparrow$ oscillates in F superimposed on an exponential decay with a coherence length of a few nanometers. Due to spin-dependent phase shifts, a spin-zero triplet pairing amplitude $\uparrow\downarrow + \downarrow\uparrow$ is generated which also rapidly decays in F, closely matching the singlet decay envelope, but vanishing in S over a singlet coherence length. By adding a HM layer with interfacial Rashba at the S/F interface, the proximity effect for spins parallel to \mathbf{M} can be extended through the generation of $\uparrow\uparrow$ and $\downarrow\downarrow$ triplet pairs. Conversely, for spins perpendicular to \mathbf{M} in F the spin zero singlet and spin zero triplet pairs remain short-ranged and oscillatory in F

in the SOC metal. The band-structure in the SOC metal is now different than in the ferromagnetic case. By considering electrons and holes with opposite spin labels, we see that such pairs have momenta $\pm k_{F\uparrow}$ or $\pm k_{F\downarrow}$, respectively. Therefore, there is no mismatch¹ in the momentum magnitude between the electrons and the Cooper pair wavefunction does not acquire any center-of-mass momentum. Thus, Andreev reflection only involves intraband (same band) excitations in the 1D case and there is no oscillatory behavior of the superconducting correlations inside the SOC metal.

The situation changes qualitatively when going to 2D. We can model a 2D system with Rashba SOC by the same \hat{H}_{SOC} , but this time with a \mathbf{g}_k -vector that depends on both k_x and k_y for a system that lies in the xy -plane, such as a 2DEG. A Rashba-like SOC is described by $\mathbf{g}_k = (-k_y, k_x, 0)$ and gives rise to the band-structure shown in the lower panel of Fig. 4.

As shown in the figure, the Fermi surface consists of two circles where the spin expectation value of an excitation on one of the circles varies as one moves around the circle. This means that the blue and red bands do not have definite spin. Assume for simplicity that we are dealing with a ballistic

SOC/S structure so that translational invariance is maintained in the direction parallel to the interface. Then, momentum in this direction is conserved during the Andreev reflection process (say k_y for a structure extending along the x -axis). Considering first the case $k_y = 0$, we recover the 1D situation shown in the upper panel of Fig. 4. But for $k_y \neq 0$ [black dashed line in the lower panel of Fig. 4], the proximity effect changes its nature. Since the Fermi surfaces do not have definite spin, an electron on the outer, blue circle (e_2) can be Andreev reflected as a hole both on the blue (h_2) and red (h_1) Fermi surface. Both of these holes carry some weight of opposite spin to the e_2 electron when $k_y \neq 0$, whereas only a hole on the same Fermi surface has opposite spin when $k_y = 0$. As a result, both intra- and interband Andreev scattering are possible. The intraband scattering gives rise to a nonoscillatory superconducting correlation decaying inside the SOC metal, like in the 1D case. But the interband Andreev scattering is seen to feature a momentum magnitude mismatch between the electron and holes involved: $k_{F1} - k_{F2}$. Thus, for interband Andreev scattering we are back to a similar situation as in the ferromagnetic case, where the induced superconducting correlations oscillate. In total, the superconducting proximity effect in a SOC metal consists of both oscillatory and nonoscillatory terms, in contrast to both the ferromagnetic and 1D SOC metal case. The spin-dependent scattering provided by SOC is thus seen to be able to cause the superconducting proximity effect to have a qualitatively different nature in materials with SOC as compared to materials with FM order.

In a S/F junction, the superconducting correlations decay rapidly inside the ferromagnet with superimposed oscillations due to the momentum-mismatch between the electrons in the pairs, as explained above. This is shown in Fig. 5. Cooper pairs consisting of electrons with spins that are collinear with \mathbf{M} in F, on the other hand, penetrate a long distance. This is because there is no longer any momentum mismatch between such electrons, as both belong to the same spin-polarized Fermi surface. Adding a thin HM as an interface layer separating the superconductor and ferromagnet introduces spin-orbit scattering. This provides a route to convert opposite spin Cooper pairs to same-spin Cooper pairs, which in turn penetrate much longer into the ferromagnet (see Fig. 5). Experiments have shown that such pairs can survive for distances of the order $\sim 1 \mu\text{m}$ even in strongly-polarized ferromagnets (Keizer *et al.*, 2006).

The superconducting proximity effect can be long-ranged in F by adding SOC e.g., (1) adding an interfacial HM layer causing SOC-scattering, or (2) F with intrinsic SOC. Case (1) is illustrated in Fig. 5 where spin-dependent scattering at the interface due to the HM layer creates long range triplet pairs in F. The number density of triplet pairs created in this way will depend on \mathbf{M} direction of the F layer (Jacobsen *et al.*, 2015). In case (2), long-ranged triplet pairs are also created, via two physical mechanisms (Bergeret and Tokatly, 2013): spin-precession induced by the SOC, and anisotropic

¹ When the Andreev reflection process involves quasiparticles with excitation energy ϵ , there is a tiny mismatch between the wavevectors due to different signs for ϵ in the wavevector expression for electrons and holes. This mismatch also occurs in the normal metal case, and does not cause oscillations of the energy-integrated superconducting correlation function in the normal metal.

spin-relaxation. One can map the diffusive-limit equation of motion for the anomalous Green functions (describing the Cooper pairs), known as the Usadel equation, to the spin-diffusion equation in (Bergeret and Tokatly, 2014). This analogy is useful since it shows that the different triplet Cooper pair components behave similarly to the spin components of an electron in a diffusive metal with SOC.

3. The Ginzburg-Landau formalism

The Ginzburg-Landau formalism is a symmetry-based method to explore the behavior of superconducting systems (Ginzburg and Landau, 1950). It involves expanding the free energy in the complex superconducting order parameter ψ , indicating the strength of the superconductivity, and is largely phenomenological. The method is highly successful, and consistent with BCS theory (Gor'kov, 1959). In the presence of SOC, the free energy density is given as (Edelstein, 1996; Kaur *et al.*, 2005; Samokhin, 2004)

$$f(\mathbf{r}) = a|\psi(\mathbf{r})|^2 + \gamma|\tilde{\nabla}\psi(\mathbf{r})|^2 + \frac{b}{2}|\psi(\mathbf{r})|^4 + \frac{B^2}{2\mu_0} - i\alpha(\mathbf{r})(\mathbf{n} \times \mathbf{h}) \left[\psi^*(\mathbf{r})\tilde{\nabla}\psi(\mathbf{r}) - \psi(\mathbf{r})(\tilde{\nabla}\psi(\mathbf{r}))^* \right], \quad (18)$$

where $\tilde{\nabla} = \nabla - (2ie/\hbar)\mathbf{A}$, $\mathbf{B} = \nabla \times \mathbf{A}$, a , b are phenomenological parameters, $\gamma = \hbar^2/2m$, and α characterize SOC. Applying Eq. (18) to a Josephson weak link, a non-zero phase difference appears between the superconducting banks (Buzdin, 2008). This is seen by minimizing Eq. (18) with respect to ψ and \mathbf{A} , giving the Euler-Lagrange equation

$$a\psi - \gamma\tilde{\nabla}^2\psi + b\psi|\psi|^2 - 2i\alpha(\mathbf{n} \times \mathbf{h}) \cdot \tilde{\nabla}\psi = 0, \quad (19)$$

$$\mathbf{j} = \frac{4e\gamma}{\hbar}\Im(\psi^*\nabla\psi) - \left(\frac{8e^2\gamma}{\hbar^2}\mathbf{A} + \frac{4e\alpha}{\hbar}(\mathbf{n} \times \mathbf{h}) \right) |\psi|^2. \quad (20)$$

Equation (19) may be solved in the normal metal, in which case ψ is interpreted as a small pair correlation present due to proximity with the superconductors. Neglecting the higher order nonlinear term, and setting $\mathbf{B} = 0$, one obtains for a 1D geometry with the exchange field pointing in the z direction,

$$\psi(x) = |\Delta| e^{i\alpha\hbar x/\gamma} \left[\frac{e^{i\phi_R} \sinh \kappa(x + L/2) - e^{i\phi_L} \sinh \kappa(x - L/2)}{\sinh \kappa L} \right], \quad (21)$$

with $\kappa^2 = a/\gamma - \alpha^2\hbar^2/\gamma^2$ and $\phi_{R/L} = \mp(\phi - \alpha\hbar L/\gamma)/2$. In Eq. (21), transparent boundary conditions have been assumed, i.e., $\psi(\pm L/2) = |\Delta| e^{i\phi_{R/L}}$, where $|\Delta|$ and ϕ is the absolute value of the superconducting gap, assumed equal in the two superconductors, and their phase, respectively. Inserting Eq. (21) into Eq. (20) one finds the current-phase relation

$$\mathbf{j} = j_c \sin(\phi - \phi_0), \quad (22)$$

where $j_c = \kappa|\Delta|^2/\sinh \kappa L$ and $\phi_0 = \alpha\hbar L/\gamma$. The presence of SOC has introduced a phase shift into the conventional Josephson current. This will be discussed in-depth later in this review.

Equation (20) also reveals spontaneous edge currents in S/F structures, as noted in Mironov and Buzdin, 2017. If the interfacial SOC is substantial, \mathbf{j} may be non-zero even if the orbital effect is negligible ($\mathbf{A} = 0$), and ψ is uniform. In this case, \mathbf{j} is directed along $\mathbf{n} \times \mathbf{h}$, parallel to the interface. This has interesting applications e.g., in a superconducting loop in proximity to a ferromagnetic insulator, circulating spontaneous supercurrents are predicted (Robinson *et al.*, 2019), which may find use in single flux quantum (SFQ) logic—similarly to proposals involving π junctions (Feofanov *et al.*, 2010). Superconducting vortices, generated solely due to these spontaneous currents, without an applied external magnetic field, have also been predicted at S/F interfaces (Olde Olthof *et al.*, 2019).

4. Bogoliubov-de Gennes method

In the following, we will consider a superconducting system within the mean-field approximation. This can be described by a Hamiltonian of the form

$$H = \sum_{ss'} \int d\mathbf{r} \psi_s^\dagger(\mathbf{r}) h_{ss'}(\mathbf{r}) \psi_{s'}(\mathbf{r}) + \frac{1}{2} \int d\mathbf{r} \left[\Delta(\mathbf{r}) \psi_\uparrow^\dagger(\mathbf{r}) \psi_\downarrow^\dagger(\mathbf{r}) + \Delta^*(\mathbf{r}) \psi_\downarrow(\mathbf{r}) \psi_\uparrow(\mathbf{r}) \right], \quad (23)$$

where $\psi_s(\mathbf{r})$ is the field operator for an electron with spin s , h is the single particle Hamiltonian, and in a homogeneous system Δ is the s -wave superconducting gap. The presence of Δ introduces the added complication that the electron and hole bands hybridize, described by using the Nambu basis,

$$\Psi(\mathbf{r}) = \left(\psi_\uparrow(\mathbf{r}) \quad \psi_\downarrow(\mathbf{r}) \quad \psi_\uparrow^\dagger(\mathbf{r}) \quad \psi_\downarrow^\dagger(\mathbf{r}) \right)^T, \quad (24)$$

in which case Eq. (23) may be written as

$$H = H_0 + \frac{1}{2} \int d\mathbf{r} \Psi^\dagger(\mathbf{r}) \hat{H} \Psi(\mathbf{r}), \quad (25)$$

where H_0 describes a trivial energy shift, and

$$\hat{H} = \begin{pmatrix} h & \Delta i\sigma_y \\ -\Delta^* i\sigma_y & -h^* \end{pmatrix}. \quad (26)$$

The diagonalization of Eq. (26) is referred to as Bogoliubov-de Gennes method (de Gennes, 1999), where it is noted that the quasiparticles (the eigenvalues) become a mixture of particles and holes.

Generally, two approaches are used when studying superconducting hybrid structures using the Bogoliubov-de Gennes method. A continuum formulation may be used, in which case the scattering at interfaces between materials is taken

into account via generalizing the Griffin-Demers or Blonder-Tinkham-Klapwijk (BTK) formalism (Blonder *et al.*, 1982; Griffin and Demers, 1971). This entails matching the wave functions obtained from Eq. (25) in adjacent materials at every interface and includes both normal reflection and tunneling processes, as well as Andreev reflection of opposite or equal spins (Žutić and Das Sarma, 1999). While BTK formalism assumes a step-function profile for the pair potential, the continuum formulation can also be solved self consistently (Halterman *et al.*, 2015; Setiawan *et al.*, 2019; Valls, 2022).

The other way of applying the Bogoliubov-de Gennes method is in a tight-binding approach on a lattice. It is appropriate when one wishes to study the equilibrium properties of superconducting systems—for instance the superconducting pair correlation in hybrid structures due to the proximity effect. The Hamiltonian then becomes a discrete $4N \times 4N$ matrix, where N is the number of lattice sites.

5. Quasiclassical theory

The Green function method is a powerful tool to describe condensed matter systems. Here, we briefly review the Keldysh technique, which is applicable to equilibrium and nonequilibrium systems. For an in-depth discussion, see (Rammer and Smith, 1986). In Keldysh space, the Green function of a fermionic system takes the form

$$\check{G} = \begin{pmatrix} \hat{G}^R & \hat{G}^K \\ 0 & \hat{G}^A \end{pmatrix}, \quad (27)$$

where \hat{G}^R , \hat{G}^A , and \hat{G}^K are the retarded, advanced and Keldysh Green functions, respectively, defined as

$$\hat{G}^R(\mathbf{r}, t; \mathbf{r}', t') = -i\theta(t-t')\hat{\tau}_z \langle \{ \Psi(\mathbf{r}, t), \Psi^\dagger(\mathbf{r}', t') \} \rangle \quad (28)$$

$$\hat{G}^A(\mathbf{r}, t; \mathbf{r}', t') = +i\theta(t'-t)\hat{\tau}_z \langle \{ \Psi(\mathbf{r}, t), \Psi^\dagger(\mathbf{r}', t') \} \rangle \quad (29)$$

$$\hat{G}^K(\mathbf{r}, t; \mathbf{r}', t') = -i \langle [\Psi(\mathbf{r}, t), \Psi^\dagger(\mathbf{r}', t')] \rangle, \quad (30)$$

with Ψ the Nambu spinor given in Eq. (24). \hat{G}^X are thus 4×4 matrices in particle-hole and spin space, making $\check{G}(\mathbf{r}, t; \mathbf{r}', t')$ an 8×8 matrix governed by the Gor'kov equations,

$$\check{\tau}_z \left(i\hbar \frac{\partial}{\partial t} - \check{H}(\mathbf{r}) \right) \check{G} = \hbar \delta(\mathbf{r} - \mathbf{r}') \delta(t - t'), \quad (31)$$

$$\check{G} \check{\tau}_z \left(i\hbar \frac{\partial}{\partial t'} - \check{H}(\mathbf{r}') \right)^\dagger = \hbar \delta(\mathbf{r} - \mathbf{r}') \delta(t - t'). \quad (32)$$

In the above $\check{\tau}_z = \hat{\tau}_z \otimes \sigma_0 = \sigma_0 \otimes \sigma_z \otimes \sigma_0$ and $\check{H} = \hat{H} \otimes \sigma_0$, where \hat{H} is given in Eq. (26). The matrices σ_i are the Pauli matrices, σ_0 is the 2×2 identity matrix, and the notation $A \otimes B$ indicates a Kronecker product. In other words, \check{H} is diagonal Keldysh space.

In many systems such as metals, the Fermi energy E_F is typically the dominating energy scale, so that all other contributions to the Hamiltonian may be considered small in com-

parison. In that case, the relevant contribution to several physical quantities of interest comes from near the Fermi level—referred to as the low-energy region. Equations (31) and (32), on the other hand, contain information about the entire spectrum, including the high-energy region. A significant simplification of these equations can be achieved if one retains only their low-energy component, keeping only terms which are at most linear in Ξ/E_F , where Ξ is any of the energy/self-energy scales involved, $\Xi \in \{|\Delta|, |\hbar\alpha|, \dots\}$. This procedure is known as the quasiclassical approximation, the details of which have been extensively reviewed elsewhere (Belzig *et al.*, 1999; Chandrasekhar, 2004; Rammer and Smith, 1986; Serene and Rainer, 1983). The resulting equation of motion for a ballistic system is known as the Eilenberger equation (Eilenberger, 1968)

$$\hbar v_F \cdot \nabla \hat{g}^R + i [\varepsilon \tau_z + \Sigma, \hat{g}^R] = 0, \quad (33)$$

where quasiparticle energy ε is the Fourier conjugate to $t - t'$, assuming a stationary system, v_F is the Fermi velocity, Σ contains the self energies under study, and $\check{g} = \frac{i}{\pi} \int d\xi \hat{G}$ is the quasiclassical Green function, with $\xi = \hbar^2 k^2 / 2m - \mu$. Uniqueness of Eq. (33) is assured by the accompanying constraint $(\check{g})^2 = \hat{I}$, with \hat{I} the 4×4 identity matrix (Shelankov, 1985).

The Green function formalism really shines when treating impurities. A high concentration of impurities may be treated within the quasiclassical approximation, using conventional impurity averaging techniques (Abrikosov *et al.*, 1975). This has the effect that quasiparticle motion takes the form of a random walker due to frequent impurity scatterings, so that momentum-dependent effects are strongly suppressed. The equation of motion then becomes,

$$D \nabla \cdot \check{g} \nabla \check{g} + i [\varepsilon \check{\tau}_z + \check{\Sigma}, \check{g}] = 0, \quad (34)$$

where D is the diffusion constant. It is noted that Eq. (34) takes the form of a diffusion equation, and a net particle current, representing a drift in the motion of the random walkers, may be identified by Fick's first law, $\check{\mathbf{j}} = -D \check{g} \nabla \check{g}$. The presence of such a drift has a profound effect on diffusive systems, as the impurity scattering becomes anisotropic, and gives rise to momentum-dependent effects which cancel out in an isotropic system.

The quasiclassical theory for SOC was established in Gorini *et al.*, 2010 and Raimondi *et al.*, 2012. Linear-in-momentum models of SOC such as Rashba and Dresselhaus models may be introduced by an effective SU(2) gauge field, for which the derivative operator may be replaced by its gauge covariant equivalent. Within the quasiclassical approximation, it is $\check{\nabla} f = \nabla f - (ie/\hbar)[\mathbf{A}, f]$, where $A_k = A_{0,k} \sigma_0 + \alpha_{klm} \sigma_l k_m$, with $A_{0,k}$ a scalar gauge field stemming from a potential external magnetic field, and α_{klm} a generic tensor describing the SOC. For ballistic systems, the SOC has the form of a momentum-dependent exchange field, which is intuitively reasonable, and has interesting consequences in *e.g.* ballistic Josephson weak links (Konschelle *et al.*, 2016).

The affect of SOC on a diffusive superconducting hybrid structure (Bergeret and Tokatly, 2013, 2014) is most evident in the limit of a weak proximity effect so that one may approximate $\hat{g}^R \simeq \hat{\tau}_z + \hat{F}$. Here, $\hat{F} = \text{antidiag}(f, \tilde{f})$, and f is the anomalous Green function, representing the superconducting correlations—which are assumed to be small. Furthermore, $\tilde{f}(\varepsilon) = f^*(-\varepsilon)$. This limit is valid, for instance, in a ferromagnet proximity-coupled to a superconductor. By parameterizing into singlet f_s and triplet \mathbf{f} components using the d vector notation (Leggett, 1975), $f = (f_s + \mathbf{f} \cdot \boldsymbol{\sigma}) i\sigma_y$, one finds that for Rashba SOC, the Usadel equation becomes

$$D\nabla^2 f_s + 2i\varepsilon f_s + 2i\mathbf{h} \cdot \mathbf{f} = 0. \quad (35)$$

$$D\nabla^2 \mathbf{f} + 4iD\alpha [\mathbf{n} \times (\nabla \times \mathbf{f}) - \nabla \times (\mathbf{n} \times \mathbf{f})] + (2i\varepsilon - 4D\alpha^2) \mathbf{f} + 2i\mathbf{h} f_s = 0. \quad (36)$$

A similar set of equations may be derived for the linear Dreselhaus model. Inspection of the above reveals that the singlet superconducting correlation is independent of the SOC to this level of accuracy, which is reasonable as it is independent of spin. The triplets, on the other hand, are influenced. Even though we are in the diffusive limit, we may still use the picture of a momentum-dependent magnetic field to understand their behavior. Indeed, the term proportional to α^2 in Eq. (36) leads to an increased decay of the triplet correlations. This is the Dyakonov-Perel-like spin relaxation (D'yakonov and Perel, 1971), where frequent scatterings is associated with fluctuations in the magnetic field perceived by the quasiparticles, leading to a loss of spin information over short distances. The terms proportional to α represent a precession of the pair correlation spins, resulting in a mixing of the triplet components. This observation, along with the experimental accessibility of the diffusive limit, has led to these systems receiving significant attention (Alidoust and Halterman, 2015a,b; Amundsen and Linder, 2017; Jacobsen *et al.*, 2015). The formalism has also been extended to incorporate magnetoelectric effects (Bobkova and Bobkov, 2017; Konschelle *et al.*, 2015; Tokatly, 2017), as well as extrinsic SOC, i.e., as induced by impurities (Bergeret and Tokatly, 2016; Huang *et al.*, 2018; Virtanen *et al.*, 2021).

It is possible to study interfacial SOC within the quasiclassical approximation. This is typically modeled as HM interlayers of sufficient thickness to be valid in the quasiclassical limit. This procedure was, for instance, used in a ferromagnetic Josephson weak link in which the central F is sandwiched between two such HM layers, revealing a spin-polarized Josephson current (Jacobsen *et al.*, 2016). This, however, does not accurately represent SOC induced by the symmetry breaking of the interface. Nevertheless, the results agree with more detailed calculations, where the SOC is introduced as a spin-dependent interface potential (Amundsen and Linder, 2019a; Linder and Amundsen, 2022).

III. EXPERIMENTAL TECHNIQUES

In this section we discuss experimental techniques that are often used to investigate the S/F hybrid structures and devices. These techniques are similar when SOC effects are included albeit with modification of the thin-film heterostructure (e.g., with the use of HM layers such as Pt with or without a magnetic spin mixer). The main purpose of this section is to provide some intuitive guidelines on designing experiments to investigate S/F proximity effects in the context of triplet pair formation. In particular, we highlight four key measurement techniques: transition temperature (T_c) measurements of S/F hybrids; JJs; magnetization dynamics; and spectroscopic techniques including tunneling spectroscopy and low-energy muon spin-rotation (LE- μ SR).

A. Transition temperature measurements

Measuring T_c of a S thin film proximity-coupled to one or more F layers is a common method of exploring S/F structures. The theory dependence of T_c on the magnetic state of the F layer is discussed in detail in Section IV B. The nature of the S/F proximity depends on the depairing effect of the magnetic exchange field on the Cooper pairs and/or the generation of triplet pairs affecting the singlet pairing amplitude in S.

The majority of T_c measurements are carried out on unpatterned thin films using a four-point current-bias technique. A low bias current is used to avoid current-induced nonequilibrium shifts in T_c . To control the magnetic state of the F layer(s), magnetic fields are applied which are negligible relative to the upper critical field of S layer. There is an orbital depairing effect due to such magnetic fields which can suppress T_c and which must be accounted for during the analyses of T_c . This is usually not a problem for in-plane magnetic fields as the coercive fields of transition metal Fs are small relative to the in-plane upper critical field of the S layer. However, the situation is more complex for out-of-plane magnetic fields where the coercive fields of F layers tend to be large and so suppress T_c , but are often comparable to or greater than the magnetic field required to nucleate superconducting vortices. This is complicated further by dipolar fields that are injected into S from magnetic domain walls. All of these factors have to be taken into account in the analyses of T_c and often required control samples including isolated S films and S/F structures with insulating barriers to break the proximity effect between S and F layers (e.g., (Banerjee *et al.*, 2018; Singh *et al.*, 2015)).

Careful consideration is required when selecting the F material. For S/F/F' or F/S/F' spin valves, the key challenge is to obtain stable parallel, antiparallel or noncollinear magnetic states over a range of reasonable magnetic fields. This means that the coercive fields of the F layers should be sufficiently mismatched. For experiments related to triplet generation in spin valves using misaligned F layers \mathbf{M} , intermediate angles, especially an orthogonal alignment, is important. This re-

quires F layers with specific anisotropies e.g., using a thin Ni layer with out-of-plane anisotropy (Singh *et al.*, 2015), using Pt/Co (Banerjee *et al.*, 2018) or Co/Ni (Satchell *et al.*, 2019) multilayers.

B. Josephson junctions

JJs with F barriers have been key to demonstrating triplet creation with one of the first experiments detecting supercurrents through the highly spin-polarized half-metallic CrO_2 (Keizer *et al.*, 2006). The absence of minority spin states in CrO_2 means that any supercurrent flowing through it must be mediated by spin-charge triplet current; however, magnetic control of singlets to triplet pair formation was found to be challenging and highly irreproducible. Since then advances in triplet supercurrent transport in JJs has been made as discussed in Section IV E.

Owing to the small electrical resistance of metallic S/F heterostructures, nanopatterning is required for straightforward measurements of device voltage e.g., in JJs. For JJs with magnetic barriers, a further advantage of nanopatterning is that the F layers can be magnetically single domain meaning that even at high applied magnetic fields, the barrier flux can be small relative to a flux quanta. This allows manipulation of the magnetic state of the barrier without significantly lowering the JJ critical current. The presence of a barrier magnetic moment adds to the magnetic flux from the external magnetic field and can distort the magnetic-field-dependence of the Josephson critical current. A further complication in nanopatterned JJs is that dipolar fields from the F layers can distort the single domain state, introducing additional complex nanomagnetic states. These issues need careful consideration when designing JJs with magnetic barriers.

Various optical or electron beam lithography techniques are routinely used for the fabrication of S/F devices including JJs. These techniques are described elsewhere e.g., see (Blamire *et al.*, 2011).

C. Magnetization dynamics

An injected normal state current from a thin film F into an S in S/F structures can introduce a nonequilibrium quasiparticle spin accumulation in which charge and spin have different relaxation rates. Due to the longer spin relaxation time in the superconducting state (Yang *et al.*, 2010), a spin imbalance can be generated without a charge imbalance (Hübler *et al.*, 2012; Quay *et al.*, 2013). Alternatively, under specific conditions it may be possible to create a superconducting spin current in the S layer mediated via triplet pairs (Jeon *et al.*, 2019b). This experiment involved spin pumping from a layer of $\text{Ni}_{80}\text{Fe}_{20}$ (Py) in a Pt/Nb/Py/Nb/Pt structure. Here, the effective Gilbert damping, α , which is proportional to the spin-current density, of the precessing \mathbf{M} of Py increased below T_c , indicating an enhancement of the spin current above the

normal state which is different from the spin pumping via the Andreev bound states (Yao *et al.*, 2021).

Spin pumping experiments on S/F structures can be performed using broadband ferromagnetic resonance (FMR) involving a microwave source, a lock-in amplifier, and a coplanar waveguide. The microwave power of -20 to +20 dBm is connected to a pulse generator allowing a microwave frequency (f_{mw}) in the GHz range to be squarely modulated with a modulation frequency f_{mod} of less than 1 kHz. The microwave signal which is transmitted through a sample fixed onto a co-planar waveguide is then rectified using a microwave diode with a bandwidth typically in the range of 40 GHz. The diode voltage is multiplied with a reference at f_{mod} with a lock-in amplifier which is subsequently integrated over a certain time period leading to a d.c. voltage from signals with the same frequency as the reference signal. Each FMR spectrum is obtained by measuring this d.c. voltage while changing the external magnetic field which is typically applied in the film plane at a fixed f_{mw} (~ 5 to 20 GHz).

For FMR experiments of S/F structures, the thickness of the S layer should be less than the magnetic penetration depth (e.g., 100 nm for thin film Nb) which can otherwise lead to a shift in the magnetic field at resonance due to the Meissner screening in the S layer (Jeon *et al.*, 2019a).

D. Spectroscopic techniques

The nature of a triplet-induced in a F, S or normal metal (N) layer is theoretically different from the usually dominant singlet state. Although the triplet and singlet states share the common feature of an s -wave order parameter, unlike the singlet state, the orbital and spin components of the triplet state are even with respect to the electron exchange and this implies their wave function must be odd in frequency with respect to time reversal symmetry (Kontos *et al.*, 2002; Petrashov *et al.*, 1999). Consequently, a triplet state in a F, S or N should enhance the quasiparticle density of states (DOS). For a singlet state, there is no enhancement in the DOS and so the observation of a conductance peak around zero voltage is considered to be the “smoking gun” proof of odd-frequency triplet superconductivity.

The standard technique to probe the induced superconducting DOS involves tunnel junctions or scanning tunneling microscopy measurements of the current-voltage, $I(V)$, characteristics. Below T_c , the $I(V)$ characteristics are nonlinear at voltages near the gap edge. For an SIN, the IVs are nonlinear around $V = \pm\Delta/e$, where e is the electron charge and Δ is half the energy gap. Such measurements can provide high-resolution spectroscopic information because dI/dV is proportional to the quasiparticle excitations, i.e., to the superconducting DOS. Tunneling studies have been extensively used to probe the singlet state (Boden *et al.*, 2011; SanGiorgio *et al.*, 2008) and the triplet state (Kalcheim *et al.*, 2014, 2015, 2012) in different S/F structures. We note that point contact Andreev spectroscopy (Soulén Jr. *et al.*, 1998) has also been used to de-

fect triplet states in S/F structures (Di Bernardo *et al.*, 2015a; Usman *et al.*, 2011; Yates *et al.*, 2017).

In recent years, LE- μ SR (or muon spin rotation spectroscopy) has been used to probe the depth-dependence of superconductivity and magnetism in S/F structures. LE- μ SR offers a high sensitivity to magnetic fluctuations and spontaneous fields < 0.1 G with a depth-resolved sensitivity of a few nanometers (Di Bernardo *et al.*, 2015b; Fittipaldi *et al.*, 2021).

Muons are spin-half elementary particles with a charge matching an electron but over two-hundred times heavier. Implanted muons can provide detailed information about their local magnetic environment within a material and so muon spectroscopy is a sensitive tool for probing sub-surface superconductivity in the Meissner state. Spin-polarized positive muons, μ^+ , are generated from π^+ decay and are moderated by passing them through a cryosolid, typically Ar, to obtain μ^+ in the low-energy range (~ 15 eV). These μ^+ are accelerated by an adjustable sample bias that tunes their energies from 0.5-30 keV, which enables precise tuning of their implantation depth within a material. The spins of the implanted μ^+ precess about a local magnetic field and a decaying μ^+ emits a positron in the direction of the μ^+ spin. This decay of the positron intensity is measured as a difference in the number of counts by two detectors placed near the sample.

To study the Meissner state of S or S/F structure, a magnetic field, B_{ext} is applied parallel to the sample plane and perpendicular to the initial spin polarization of the μ^+ beam. This induces a precession of the μ^+ spins at an average frequency of $\bar{\omega}_s = \gamma_\mu \bar{B}_{loc}$ where \bar{B}_{loc} is the average local field experienced by the implanted muons and $\gamma_\mu = 2\pi \times 135.5 \text{ MHzT}^{-1}$ is the gyromagnetic ratio of the μ^+ . If the stopping distribution is $p(z, E)$ at a depth z and energy E of the implanted muons, then the precession frequency is $\bar{\omega}_s = \gamma_\mu \int B_{loc}(z) p(z, E) dz$. The asymmetry spectrum $A_s(t, E)$, which measures the normalized difference in the counts of the left and right detectors is proportional to $e^{-\bar{\lambda}t} [\cos \gamma_\mu \bar{B}_{loc} t + \phi_0 t]$ for a given implantation energy E . Here, $\bar{\lambda}$ is the mean muon depolarization rate and $\phi_0 E$ the starting phase of the muon precession. A series of mean-field values \bar{B}_{loc} is determined from the asymmetry fits as a function of the muon implantation energy E which provides the final $B_{loc}(z)$ profile inside the sample.

In the context of S/F proximity effects and triplet pairs, this technique has shown evidence for a paramagnetic Meissner effect in Au/Ho/Nb (Di Bernardo *et al.*, 2015b) and Au/C₆₀/Cu/C₆₀/Nb (Rogers *et al.*, 2021) structures, observed as a local enhancement of the magnetic field in Au above the externally applied field, in contrast to the diamagnetic repulsion which is a hallmark of the superconducting state.

IV. RECENT DEVELOPMENTS

This section reviews developments in superconducting thin-film hybrids with SOC.

A. Majorana zero modes

Majorana fermions are particles which have the peculiar property of being their own anti-particle. They are real solutions of the Dirac equation and represent a potential new, as of yet, undetected fundamental particle (Elliot and Franz, 2015). In condensed matter systems, predicted Majorana fermions are chargeless quasiparticle excitations (Aguado, 2017). This property makes superconductors ideal candidates to host such states, as the quasiparticles of superconducting systems—the bogoliubons—can consist of an equal mixture of the electron-like and hole-like excitations of the normal state system, as discussed in section II.D.4. However, these superconductors cannot be conventional with a spin-singlet configuration. Of particular interest are a class of materials known as topological superconductors with equal-spin (also referred to as spinless) pairing which, as topological insulators, feature a band inversion and a nontrivial topology (Culcer *et al.*, 2020; Shen, 2012). Defects (such as vortices) and quasiparticles in topological superconductors or boundaries between topological and trivial regions, can bind localized Majorana zero-energy modes (MZM) (Aasen *et al.*, 2016). These zero-energy (pinned at the Fermi level) topologically-protected degenerate states, in which quantum information can be nonlocally stored, are separated by the topological gap from the excited states.

A huge interest in MZM comes from their exotic non-Abelian statistics (unlike the Majorana fermions in particle physics), which is both fundamentally exciting and offers prospect for fault-tolerant topological quantum computing (Alicea *et al.*, 2011; Das Sarma *et al.*, 2015; Ivanov, 2001; Kitaev, 2003; Nayak *et al.*, 2008). An interchange of the position of two such MZM, known as braiding, yields a non-Abelian phase and transforms one to another quantum state within a degenerate ground-state manifold. The result is a quantum gate, topologically-protected from local perturbations (Lahtinen and Pachos, 2017) that typically plague conventional quantum computers. A complementary signature of the non-Abelian statistics comes from bringing together, or fusing, two MZM which removes their degeneracy and yields either an ordinary fermion or a vacuum state (Cooper pair condensate) (Beenakker, 2020).

While experimental reports of MZM detection remain debated and do not include their non-Abelian statistics, these efforts coupled with related theoretical studies have enabled a remarkable progress in understanding SOC effects in hybrid superconducting structures and advances in their fabrication.

In 1D, MZM are found at the ends of the well-known Kitaev chain (Kitaev, 2001), with triplet p -wave superconductivity. In 2D, MZM appear in $p_x \pm ip_y$ superconductors as localized states bound to vortices, as well as distributed chiral edge states at interfaces (Read and Green, 2000). Materials of dimension higher than one also offer the possibility of hosting MZM on surfaces of codimension larger than one, e.g., in the 0D corners of 2D systems, or 1D hinges of 3D systems. These materials are known as higher-order topological superconduc-

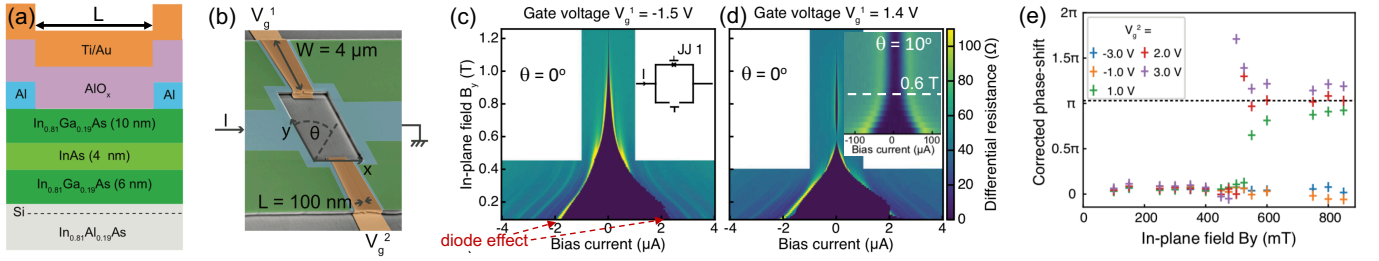


FIG. 6 Experimental evidence for topological superconductivity. (a) Schematic diagrams of a planar JJ. (b) SEM micrograph of a SQUID formed of two JJs with width $W = 4 \mu\text{m}$ and separation between the S contacts (Al) $L = 100 \text{ nm}$. Each JJ is independently gated with the voltage tuning both the carrier density and the SOC. The x-direction is colinear to the current flow in the JJs. Differential resistance of JJ1 as function of an applied in-plane field at gate voltages: (c) $V_g^1 = -1.5 \text{ V}$, (d) $V_g^1 = 1.4 \text{ V}$. In both cases, JJ2 is depleted ($V_g^2 = -7 \text{ V}$) and does not participate in the transport. Marked asymmetry signifies the superconducting diode effect. In (d), as expected for the transition to topological superconductivity, a minimum of the critical current is observed around 0.6 T for JJ1 for the in-plane field, B_y , at $\theta = 0^\circ$ [see Fig. 6(b)]. Inset: For $\theta = 0^\circ$ such minimum is lost. (e) Phase signature of topological transition from SQUID interferometry. Phase shift between the SQUID oscillation at $V_g^2 = -4 \text{ V}$ and the oscillation at a different value as a function of B_y . The linear B_y -contribution (due to anomalous Josephson effect) has been subtracted to highlight the phase jump of $\sim \pi$ at three higher V_g^2 values. From Dartailh *et al.*, 2021.

tors, in correspondence with their insulating counterparts (Benalcazar *et al.*, 2017; Schindler *et al.*, 2018a,b).

There are materials believed to exhibit intrinsic topological superconductivity, such as Sr_2RuO_4 (Kallin, 2012; Mackenzie and Maeno, 2003) and $\text{Cu}_x\text{Bi}_2\text{Se}_3$ (Kriener *et al.*, 2011; Sasaki *et al.*, 2011). However, challenges in relying on them can be seen from the extensively studied Sr_2RuO_4 . While doubts about the claimed $p_x \pm ip_y$ (Kallin, 2012; Mackenzie and Maeno, 2003) were raised before (Žutić and Mazin, 2005), an experimental evidence against the p -wave (Petsch *et al.*, 2020) now even involves some of the original discoverers of Sr_2RuO_4 (Maeno *et al.*, 1994).

Instead of the elusive intrinsic p -wave superconductors, there are alternative approaches to realize proximity-induced topological superconductivity. Chiral triplet superconducting correlations can be induced on the semimetallic surface states of a topological insulator in proximity to a conventional s -wave superconductor (Fu and Kane, 2008; Rosenbach *et al.*, 2021). It has been predicted that proximity-induced topological superconductivity is also generated when the topological insulator is replaced by a conventional semiconductor nanowire, provided it contains strong SOC and a Zeeman field (Alicea, 2010; Brouwer *et al.*, 2011; Das *et al.*, 2012; Deng *et al.*, 2012; Lutchyn *et al.*, 2010; Mourik *et al.*, 2012; Oreg *et al.*, 2010; Rokhinson *et al.*, 2012; Sau *et al.*, 2010).

Other viable candidates for topological superconductivity and MZM are the noncentrosymmetric superconductors. The strong SOC in these materials typically lead to a parity mixing, giving rise to a simultaneous presence of both p -wave and s -wave superconducting correlations. It has been shown theoretically that when the former are greater than the latter, the system enters a topologically nontrivial state featuring edge modes (Smidman *et al.*, 2017; Tanaka *et al.*, 2009). In a thin film of such a superconductor, the possibility of generating tunable higher-order topological states by external means has been theoretically predicted. This can be achieved by applying an in-plane magnetic field, $B_{||}$. In that case, the p -wave

correlations, SOC and the resulting Zeeman field together create a gap in the edge states—the size of which depends on the direction of $B_{||}$. The gapless edge states of a Rashba superconductor are immune to exchange fields applied normal to the edge, thus providing the ability of switching between corner and edge modes by rotating $B_{||}$ (Ikegaya *et al.*, 2021; Pahomi *et al.*, 2020; Zhu, 2018).

Instead of relying on native SOC, MZM can be hosted in systems where a suitable synthetic SOC is realized through magnetic textures and the resulting fringing fields (Desjardins *et al.*, 2019; Fatin *et al.*, 2016; Güngördü and Kovalev, 2022; Kim *et al.*, 2018, 2015; Kjaergaard *et al.*, 2012; Klinovaja *et al.*, 2012; Nadj-Perge *et al.*, 2014). Magnetic textures, $\mathbf{B}(\mathbf{r})$, remove the need for an applied magnetic field, while their tunability reconfigures regions that support topological superconductivity to create and control MZM (Boutin *et al.*, 2018; Fatin *et al.*, 2016; Mohanta *et al.*, 2019; Yang *et al.*, 2016; Zhou *et al.*, 2019). The emergent SOC arising from $\mathbf{B}(\mathbf{r})$, can be understood by recognizing that the Zeeman interaction, $g_{\text{eff}}\mu_B\mathbf{B}(\mathbf{r})/2$, where g_{eff} is the effective g -factor, is diagonalized by performing local spin rotations aligning the spin-quantization axis to the local $\mathbf{B}(\mathbf{r})$, a procedure known for over 45 years (Matos-Abiague *et al.*, 2017). In a rotated frame, the Zeeman energy attains a simple form, $|g_{\text{eff}}\mu_B\mathbf{B}(\mathbf{r})/2|\sigma_z$, while the kinetic energy acquires an extra term due to the non-Abelian field that yields the synthetic SOC.

Since the role of magnetic textures would be more pronounced in proximitized materials with large $|g_{\text{eff}}|$, such as narrow-band semiconductors or magnetically-doped semiconductors (Fatin *et al.*, 2016; Mohanta *et al.*, 2019; Zhou *et al.*, 2019), it was surprising that a support for MZM was reported in a carbon nanotube (Desjardins *et al.*, 2019; Yazdani, 2019), where the weak inherent SOC renders $|g_{\text{eff}}|$ small. Experimentally, a multilayer Co/Pt magnetic textures generated strong fringing field $\approx 0.4 \text{ T}$ in the nearby carbon nanotube which resulted both in the Zeeman interaction and the characteristic SOC energy $\approx 1.1 \text{ meV}$ (Desjardins *et al.*, 2019), ex-

ceeding the SOC values for InAs or InSb, common candidates sought to support the MZM. Tuning the magnetic textures, which needs to be accurately studied through micromagnetic simulations (Desjardins *et al.*, 2019; Mohanta *et al.*, 2019; Zhou *et al.*, 2019), revealed through the oscillations of the superconductivity-induced subgap states in carbon nanotube-based JJs with *s*-wave Pd/Nb electrodes. This realization of tunable magnetic textures and synthetic SOC which modifies proximity-induced superconductivity is encouraging for the feasibility of versatile control of MZM and demonstrating their non-Abelian statistics through braiding (Fatin *et al.*, 2016; Güngördü *et al.*, 2018; Matos-Abiague *et al.*, 2017).

Experiments in 2DEGs have also revealed a strong proximity effect when coupled to a superconductor, even in the presence of strong SOC (Kjaergaard *et al.*, 2016; Shabani *et al.*, 2016; Wan *et al.*, 2015). Several proposals suggest to use planar JJs with B_{\parallel} , where the superconducting correlations in the 2DEG can be tuned into a topologically nontrivial phase by a phase difference between the superconducting banks, thus producing MZM (Hell *et al.*, 2017a,b; Pientka *et al.*, 2017; Stern and Berg, 2019; Zhou *et al.*, 2020) and accompanied by related experiments reporting topological superconductivity (Fornieri *et al.*, 2019; Ren *et al.*, 2019). Using a SQUID geometry as shown in Figs. 6 (a) and (b), gate voltage can change both the carrier density and the strength of the Rashba SOC, which can determine the presence or absence of the topological superconductivity. Two individually gated JJs in the SQUID thus control the current to flow through both or just one of them (Dartiailh *et al.*, 2021). Figures 6(c) and (d) show that with gate control the JJ current can become non-monotonic with B_{\parallel} , as expected from the closing of the *s*-wave and the reopening of the *p*-wave superconducting gap, predicted in proximitized nanowires (Alicia, 2010; Lutchyn *et al.*, 2010; Oreg *et al.*, 2010; Sau *et al.*, 2010). The observed anisotropy of the JJ current, where its nonmonotonic character is lost for B_{\parallel} which is sufficiently misaligned with the N/S interface [Fig. 6(d), inset], further supports the expected proximity-induced *p*-wave superconductivity.

An independent signature of the topological superconductivity is obtained from the SQUID measurements which in Fig. 6(e) reveal an approximate π jump in the superconducting phase difference, expected across the transition to topological superconductivity (Hell *et al.*, 2017b; Pientka *et al.*, 2017). These various signatures of the topological superconductivity are obtained on the same sample and indicate topological transition at ~ 0.6 T. In contrast, B_{\parallel} required to reach $0 - \pi$ transition expected from the FFLO-like mechanism (Yokoyama *et al.*, 2014) in the studied samples is $B_{0-\pi} = (\pi/2)\hbar v_F / (g\mu_B L) \approx 14.4$ T (Dartiailh *et al.*, 2021). In another Al/InAs planar JJ, topological superconductivity was reported at an even lower $B_{\parallel} \sim 0.2$ T (Banerjee *et al.*, 2022). With multiple gates, planar JJs can be used to fuse MZM and probe the non-Abelian statistics (Zhou *et al.*, 2022).

Curved nanostructures, which have been suggested as viable systems for next generation spintronic devices (Chang and Ortix, 2017; Das *et al.*, 2019; Francica *et al.*, 2019; Gen-

tile *et al.*, 2015; Nagasawa *et al.*, 2013; Ying *et al.*, 2016), is another candidate to host MZM. In the presence of SOC, forcing motion along curved geometries can lead to non-trivial spin-dependent effects. Furthermore, bending, e.g., a nanowire, introduces a strain field which itself acts as a source of SOC. When superconducting order is introduced to such systems, curvature-dependent triplet superconducting correlations may appear (Ying *et al.*, 2017), a necessary ingredient for MZM. The manipulation of curvature can be used to exert control over, and even induce, nontrivial topology and MZM (Chou *et al.*, 2021; Francica *et al.*, 2020).

B. Superconducting critical temperature

Measurement of the superconducting critical temperature in S/F hybrids S/F1/F2 or F1/S/F2 spin-valve type configuration has been widely used study S/F proximity effects both in the context of singlet and triplet superconductivity. Theory (Baladié *et al.*, 2001; Tagirov, 1999) and experiments (Gu *et al.*, 2002; Moraru *et al.*, 2006) on F/S/F trilayers with both weak (CuNi) and strong (NiFe) F layers showed that the superconducting T_c is higher when the F layer moments are antiparallel compared to when they are parallel. In the singlet picture this can be understood easily from the higher net pair-breaking exchange field arising for the parallel F layer moments which suppresses superconductivity. For noncollinear F-moment alignments in F/S/F and S/F/F systems (Leksins *et al.*, 2012; Wang *et al.*, 2014), the proximity effect between the S and F layers is enhanced due to the generation of triplet Cooper pairs. The increased proximity effect results in a reduction of T_c by up to 120 mK for 3d ferromagnets (Leksins *et al.*, 2012; Wang *et al.*, 2014) to as large as a 1K for half-metallic ferromagnets like CrO₂ (Singh *et al.*, 2015).

This principle of detecting triplets using magnetic state-dependent modulation of the transition temperature was experimentally used to detect control of short-ranged triplets (Banerjee *et al.*, 2018). Using a Pt/Co/Pt trilayer proximity-coupled to an *s*-wave superconductor (Nb), a strong suppression of T_c for magnetic fields applied in-plane and partial compensation of T_c suppression for out-of-plane fields was detected. This was in sharp contrast to a pure Nb or Nb/Co multilayers where relatively little T_c suppression is seen for in-plane fields with negligible orbital depairing and a strong out-of-plane T_c suppression arising from orbital effects. The unconventional modulation is explained by the fact that in S/F structures without SOC, the short-ranged triplet energy does not depend on \mathbf{M} orientation thereby making the T_c independent of \mathbf{M} angle θ with the film plane. However, in presence of SOC arising from the interfacial symmetry breaking in Pt/Co/Pt trilayers, an increasing in-plane field increases the “leakage” of the Cooper pairs through the triplet channel. This leakage drains the superconductor of Cooper pairs and the superconducting gap is reduced. An out-of-plane has an opposite effect and closes this parallel triplet channel, thereby reducing the T_c suppression. The role of long-ranged triplets are

somewhat unclear. Numerically, short-range energy penalty due to change in \mathbf{M} is greater than the long-ranged triplets, but a comprehensive study is lacking. Likely progress may come from local scanning probe microscopy similar to earlier work carried out to detect triplets using the zero-bias conductance in S/F hybrids (Di Bernardo *et al.*, 2015a). Furthermore, the dependence of the magnitude of T_c modulation is expected to depend both on the strength of the SOC and \mathbf{M} with the former most likely depending on the exact interface structure and is currently not understood.

C. Modification of magnetic anisotropy

A consequence of a SOC-driven modulation of superconductivity is the potential for a reciprocal effect i.e., a reorientation of \mathbf{M} due to superconductivity (Johnsen *et al.*, 2019). A reduction in T_c of the superconductor for an in-plane \mathbf{M} translates to a reduction in the condensation energy due to a suppression of the superconducting gap. The free energy of the superconducting state will thus favour an out-of-plane \mathbf{M} . \mathbf{M} -angle-dependence of free energy means that for a sufficiently low-anisotropy barrier in the F layer, T_c can trigger an in-plane to out-of-plane \mathbf{M} reorientation. This is modeled as a S/HM/F structure. Using the tight-binding Bogoliubov-de Gennes method on a lattice (see Section 3), the system is described by the Hamiltonian

$$\begin{aligned}
H = & -t \sum_{\langle i,j \rangle, \sigma} c_{i,\sigma}^\dagger c_{j,\sigma} - \sum_{i,\sigma} \mu_i c_{i,\sigma}^\dagger c_{i,\sigma} - \sum_i U_i n_{i,\uparrow} n_{i,\downarrow} \\
& - \frac{i}{2} \sum_{\langle i,j \rangle, \alpha, \beta} \lambda_i c_{i,\alpha}^\dagger \hat{n} \cdot (\boldsymbol{\sigma} \times \mathbf{d}_{i,j})_{\alpha,\beta} c_{j,\beta} \\
& + \sum_{i,\alpha,\beta} c_{i,\alpha}^\dagger (\mathbf{h}_i \cdot \boldsymbol{\sigma})_{\alpha,\beta} c_{i,\beta}
\end{aligned} \quad (37)$$

Here, t is the hopping integral, μ_i is the chemical potential at lattice site i , $U < 0$ is the attractive on-site interaction which gives rise to superconductivity, λ_i is the Rashba SOC magnitude at site i , \hat{n} is a unit vector normal to the interface, $\boldsymbol{\sigma}$ is the vector of Pauli matrices, $\mathbf{d}_{i,j}$ is the vector from site i to site j , and \mathbf{h}_i is the local magnetic exchange field. $c_{i,\sigma}^\dagger$ and $c_{i,\sigma}$ are the second quantization electron creation and annihilation operators at site i with spin σ , and $n_i \equiv c_{i,\sigma}^\dagger c_{i,\sigma}$. The superconducting term in the Hamiltonian is treated by a mean field approach, where $c_{i,\uparrow} c_{i,\downarrow} = \langle c_{i,\uparrow} c_{i,\downarrow} \rangle + \delta$ and $c_{i,\uparrow}^\dagger c_{i,\downarrow}^\dagger = \langle c_{i,\uparrow}^\dagger c_{i,\downarrow}^\dagger \rangle + \delta^\dagger$ is inserted into Eq. (37) and neglect terms of second order in the fluctuations δ and δ^\dagger . $\Delta_i \equiv U_i \langle c_{i,\uparrow} c_{i,\downarrow} \rangle$ is the superconducting order parameter which is solved self-consistently. In presence of a strong shape anisotropy favouring an in-plane orientation, this model predicts a $\pi/4$ rotation in the plane of the film below the superconducting transition.

These predictions were recently realised in magnetic tunnel junctions containing epitaxial V(40)/MgO(2)/Fe(10)/MgO(2)/Fe(10)/Co(20) (González-Ruano *et al.*, 2021) grown using molecular beam epitaxy. The

number in parentheses denotes the thicknesses of individual layers in nanometres. The Rashba SOC arises from the MgO/Fe interface which is also responsible for a well-defined perpendicular magnetic anisotropy (PMA) in addition to the required cubic symmetry of Fe(001). The top Fe/Co bilayer acted as an analyser to detect superconductivity-driven orientational changes of the Fe(001) layer through tunnel magneto-resistance. Below the transition temperature of the V layer, the Fe layer showed a pronounced reduction in the field required to orient the OOP \mathbf{M} or for larger junctions a spontaneous reorientation in the OOP direction at zero field. Interestingly, an electric field effect was also reported in the superconducting state where the OOP switching fields dependent on the strength and direction of the applied field. This field-dependent behaviour arises from an electric field-induced modification of the Rashba SOC. A similar effect, albeit IP rotation of the Fe(001) layer magnetic moment, was also observed in this system (González-Ruano *et al.*, 2020) as predicted by the theoretical model described above. We note here that although the free energy considerations are somewhat similar, this is fundamentally different from the superconducting exchange coupling observed in GdN/Nb/GdN trilayers (Zhu *et al.*, 2017) and originally predicted by de Gennes (de Gennes, 1966). This SOC-induced modification of magnetic anisotropy establish superconductors as active and tunable components in the design of cryogenic magnetic memories.

D. Interfacial magnetoanisotropy

Tunneling magnetoresistance (TMR) (Tsymbal and Žutić, 2019) is an important effect in spintronics where the tunneling probability, and thus the resistance, of a thin film heterostructure consisting of F/I/F trilayers (I is an insulator separating the two ferromagnetic leads), depends on the orientation of the two ferromagnets. Due to the higher tunneling probability, the resistance in the parallel state is higher than the resistance in the antiparallel state. In a normal metal/F bilayer, a similar effect can be achieved if there is significant interfacial SOC, in which case the resistance depends on the \mathbf{M} orientation—an effect called the tunneling anisotropic magnetoresistance (TAMR) (Gould *et al.*, 2004; Moser *et al.*, 2007), recall section II.A. Such a TAMR device has a clear advantage over TMR equivalents as it requires only a single ferromagnet thereby reducing the number of interfaces and potential alignment problems due to magnetostatic coupling between the two F layers in devices. When the normal metal is replaced with a superconductor, Andreev reflection provides an additional source of magnetoanisotropy through a process known as magnetoanisotropic Andreev reflection (MAAR) (Högl *et al.*, 2015). The transport properties of such a bilayer has been explored in (Veziñ *et al.*, 2020) using the BTK formalism outlined in section II.D.4, within which the interfacial SOC may be included as a boundary potential. With the F/S interface

located at a position $z = 0$, the Hamiltonian is

$$H = \frac{\hbar^2 \mathbf{k}^2}{2m} - \boldsymbol{\mu} + \mathbf{h} \cdot \boldsymbol{\sigma} \theta(z) + V_B(z), \quad (38)$$

where \mathbf{h} is the exchange field of the ferromagnet, $\boldsymbol{\sigma}$ is a vector of Pauli matrices and $\theta(z)$ is the Heaviside step function. The boundary potential is assumed to contain a spin-independent contribution, V_0 , as well as Rashba SOC,

$$V_B(z) = [V_0 d + \alpha(k_x \sigma_y - k_y \sigma_x)] \delta(z), \quad (39)$$

with d the barrier thickness. It is convenient to introduce the dimensionless quantities: spin polarization $P = |\mathbf{h}|/(2\mu_F)$, barrier strength $Z = V_0 d \sqrt{m}/(\hbar^2 \sqrt{k_F q_F})$, and Rashba SOC strength $\lambda = 2\alpha \sqrt{m}/\hbar^2$, where μ_F is the chemical potential in the F region, m the effective mass, while k_F (q_F) is the magnitude of the (spin-averaged) wave vector in the F (S) region.

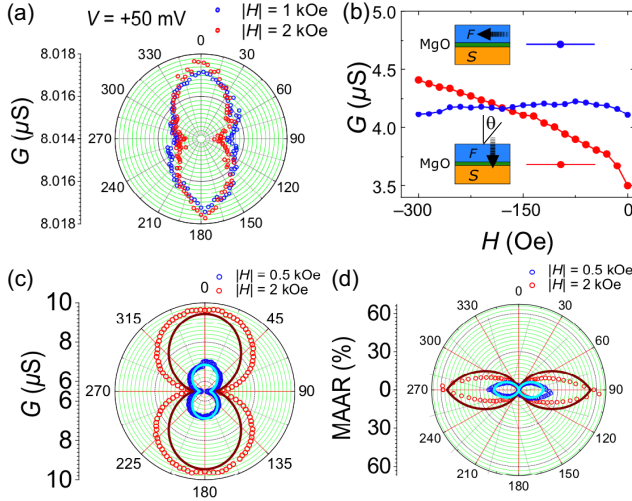


FIG. 7 (a) Angular dependence of conductance, $G(V)$, for an out-of-plane rotation of \mathbf{M} in Fe/MgO/V junction at bias $V = +50$ mV and magnetic fields $H = 1, 2$ kOe, yields a negligible TAMR $\sim 0.01, 0.02\%$, respectively. (b) Evolution of $G(0)$, with in-plane and out-of-plane H . The two remanent perpendicularly oriented \mathbf{M} (black arrows) with different $G(0)$ reveal MAAR $\sim 17\%$ at $H = 0$. (c) Out-of-plane $G(0)$ at $H = 0.5, 2$ kOe (blue, red dots) compared with a phenomenological model (lines). (d) The same approach for out-of-plane MAAR. All results are for $T = 0.3$ K. From Martínez *et al.*, 2020.

This model showed that even a small P and λ resulted in a remarkable increase in the zero-bias conductance, due to spin-flip Andreev reflection (Vezin *et al.*, 2020). For a moderate value of $P = 40\%$ the MAAR is 10 times greater than the TAMR in the normal state while for spin polarizations approaching that of a half metal ($P \gtrsim 80\%$), MAAR could be even 100 times more than TAMR. In the fully half-metallic limit, the MAAR depends universally on spin-orbit fields only (Högl *et al.*, 2015).

Experimentally, the existence of a large out-of-plane MAAR has been recently demonstrated in all-epitaxial Fe/MgO/V junctions (Martínez *et al.*, 2020). By defining an

angle θ , measured between \mathbf{M} and the interface normal of the junction, both an out-of-plane TAMR and MAAR can be expressed from the magnetoanisotropy of the conductance, G ,

$$\text{TAMR(MAAR)} = \frac{G(0^\circ) - G(\theta)}{G(\theta)}. \quad (40)$$

In the same Fe/MgO/V junction, the conductance anisotropy and TAMR can be measured by rotating \mathbf{M} , either by raising the temperature above the superconducting transition of V or applying the bias, to exceed Δ for V, as shown in Fig. 7(a). While with a modest SOC in Fe/MgO/V junction there is only a negligible TAMR of $\sim 0.01\%$ at applied field $|H| = 1$ kOe, at the same temperature of $T = 0.3$ K, a measured zero-bias conductance anisotropy in Figs. 7(b)-(d) reveals that MAAR is enhanced by several orders of magnitude. By carefully designing the magnetic anisotropies, two remanent states with perpendicular \mathbf{M} in Fe/MgO/V junctions (Martínez *et al.*, 2020) were obtained. The observed giant increase of MAAR $\sim 17\%$ at $H = 0$ thus excludes any role of an applied magnetic field in enhanced MAAR.

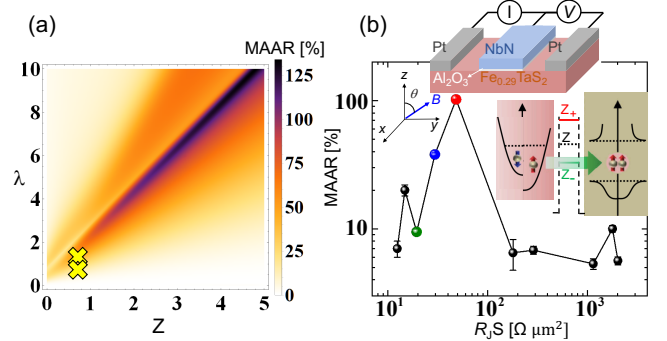


FIG. 8 (a) Out-of-plane MAAR amplitude at zero bias as function of normalized strengths of the interfacial barrier, Z , and the Rashba SOC, λ , for spin polarization $P = 0.7$. Crosses mark the parameters modeling Fe/MgO/V junctions (Martínez *et al.*, 2020). From Vezin *et al.*, 2020. (b) Nonmonotonic dependence of the out-of-plane MAAR amplitude of the quasi-2D van der Waals $\text{Fe}_{0.29}\text{TaS}_2/\text{Al}_2\text{O}_3/\text{NbN}$ junctions (upper inset) on the interface resistance area product, $R_J S$, near zero-bias, where $R_J = V/I$. SOC-modified barrier (lower inset). From Cai *et al.*, 2021.

A closer analysis of the MAAR reveals that its large amplitude can be connected to the the proximity-induced equal-spin-triplet superconductivity (Vezin *et al.*, 2020). The conductance from the spin-flip Andreev reflection dominates the same triangular region, shown in Fig. 8(a) to have an enhanced MAAR (Vezin *et al.*, 2020). The nonmonotonic behavior of the spin-flip Andreev reflection can be understood from the effective barrier strength (Vezin *et al.*, 2020),

$$Z_{\text{eff}}^+ = Z + \frac{\lambda k_{\parallel}}{2\sqrt{k_F q_F}}, \quad Z_{\text{eff}}^- = Z - \frac{\lambda k_{\parallel}}{2\sqrt{k_F q_F}}, \quad (41)$$

where Z_{eff}^+ (Z_{eff}^-) is for inner (outer) Rashba bands [see Fig. 1]. When $Z \geq 0$ and $\lambda \geq 0$, $Z_{\text{eff}}^+ \geq Z$ cannot be suppressed. However, at $k_{\parallel} = (2Z/\lambda)\sqrt{k_F q_F}$, Z_{eff}^- becomes completely

transparent and gives a dramatically increased conductance. The maximum of the total conductance is achieved when the amount of the open channels, $\propto k_{\parallel}$, is maximized. Therefore, the maximum spin-flip Andreev reflection is located near $q_F = (2Z/\lambda)\sqrt{k_F q_F}$, i.e., $\lambda = 2Z$ when $k_F = q_F$.

Unlike common expectations that a strong SOC is desirable for equal-spin-triplet superconductivity, this analysis reveals a more complex picture in which a desirable SOC strength nonmonotonically depends on the interfacial barrier. This trend is confirmed in Fig. 8(b) for F/S junctions with quasi-2D van der Waals (vdW) ferromagnets where, together with a large MAAR, such a measurement is a support for the equal-spin-triplet superconductivity (Cai *et al.*, 2021). Conversely, while a weak interfacial barrier that enables a robust proximity-induced superconductivity seems suitable to enhance the spin-triplet superconductivity, the most enhanced spin-triplet contribution is obtained for the interfacial barrier that nonmonotonically depends the SOC strength. A large conductance anisotropy is also found in all-vdW F/S tunnel junctions (Kang *et al.*, 2021; Lv *et al.*, 2018).

Combined interfacial Rashba and Dresselhaus SOC coupling has also been investigated in Costa and Fabian, 2020; Costa *et al.*, 2019; and Högl *et al.*, 2015, in which case the boundary potential takes the form,

$$V_B(z) = [V_0 d + \mathbf{h} \cdot \boldsymbol{\sigma} + \alpha (k_x \sigma_y - k_y \sigma_x) - \beta (k_x \sigma_x + k_y \sigma_y)] \delta(z). \quad (42)$$

Since the tunneling barrier depends on spin and momentum, it was found that so-called skewed Andreev processes, where the reflection amplitude is asymmetric in momentum space, resulted in a large anomalous Hall effect.

Another interesting manifestation of spin-anisotropy due to SOC has been predicted to occur at the interface of a ballistic S/HM bilayer when the symmetry breaking axis \mathbf{n} of the spin-orbit field is rotated (Johnsen *et al.*, 2020). Such an effect may be achieved by combining bulk and interfacial SOC. Depending of the direction of \mathbf{n} a significant modulation of the critical temperature was found. This effect is explained by the anisotropic conversion of the conventional s -wave even frequency superconducting correlations into other pair correlations of different symmetries.

E. Josephson junctions

JJs with weak links featuring SOC have been studied for decades in the form of supercurrents through 2DEGs (Mayer *et al.*, 2020; Takayanagi and Kawakami, 1985). However, only more recently has the role of SOC with regard to the spin degree of freedom in the Cooper pairs carrying the supercurrent been explored more carefully. Recent developments for JJs involving spin-orbit coupled layers typically also include magnetic elements for purposes such as (i) inducing Majorana modes and related topological phenomena, (ii) creating long-ranged triplet supercurrents carrying both charge and spin,

or (iii) creating phase-batteries where the ground-state phase-difference in the JJ is arbitrary (not restricted to 0 or π). MZM and topological phenomena in JJs was covered in the beginning of this section, so we focus here on point (ii) and (iii).

Long-ranged triplet supercurrents. Whereas magnetically inhomogeneous structures are known to support long-ranged spin-polarized supercurrents in diffusive systems, despite the pair-breaking effect of an exchange field, SOC can accomplish this even in homogeneous ferromagnets. This can be understood by considering an inhomogeneous \mathbf{M} along the x -direction, such as a domain wall, written as

$$\mathbf{h} = h \sin(Qx) \hat{\mathbf{y}} + h \cos(Qx) \hat{\mathbf{z}}, \quad (43)$$

where Q is the wavevector describing the \mathbf{M} rotation (Bergeret and Tokatly, 2014). By performing a unitary transformation U on the Green function describing such a system, corresponding to a local SU(2) rotation $U(x) = e^{-\frac{i}{2} Qx \sigma_x}$, one finds that the resulting equation of motion for the transformed Green function describes a system with homogeneous \mathbf{M} $\mathbf{h} = h \hat{\mathbf{z}}$, but now with an effective SOC which enters the effective gradient operator $\tilde{\nabla}$ like an SU(2) gauge field:

$$\tilde{\nabla} = \nabla + \frac{iQ}{2} [\sigma^x, \cdot] \hat{\mathbf{x}}. \quad (44)$$

Details are given in Bergeret and Tokatly, 2014. The result of this transformation is that the singlet-triplet conversion in a S/inhomogeneous F structure is equivalent to the singlet-triplet conversion in a S/homogeneous F structure with SOC. This explains why spin-orbit interactions, described by an SU(2) gauge field can produce long-ranged triplet correlations inside a ferromagnetic material. The equivalence between an inhomogeneous \mathbf{M} and the combination of a homogeneous exchange field and SOC has an interesting application, as was recently theoretically predicted. Considering a ferromagnetic nanowire, with an easy-axis anisotropy, proximitized to superconducting leads, and neglecting all forms of intrinsic SOC, one would expect only singlet and short-ranged triplet correlations to be present. Nevertheless, it is still possible to produce long-ranged triplet correlations by bending the nanowire. If the resulting curvature is not so large that the exchange interaction of \mathbf{M} overcomes the anisotropy, it is reasonable to expect that \mathbf{M} follows the bend of the wire, thereby producing a rotation of \mathbf{M} . As a result, an artificial, effective SOC appears by the mechanism of Eqs. (43) and (44). This can therefore give rise to long-ranged triplet supercurrents, and may even induce 0 to π transitions in JJs (Salamone *et al.*, 2021).

Historically, the first experiments to detect long-ranged triplet were carried out in JJs with disordered magnetic interface (Keizer *et al.*, 2006) or spin-mixer layers (Khair *et al.*, 2010; Robinson *et al.*, 2010). These spin-mixer layers generated the triplets which was subsequently passed through a thick F (e.g. Co) to filter out the singlets. In fact, the characteristic algebraic decay of the Josephson critical current as a function of the thickness of the ferromagnetic layer was used as an indirect evidence of the presence of triplets in contrast

to the exponential decay of the singlet correlations without the spin-mixer layers. However, a key limitation was the use of these spin-mixer layers itself which added to the complexity of the structure and reduced the efficiency of triplet generation. Therefore, the proposal to create triplets in JJs with SOC weak links is attractive as it removes the requirement of complex spin-mixer layers.

So far, direct experimental evidence in this direction in thin-film hybrids have been inconclusive. Initial attempts (Satchell and Birge, 2018) with Nb/Pt/F/Pt/Nb, where F is a synthetic antiferromagnet composed of Co/Ru/Co showed a significant enhancement in the characteristic voltage of the JJs compared to devices without the Pt layer. However, the decay length of the supercurrent as a function of the Co layer thickness was not as expected for long-range triplets. The higher characteristic voltage values was attributed to the improved growth of Co on Pt leading to fewer stacking faults and dislocations. The major limitation, and perhaps the main reason for the failure to observe triplets in this experiment, is the predominant IP magnetic anisotropy of the F layer instead of the canted magnetic anisotropy required to observe the long-range triplets (Jacobsen *et al.*, 2015). Interestingly, overcoming this limitation by replacing the Pt/F/Pt weak link with a [Co/Ni]_n/Co multilayer with a canted magnetic anisotropy, also failed to show evidence of triplet supercurrents. It is not clear whether this discrepancy between theory and experiments is merely due to a poor singlet-to-triplet conversion efficiency in these systems or something more fundamental.

For more stringent observation requirements of triplets in transverse junctions with current flow perpendicular to the plane of the layers, lateral JJs with the current flowing in the plane of the layers are more flexible in terms of satisfying the conditions for SOC-mediated triplet generation. In fact, the original experiment observing supercurrent flow through half-metallic CrO₂ in a lateral JJ can equally be explained (Bergeret and Tokatly, 2014) as arising from the SOC in the contact region instead of surface magnetic inhomogeneity in CrO₂ as previously assumed. This SOC can be attributed to crystallographic or structural inversion asymmetry (Ast *et al.*, 2007; Miron *et al.*, 2010). Interestingly, in the lateral geometry in a disk-shaped JJ containing a Nb/Co bilayer, triplet supercurrents have been detected which are confined to the rim of the disk (Fermin *et al.*, 2022). This confinement was explained to arise as a result of an effective SOC that results from the vortex in Co which forms in the disk-shaped junction.

An additional advantage of the lateral geometry is the possibility to study the dependence of the triplet supercurrent as a function of the \mathbf{M} direction of F as proposed theoretically in Eskilt *et al.*, 2019 and later in Bujnowski *et al.*, 2019. Here, a lateral JJ with SOC is in contact with an underlying F with IP anisotropy (see Fig. 9). The supercurrent was shown to be highly sensitive to the IP \mathbf{M} rotation with the triplet supercurrent reducing by several orders of magnitude with a $\pi/2$ rotation. Not only this dependence is a clear evidence of the presence of triplet supercurrents, but the device also acts as a magnetic transistor for supercurrents which can be experi-

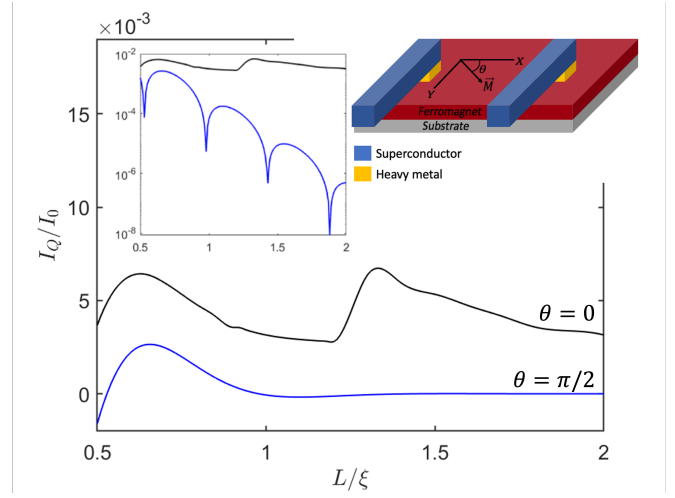


FIG. 9 Normalized supercurrent vs. F barrier length of a planar S/F/S JJ. The black (blue) trace shows the supercurrent density for $\theta = 0$ ($\theta = \pi/2$), where θ is the in-plane angle of \mathbf{M} in F (right inset). The SOC originates from the HM layer. The left inset plots the absolute value of the supercurrent, showing a slow decay in F for $\theta = 0$ and a rapid decay for ($\theta = \pi/2$). The sharp drop of the supercurrent for ($\theta = \pi/2$) indicates a sign reversal of the short-ranged supercurrent. The main panel shows that for a fixed F barrier length, rotating θ induce $0-\pi$ oscillations. Adapted from Eskilt *et al.*, 2019.

mentally studied for a wide range of ferromagnets without the constraint for complex magnetic anisotropies.

An alternative strategy is to focus on entirely different materials such as the 5d transition metal oxide Sr₂IrO₄ with canted antiferromagnetism and high SOC (Petrzhik *et al.*, 2019). Supercurrents observed in Nb/Au/Sr₂IrO₄/YBa₂Cu₃O_x have been attributed to triplet correlations arising from the singlet-triplet conversion mediated by SOC at the Sr₂IrO₄/YBCO interface. Although inconclusive, the results indicate the need to widen the search to materials with intrinsic SOC as in the 5d transition metal oxides.

Before discussing the final aspect of incorporating SOC in JJs, we note that while the normal-state properties of heterostructures typically consider SOC linear in momentum described by models from Eqs. (9) and (10), there is a growing class of materials where the SOC cubic in momentum is not just a small perturbation, but instead provides a dominant contribution (Cottier *et al.*, 2020; Krich and Halperin, 2007; Liu *et al.*, 2018; Nakamura *et al.*, 2012; Winkler *et al.*, 2002). However, the role of such SOC in JJs is largely unexplored (Alidoust *et al.*, 2021). The corresponding Hamiltonian can be written as

$$H_{so} = \frac{i\alpha_c}{2\hbar^3}(p_-^3\sigma_+ - p_+^3\sigma_-) - \frac{\beta_c}{2\hbar^3}(p_-^2p_+\sigma_+ + p_+^2p_-\sigma_-), \quad (45)$$

expressed using cubic strengths α_c and β_c , for Rashba and Dresselhaus terms, where $p_{\pm} = p_x \pm ip_y$, and $\sigma_{\pm} = \sigma_x \pm i\sigma_y$.

A hallmark of JJs with cubic SOC goes beyond current-phase relations (including the anomalous Josephson effect,

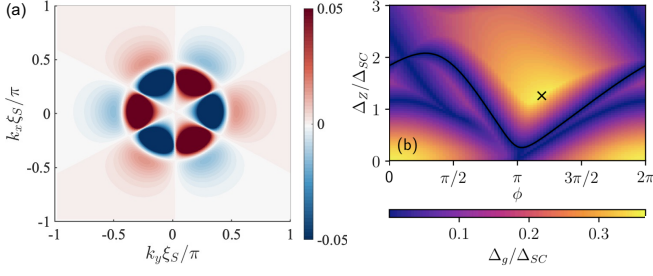


FIG. 10 Signatures of cubic SOC. (a) The real part of equal-spin superconducting correlations in \mathbf{k} -space, $\xi_S = \hbar/\sqrt{2m^*\Delta}$ is the characteristic length, m^* is the effective mass and Δ the superconducting gap. $\alpha_c = 1$ cubic SOC (in the units of ξ_S^3). From Alidoust *et al.*, 2021. (b) Bulk gap, Δ_g , for the N region in the topological phase as a function of the Zeeman energy, Δ_z , and the phase difference, ϕ . Black line: gap closing at $k_x = 0$, black cross: maximum $\Delta_g = 0.37$ (in the units of the superconducting gap $\Delta_{SC} = \mu/3$). From Luethi *et al.*, 2022.

discussed below in the context of phase batteries) and also influences the spin structure and symmetry properties of superconducting proximity effects. Unlike the p -wave symmetry for linear SOC, the f -wave symmetry of superconducting correlations in Fig. 10(a) is the fingerprint for cubic SOC, which supports MZM (Alidoust *et al.*, 2021). Cubic Rashba SOC also provides an effective low-energy description for the heavy holes in Ge-based planar JJs (Luethi *et al.*, 2022), experimentally realized (Tosato *et al.*, 2022). Proximity-induced topological superconductivity, calculated in Fig. 10(b), can host MZM at low applied B_{\parallel} for the phase bias π . Determining the optimal topological gap is complicated by crystalline and magnetic anisotropy and a finite geometry (Paudel *et al.*, 2021; Pekerten *et al.*, 2022).

Phase-batteries. The supercurrent flowing through a JJs depends sensitively on the phase difference ϕ between the superconductors. A finite phase difference usually drives a supercurrent through the system and the ground-state of the system is usually $\phi = 0$ or $\phi = \pi$. But this is not always the case. To see this, it is useful to recall some basic and model-independent properties of JJs, following Golubov *et al.*, 2004.

Firstly, advancing the phase difference ϕ of the superconducting order parameters by $2\pi n$ where n is an integer should correspond to exactly the same physical state. Therefore, a supercurrent $I = I(\phi)$ must be $2\pi n$ -periodic. Moreover, a dc supercurrent flows if a gradient exists in the phase of the superconducting order parameter in the junction. If $I(0) = 0$, it follows that $I(2\pi n) = 0$. Finally, performing a time-reversal operation on the system must reverse any supercurrent present. Since time-reversal includes complex conjugation, the phase changes sign and $\phi \rightarrow -\phi$. Therefore, one usually has $I(\phi) = -I(-\phi)$.

From the above properties, it follows that the supercurrent should vanish whenever $\phi = \pi n$. As a consequence, the ground-state phase difference of a JJ, being the state with no supercurrent, is usually either 0 or π . However, this can change if time-reversal symmetry (TRS) and inversion sym-

metry is broken in the system. In JJs with superconductors breaking TRS, such as $d + id$ superconductors, the relation $I(\phi) = -I(-\phi)$ is not necessarily fulfilled (Liu *et al.*, 2017). Instead, the phase difference ϕ that minimizes the Josephson energy of the system can be neither 0 or π , but a different value denoted ϕ_0 . There is no supercurrent for the ground-state phase difference ϕ_0 , so that $I(\phi_0) = 0$. Instead, spontaneous surface currents flowing in the interface plane exist due to the spontaneously broken TRS (Kolesnichenko and Omelyanchouk, 2004).

JJs where the ground-state phase difference is neither 0 or π , but some arbitrary value ϕ_0 are known as ϕ_0 junctions (Buzdin, 2008). Assuming that the value of ϕ_0 is tunable, a suitable name for such systems is in fact *phase-batteries*. By tuning ϕ_0 via external parameters, such a JJ provides a phase bias to a macroscopic wavefunction (the superconducting order parameter) in a quantum circuit. This is conceptually similar to how a classical battery provides a voltage bias in an electronic circuit. The question is then if controllable ϕ_0 junctions can be tailored by combining materials with the right properties into a JJ. It turns out that this is indeed possible, even when using conventional BCS s -wave superconductors, as we will proceed to explain.

Based on the above example with superconductors that break TRS, one might think that a ϕ_0 junction can be created using conventional superconductors if the weak link separating them TRS instead. An example of such a system is S/F/S JJ, but in such junctions the condition that $I(\phi) = -I(-\phi)$ is satisfied and the ground-state phase difference remains 0 or π .

The key to achieving a phase-battery using conventional superconductors is combining antisymmetric SOC (e.g., linear-in-momentum Rashba coupling) with a spin-splitting Zeeman field in the weak link. This breaks TRS and inversion symmetry which can result in a finite supercurrent even at zero phase difference (Buzdin, 2008; Zazunov *et al.*, 2009). Here "breaking inversion symmetry" is generally applied meaning it points to the fact that some particular operation on the spatial degrees of freedom in the system, such as a mirror, parity, or rotation operation (or combination thereof) does not leave the Hamiltonian of the weak link invariant. The precise mathematical description of which spatial symmetry that needs to be broken in order for the ϕ_0 junction to appear is system-specific, depending *e.g.* on the direction of the spin-splitting field (Liu and Chan, 2010; Rasmussen *et al.*, 2016).

A microscopic explanation of the ϕ_0 -effect in JJs with quantum dots (QDs) was given in Szombati *et al.*, 2016 and Zazunov *et al.*, 2009 as follows. Consider a Cooper pair tunneling from the left to the right superconductor through a two-level, orbital, QD which has Rashba SOC and a suitably oriented Zeeman field. The Hamiltonian of the QD is (Szombati *et al.*, 2016)

$$H_{\text{QD}} = (E_{\text{orb}}\tau_z - \mu\tau_0)\sigma_0 + B\tau_0\sigma_z + \alpha\tau_y\sigma_x, \quad (46)$$

where μ is the chemical potential, E_{orb} is the orbital energy, α parametrizes the SOC strength, B is the Zeeman splitting, while $\tau_{0,x,y,z}$ and $\sigma_{0,x,y,z}$ are the identity and Pauli matrices

acting on orbital and spin space, respectively. Without SOC, $\alpha = 0$ and the two orbitals do not mix. Transfer of electrons in the Cooper pair through the QD then takes place in one level at the time. Consider one electron tunneling via level 1 and the second via level 2: the corresponding tunneling coefficient or matrix element for such a process is $t_L^{(1)} t_R^{(1)} t_L^{(2)} t_R^{(2)}$, where $t_L^{(i)}$ are the hybridization amplitudes between level i in the QD and the left lead and are assumed to be real. Similarly, for $t_R^{(i)}$. Therefore, the matrix element describing tunneling from right to left is exactly the same as left to right when $\phi = 0$, hence no current flows.

When $\alpha \neq 0$, the eigenstates of H_{QD} are a mix of the two orbital states. As shown in Szombati *et al.*, 2016, this results in new single level hybridization amplitudes $T_L^{(1,2)}$ for level 1 and 2 with the left lead (determining the probability for electron transfer between the level and the lead). For spin- \uparrow electrons, one finds

$$\begin{aligned} T_L^{(1)} &= t_L^{(1)} \cos \varepsilon + i \sin \varepsilon t_L^{(2)}, \\ T_L^{(2)} &= t_L^{(2)} \cos \varepsilon - i \sin \varepsilon t_L^{(1)}. \end{aligned} \quad (47)$$

The expressions for $T_R^{(i)}$ are obtained by $L \rightarrow R$. For spin-down electrons, the $+$ and $-$ signs in Eq. (47) are exchanged.

A key observation at this point is to note that the amplitudes $T_{L(R)}^i$ describing tunneling between the leads and the QD levels are now complex. This means that as electrons make their way across the QD, they gain a finite phase. The phase of the resulting matrix element is opposite for electrons tunneling in one direction (say, left to right) compared to the opposite direction (right to left). Since the imaginary part of the the rightward and leftward total tunneling coefficients are then different, leftward and rightward tunneling do not cancel each other exactly for a given spin species σ . If the tunneling probabilities are now also different *in magnitude* for spin \uparrow and \downarrow , which is the case for $B \neq 0$, the Cooper pairs acquire a net phase upon tunneling despite the intrinsic superconducting phase difference being $\phi = 0$.

The ϕ_0 has also been predicted in JJs with metallic interlayers, such as multilayered ferromagnets (Braude and Nazarov, 2007; Grein *et al.*, 2009; Kulagina and Linder, 2014; Liu and Chan, 2010) and through metallic weak links that contain both SOC and ferromagnetic order (Buzdin, 2008). In this case, the physics behind the effect can be understood in terms of Andreev bound states that form in the junction. Such a bound state is comprised of a counterpropagating electrons and holes which transfer Cooper pairs between superconductors via Andreev reflection. These bound states come in pairs $\pm E_i$ where i is an index characterizing internal degrees of freedom such as the spin of the electron and hole that comprise the bound state. Consider first a simple S/F/S JJ. In the limit of weak Zeeman splitting h and assuming a high-transparency junction for simplicity, one finds energies (Annunziata *et al.*, 2011)

$$E_i = E_\sigma = E_0 \cos(\phi/2 + \sigma ch), \quad \sigma = \pm 1, \quad (48)$$

where c is a constant whose exact expression is not important for the present discussion and $E_0 = \Delta$. The current carried by

these Andreev bound states is proportional to $dE_\sigma/d\phi$. Despite that each bound state is phase-shifted by σch , the total current at $\phi = 0$ then vanishes since the magnitude of each current is identical. Thus, a phase-shift in the Andreev bound states is not sufficient for creating a ϕ_0 junction.

The situation changes when considering a JJ with a magnetic trilayer, in effect a S/F₁/F₂/F₃/S junction. When the magnetization \mathbf{M}_i of the ferromagnets is such that the spin-chirality defined as

$$\mathbf{M}_1 \cdot (\mathbf{M}_2 \times \mathbf{M}_3) \quad (49)$$

is non-zero, an anomalous ϕ_0 JJ emerges. For instance, when all \mathbf{M} are perpendicular to each other, the spin-chirality is maximized. The reason for why the spin-chirality needs to be finite is precisely that both time-reversal symmetry and inversion symmetry are now broken in a manner that permits the ϕ_0 -effect (recall that \mathbf{M}_j is a pseudovector). As discussed in Liu and Chan, 2010, the Andreev bound states in the junction may now be written

$$E_i = E_\eta = E_{\eta,0} \cos(\phi + \eta c' h), \quad \eta = \pm 1, \quad (50)$$

where c' is a new constant depending on details of the junction geometry, under the simplifying assumptions that the Zeeman-splitting in each F layer is equal and that the spin-chirality product is maximized. The index η is related to the spin of the Andreev bound state. The crucial difference from the S/F/S case is that the amplitude $E_{\eta,0}$ of the bound state is now unequal for the two bound states $\eta = \pm 1$. Therefore, the total current at $\phi = 0$ does not cancel out and a net anomalous supercurrent exists even at zero superconducting phase difference.

A pictorial argument shows when a ϕ_0 -effect can appear, which is intuitively easier to understand than using matrix symmetry operations applied to the Hamiltonian of the system. Consider first a magnetic JJ with an arbitrary number of magnetic layers. Without SOC, there is no coupling between the spin degree of freedom and orbital motions of the electrons. Therefore, a global spin rotation should leave the supercurrent invariant: if all \mathbf{M} are rotated in the same way, the current stays the same. The goal is now to use this global spin rotation invariance as well as a spatial rotation of the entire JJ (imagine just taking the junction in your hands and turning it) to prove that $I(\phi) = -I(-\phi)$. As explained in Fig. 11, this is possible to accomplish for arbitrary \mathbf{M} directions with both one and two ferromagnets, but not with three (lower row) if the spin-chirality is finite. The pictorial proof shown in the figures can thus be used to prove if the ϕ_0 -effect is absent.

Interestingly, we note that the same type of pictorial proof should be possible to use for non-reciprocal dissipative transport by replacing the superconducting phase differences $\pm\phi/2$ with voltages $\pm V/2$. In this way, using the described set of rotations it is possible to prove that in some junctions $I(V) = -I(-V)$ is satisfied, i.e. there is no non-reciprocal dissipative transport.

We can use the pictorial proof also for a S/F/S junction with SOC to infer which \mathbf{M} directions that do not permit a ϕ_0 -state.

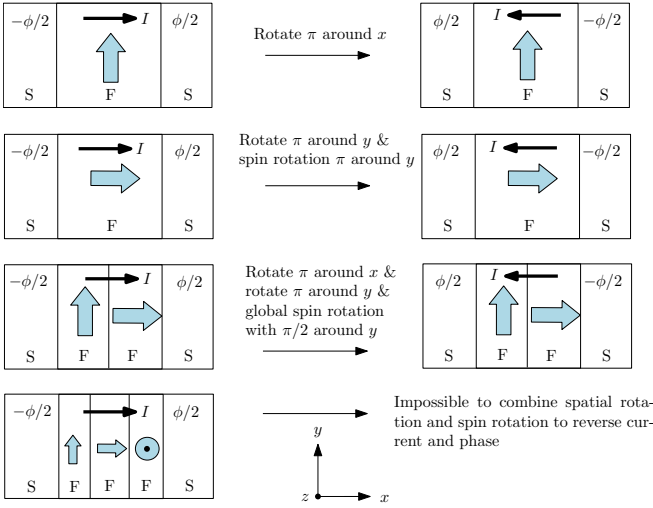


FIG. 11 Illustration of how a combination of spatial rotation of the entire junction and a global spin rotation allows one to prove $I(\phi) = -I(-\phi)$ for magnetic JJs with zero spin-chirality. The blue arrows show the \mathbf{M} in each layer.

We consider a Rashba-type SOC $\propto \alpha \sigma_z k_x$ in a 1D geometry for simplicity since this suffices to show the principle. This is shown in Fig. 12. For instance, the upper row shows that if \mathbf{M} points in the z -direction, physically rotating the entire junction two times brings it back to its original state except for a reversed current and phase. Therefore, one concludes $I(\phi) = -I(-\phi)$: no ϕ_0 -state. When the \mathbf{M} points along the x -direction, a global spin rotation around the y -axis is still permitted without changing the supercurrent. The reason is that performing this spin rotation does not change the SOC-term nor the absolute or relative magnitude of the momentum-dependent total exchange-field of the carriers. Making use of this, combined with a physical rotation of the entire system, one proves again that $I(\phi) = -I(-\phi)$. On the other hand, this is not possible to do when \mathbf{M} points in the y -direction, consistent with the known result in the literature that such a system hosts a ϕ_0 -state. A further manipulation of such ϕ_0 -state is possible with the contribution of Rashba and Dresselhaus SOC (Alidoust, 2020) and experimentally-demonstrated gate-controlled SOC (Dartiailh *et al.*, 2021; Mayer *et al.*, 2020).

Besides the phase-shift obtained due to the broken time-reversal and inversion symmetry in the junction, the magnitude of the critical current also becomes direction-dependent, which we discuss in more detail in the following subsection. Finally, the presence of SOC in magnetic JJs has also been shown to induce interesting phenomena like electrically-controlled \mathbf{M} dynamics (Nashaat *et al.*, 2019).

F. Supercurrent diodes

There has been a resurgence in the interest of the superconducting diode effect, which shares a curious history with

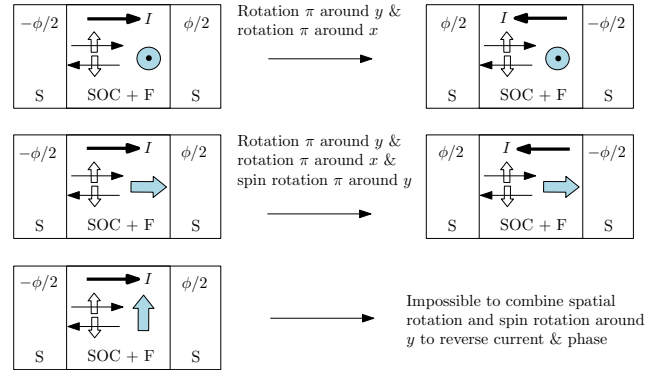


FIG. 12 Illustration of how a combination of spatial rotation of the entire junction and a particular global spin rotation allows one to prove $I(\phi) = -I(-\phi)$ for magnetic JJs with SOC.

the spin Hall effect (Žutić *et al.*, 2004), predicted decades before (D'yakonov and Perel, 1971; D'yakonov and Perel', 1971) the current terminology was established (Hirsch, 1999). The observation of the superconducting diode effect by Ando *et al.*, 2020, where the magnitude of the critical supercurrent was directionally dependent with the magnitude of I_c^+ in the forward direction mismatched to I_c^- in the reverse direction, confirming the prediction from the abstract of Edelstein, 1996. This means that there exists a magnitude range $I_c^- < I < I_c^+$ where the current I is dissipationless in one direction, but resistive in the other. The term ‘‘Josephson diode’’ was also used in 2007 (Hu *et al.*, 2007) with the proposed implementation of the p - and n -doped region resembling conventional semiconductor diodes without SOC, but with a broken inversion symmetry and a rectifying behavior (Shockley, 1949). Many recent experimental realizations of the superconducting diode effect closely follow theory (Reynoso *et al.*, 2008), appearing in JJs with spin splitting and SOC. However, while some measurements show the diode effect (Dartiailh *et al.*, 2021; Mayer *et al.*, 2020) prior to Ando *et al.*, 2020, such an effect was overlooked, focusing on other SOC-related phenomena, including topological superconductivity as a host of MZM. Figures 6(c), (d) show such a supercurrent diode effect, where the normalized critical current asymmetry reaches $\approx 10 - 20\%$ (Dartiailh *et al.*, 2021).

Recent theory (Davydova *et al.*, 2022; He *et al.*, 2022; Scammell *et al.*, 2022; Yuan and Fu, 2022) and experiments (Ando *et al.*, 2020; Baumgartner *et al.*, 2022; Pal *et al.*, 2022) have investigated non-reciprocal critical currents in superconducting wires.

The supercurrent diode effect in a JJ is related to the appearance of an anomalous phase, although they do not go hand-in-hand i.e., it is possible to have a ϕ_0 JJ without any accompanying diode effect. A current-phase relation of $I = I_0 \sin(\phi + \phi_0)$ gives an anomalous phase difference, but no diode effect since the positive and negative critical currents match. Since $\delta \sin(\phi + \phi_0)$ can be written as $\alpha \sin \phi + \beta \cos \phi$ for real coefficients $\alpha, \beta, \delta, \phi_0$, for the diode effect one additionally requires higher-order harmonics in the current-phase relation beyond

$\sin\phi$ and $\cos\phi$, in order to achieve different magnitudes of the positive and negative critical current (Baumgartner *et al.*, 2022). A skewed current-phase relation is therefore a necessary condition for the appearance of this effect.

Several studies have focused on superconducting systems where time-reversal and inversion symmetry breaking are modelled via ferromagnetism/a magnetic field and antisymmetric SOC interactions, such as Rashba SOC. Nonreciprocal supercurrents have also been observed in materials with valley-Zeeman spin-orbit interaction where, unlike the Rashba SOC, the rectification of supercurrent depends on the out-of-plane magnetic field (Bauriedl *et al.*, 2022). Figure 13 shows rectification efficiency of 60% measured in transition metal dichalcogenide NbSe₂ sandwiched between hBN layers which is significantly larger than those observed in Rashba SOC systems. The rectification saturates at low temperature with a maximum observed around $T = T_c/2$, unlike the observations by Ando *et al.*, 2020 where the diode effect was observed near T_c . The unusual temperature dependence together with the rectification appearing with an out-of-plane applied magnetic field indicates a fundamentally different origin of the diode effect in comparison to those observed in Rashba superconductors. One notable exception, which does not require SOC, is Davydova *et al.*, 2022 where it was argued that the diode effect could arise due to Meissner screening in S, causing a finite center-of-mass momentum state in S which removes inversion symmetry. Another interesting case is twisted trilayer graphene a zero magnetic field diode effect was reported (Lin *et al.*, 2021; Scammell *et al.*, 2022).

There are aspects of the supercurrent diode effect which remain poorly understood. For instance, the experimental ob-

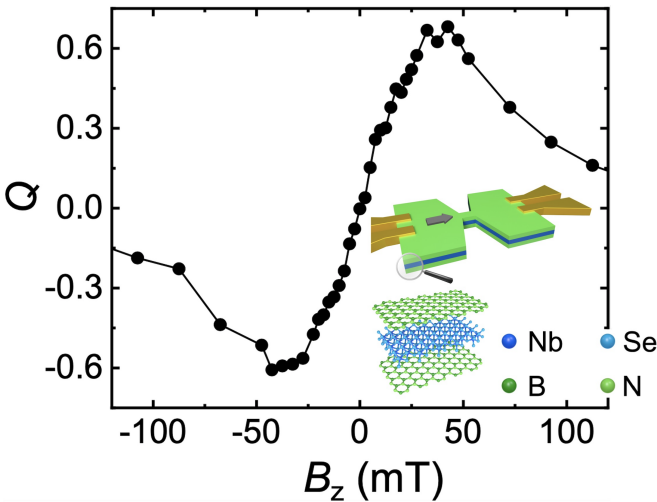


FIG. 13 The supercurrent rectification efficiency, $Q \equiv 2(I_c^+ - |I_c^-|)/(I_c^+ + |I_c^-|)$, as a function of the out-of-plane applied magnetic field measured at 1.3 K. Q is maximum around 35 mT. Inset: the device structure with a 250 nm long and wide central constriction and the z direction is perpendicular to the crystal plane. The hybrid stack consists of 10 nm hBN sandwiching 2, 3 or 5-layer NbSe₂. From Bauriedl *et al.*, 2022.

servation of the diode effect in Ando *et al.*, 2020 only occurred near T_c , vanishing far below T_c . This suggests a different origin of the effect than purely symmetry breaking mechanisms, since those would be in play also for $T \ll T_c$, and instead points to a key role played by fluctuations.

G. Spin-pumping

While significant research has been carried out to understand the generation of triplet pairs using inhomogeneous magnetism or SOC in S/F hybrids, few experiments have focused on triplet transport through a superconductor. Traditional studies of spin transport in superconductors involve quasiparticle injection at voltages above the superconducting gap. These show evidence for spin and charge decoupling (Hübler *et al.*, 2012; Quay *et al.*, 2013) and in some experiments and enhancement of the spin relaxation times (Yang *et al.*, 2010). Previous experiments demonstrated that Andreev reflection essentially excludes transport of dynamically driven spin currents through the superconducting energy gap and so the spin-current-induced broadening of the FMR linewidth is suppressed by the opening of the superconducting gap.

Recent experiments (Jeon *et al.*, 2018) compared FMR results on Nb/Ni₈₀Fe₂₀/Nb trilayers with Pt/Nb/Ni₈₀Fe₂₀/Nb/Pt structures in which the outer layers of Pt are effective spin sinks with strong SOC. The authors investigated the T -dependence of the FMR linewidth ($\mu_0\Delta H$ proportional to α) and the resonance field $\mu_0 H_{\text{res}}$ across T_c . Where Pt (or other large SOC spin sinks) are present, a substantially increased FMR damping for a SC layer thickness of the order the coherence length is interpreted as evidence for superconducting pure spin (triplet) supercurrent pumping. The key mechanism driving the spin current through superconducting Nb involves an interaction of the SOC in Pt with a proximity exchange field from Ni₈₀Fe₂₀, which passes through Nb. Theoretically, this requires Landau Fermi liquid interactions and a non-negligible spin splitting in Pt, creating a triplet channel in the superconducting density of states of Nb around zero energy (Montiel and Eschrig, 2018).

In Jeon *et al.*, 2020, Pt is substituted for a perpendicularly magnetized Pt/Co/Pt spin sink. This experiment enable them to isolate the role of SOC and show that the pure spin supercurrent pumping efficiency across Nb is tunable by controlling the \mathbf{M} angle of Co with respect to the SOC. Furthermore, by inserting a Cu spacer with negligible SOC in-between Nb and the Pt/(Co/Pt) spin sink, they were able to show that Rashba-type SOC is responsible for forming and transmitting the pure spin supercurrent across Nb.

H. Spin-Hall phenomena with superconductors

The spin Hall effect (Sinova *et al.*, 2015) and its inverse are key in spintronics, providing a method to electrically de-

tect spin currents. The spin Hall effect also takes place theoretically in superconducting materials where a longitudinal flow of charge or spin converts to a transverse flow of spin or charge. Experimentally demonstrating a superconducting spin Hall effect would provide a means to electrically detect the polarization of spin supercurrents and potentially control spin in the superconducting state.

To understand this prospect, we start with the magneto-electric phenomena in superconductors which were already studied in 1995 by Edelstein (Edelstein, 1995). Considering a superconductor lacking spatial reflection symmetry, Edelstein predicted that the supercurrent must be accompanied by an induced spin-polarization among the itinerant electrons. Spin Hall effects in superconductors were later considered in Mal'shukov and Chu, 2008, predicting an induced edge spin polarization in a JJ with a spin-orbit coupled layer separating the superconductors. Kontani *et al.*, 2009 considered instead the dissipative spin Hall effect in a superconductor with Rashba SOC, predicting a large negative spin Hall conductivity in the superconducting state. Several works followed, considering the spin Hall effect in different types of JJ geometries, including an AC Josephson bias (Mal'shukov and Chu, 2011; Mal'shukov *et al.*, 2010).

An important experimental breakthrough was published in 2015, when Wakamura *et al.*, 2015 reported observation of a giant quasiparticle-mediated inverse spin Hall effect in the superconductor NbN, which exceeded the effect in the normal state by three orders of magnitude. The signal diminished when the distance between the voltage probes in the setup exceeded the charge imbalance length, indicating that the inverse spin Hall signal was indeed carried by quasiparticles. This quasiparticle-mediated spin Hall effect in the superconducting state was measured by the spin absorption technique using a lateral structure composed of Ni₈₁Fe₁₉ (referred to as Py) and a superconducting NbN wire joined by a nonmagnetic Cu bridge as illustrated in the inset of Fig. 14. The spin current injected via Py diffuses towards the NbN wire and is partly absorbed by it owing to the high SOC in NbN where it is converted to a charge current (quasiparticle current in the superconducting state) via the inverse spin Hall effect.

Theoretical studies followed shortly (Espedal *et al.*, 2017; Huang *et al.*, 2018), utilizing the quasiclassical theory of superconductivity. With this methodology, one derives kinetic equations for the distribution functions for energy, charge, and spin-excited modes in the system, which permits computation of currents. The coefficients in these kinetic equations are determined by the spectral properties of the material and therefore can be very different in the normal and superconducting state. Espedal *et al.*, 2017 computed the various contributions to the spin Hall effect in a conventional superconductor, including side-jump, skew scattering, and anomalous velocity operators. They found that the inverse spin Hall current (i.e. a charge current) j_i^{SH} flowing in the i -direction could be computed from the injected spin-current j_{jk}^s flowing in the j -

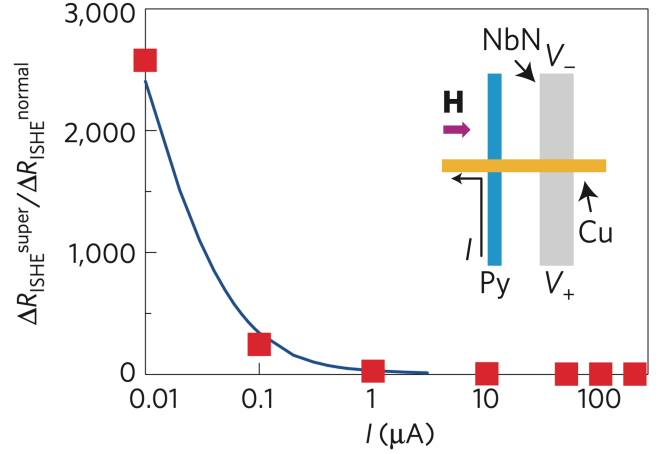


FIG. 14 Inverse spin Hall signal at 3 K, quantified by $\Delta R_{\text{ISHE}}^{\text{super}}$ versus injected spin current I . The signal is normalized by the measured value at 20 K in the normal state $\Delta R_{\text{ISHE}}^{\text{normal}}$. The blue line is the fit to the model as discussed in Wakamura *et al.*, 2015.

direction and polarized along the k -direction according to

$$j_i^{\text{SH}} = \theta^{\text{SH}} \varepsilon_{ijk} j_{jk}^s \quad (51)$$

where ε_{ijk} is the Levi-Civita tensor while θ^{SH} is the spin Hall angle. In the superconducting state, in the diffusive limit, it is

$$\theta^{\text{SH}} = \chi^{\text{SH}} N_S D / D_E. \quad (52)$$

Here, χ^{SH} is the normal-state spin Hall angle whereas D and D_E are renormalized, energy-dependent diffusion coefficients in the superconducting state with a ratio D/D_E which depends only weakly on energy. Instead, the key factor in the expression for θ^{SH} is the superconducting density of states N_S which depends strongly on energy near the gap edge $E \simeq \Delta$. This result predicts a strong enhancement in the spin Hall angle for quasiparticle energies near the gap Δ , consistent with the experimental findings of (Wakamura *et al.*, 2015).

Another interesting aspect regarding spin Hall phenomena in superconductors involves pure supercurrent-transport: conversion of Cooper pair charge currents to Cooper pair spin currents and vice versa. Linder *et al.*, 2017 and Yang *et al.*, 2012 considered this phenomenon in JJs with interfacial SOC and a Zeeman field. Here, it was found that applying a phase gradient between the superconductors produces a transversal spin current at the junction interfaces. The physical origin of this effect stems from the p -wave superconducting correlations induced by the SOC. As was explained in Sec. II.D.1, they can give rise to equilibrium spin currents provided they are not phase shifted by $\pi/2$ with respect to the singlet correlations. In a S/F bilayer, the Zeeman field in F will indeed cause such $\pi/2$ -shifted p -wave triplets to appear, having seemingly no observable consequences. However, in a JJ with a phase gradient, p -wave triplets induced at the interface to one of the superconductors can be non-zero at the other S interface, modifying the singlet-triplet phase-shift, and thereby yielding spin currents.

In typical spin Hall phenomenology, an injected current in a given direction is deflected transversely to the injected current while being polarized in a direction transverse to both the injection and deflection axis. The spin Hall supercurrent considered above behaves similarly, with the polarization of the triplet Cooper pairs carrying the current taking the role of the spin-polarization of the resistive current in the conventional case. The superspin Hall effect was later studied in a finite size structure (Risinggård and Linder, 2019), demonstrating that the induced transverse spin supercurrent flow would produce an edge spin \mathbf{M} , similarly to the conventional resistive spin Hall effect. In this context, it is also worth to mention the prediction of an anomalous supercurrent Hall effect in ferromagnets with a nontrivial spin texture (Yokoyama, 2015). This finding indicated that similar effects could take place in homogeneously magnetized systems with SOC, since conversion processes between singlet and triplet Cooper pairs can be shown to be similar in systems with inhomogeneous \mathbf{M} and systems with homogeneous \mathbf{M} and SOC (Bergeret and Tokatly, 2014). Indeed, (Costa and Fabian, 2020) predicted an anomalous Josephson Hall effect and transverse spin supercurrents in JJs with a macrospin \mathbf{F} and interfacial SOC.

Whereas the above studies considered intrinsic SOC of the Rashba-type, (Bergeret and Tokatly, 2016) predicted that dissipationless magnetoelectric phenomena like spin Hall effects with supercurrents should also occur with extrinsic (impurity) SOC. Considering the diffusive limit of transport, (Bergeret and Tokatly, 2016) predicted a nondissipative spin-galvanic effect, corresponding to generation of a supercurrent by a spin-splitting field, in addition to its inverse – a magnetic moment induced by a supercurrent. Edge \mathbf{M} induced by supercurrents due to interfacial SOC was very recently studied in Linder and Amundsen, 2022 and Silaev *et al.*, 2020. Long-ranged triplets and controllable $0 - \pi$ switching has also been predicted in such systems (Mazanik and Bobkova, 2022).

V. OPEN QUESTIONS AND FUTURE DIRECTIONS

We close the review by discussing some outstanding theoretical and experimental issues.

One of the key advantages to using SOC for generation of polarized triplet Cooper pairs rather than magnetic order, is that the SOC can be tuned electrically *e.g.* via gate voltages in thin-film structures. Local electric control is preferable to using complex magnetic structures due to stray-field effects. However, clear experimental evidence of electric-field controlled triplet Cooper pairs is still missing, such as a tunable critical temperature T_c due to a triplet proximity effect switchable via gate voltage (Ouassou *et al.*, 2016). A preliminary support for the feasibility of such a gate-controlled SOC and the resulting singlet-to-triplet transition is indicated in experiments from Figs. 6(c) and (d).

Another interesting avenue to explore experimentally is the role of SOC in structures where supercurrents can induce magnetization dynamics. In the absence of SOC,

supercurrent-induced magnetization dynamics was proposed two decades ago (Waintal and Brouwer, 2002) and studied from first principles (Wang *et al.*, 2010). The role of SOC, including the spin-orbit and spin-transfer torques generated by spin-triplet supercurrents, was considered more recently (Hals, 2016; Nashaat *et al.*, 2019; Takashima *et al.*, 2017).

Experimentally, the key limitation is that, even without SOC, supercurrent densities are generally too low to compete with the magnetic anisotropy of ferromagnets, but may influence a nanomagnet (Cai and Chudnovsky, 2010).

Magnetization dynamics in superconducting hybrid structures is an example of nonequilibrium phenomena where, in addition to solving the kinetic equations, it is also required to establish suitable boundary conditions describing the interfaces between the different layers of the system. Only very recently (Bobkova *et al.*, 2021) has the time-dependent interplay between SOC and superconducting order in a single layer been successfully modelled, which is a significant achievement. A gate-controlled time-dependent SOC can strongly modify the current-phase relations and drive the JJ dynamics even without any bias current (Monroe *et al.*, 2022). Such time-dependent tunability, supported by the experiments in planar JJs (Dartiailh *et al.*, 2021), has implications for superconducting spintronics, Majorana states, and emerging qubits. Experiments probing the time-dependent interaction between SOC and superconducting order are currently lacking.

Moreover, recent theory has derived suitable boundary conditions (Amundsen and Linder, 2019b; Linder and Amundsen, 2022; Silaev *et al.*, 2020) for interfaces with SOC in superconducting structures. This enables the description of effects such as a superconducting spin Hall effect, magnetization dynamics, and thermoelectric currents in S/F hybrids. Such theory progress opens possibilities for nonequilibrium phenomena in superconducting structures with SOC. Nevertheless, the theory has advanced further than experiments in this area which, on a historical note, is similar to the original development of the proximity effects in S/F systems *e.g.*, the theory for $0-\pi$ junctions (Bulaevskii *et al.*, 1977; Buzdin *et al.*, 1982) predated experimental confirmation by two decades (Kontos *et al.*, 2002; Ryazanov *et al.*, 2001). The experimental observation of the superconducting analogue of spin Hall currents could be high impact, providing the interconversion between dissipationless charge and spin flow.

One of the key outstanding experimental issues is the observation a long-ranged Josephson current without magnetic inhomogeneities (Bergeret and Tokatly, 2013). A few experiments have attempted (Petrzhik *et al.*, 2019; Satchell and Birge, 2018; Satchell *et al.*, 2019) to measure this effect, but no observation has been reported so far. So far, in the context of JJs, we have focused on SOC mediated generation of triplet pairs, but understanding transport of already generated triplet pairs is also in its beginning stages. Two interesting problems to consider are the scattering mechanisms of triplet pairs in a weak link with a strong SOC, and the dynamical coupling of *s*-wave singlet and triplet states. A recent experiment (Ko-

mori *et al.*, 2020) partly addressed this problem by measuring the triplet coherence length in Nb' in Nb/Cr/Fe/Nb'/Fe/Cr/Nb JJs. Here, the thinner Nb' layer has a lower T_c , compared to the Nb leads. A strong suppression of triplet pairs generated at Cr/Fe interfaces were observed both in the normal and superconducting states of this middle Nb' layer. This indicates scattering of triplet pairs in Nb in the normal state due to high intrinsic SOC and blocking of the triplet pairs in the superconducting state of Nb. The competition between triplet pair suppression and singlet-triplet conversion in materials with strong SOC requires further studies.

We have summarized key developments in superconducting spintronics in the presence of SOC and outlined avenues where future developments could lead to a deeper understanding of the interplay between superconductivity, magnetism, and SOC. We envision that such an interplay will stimulate research leading to the discovery of new emergent physical phenomena and devices that are of fundamental interest to superconducting spintronics and quantum technologies.

ACKNOWLEDGMENTS

The authors thank J. A. Ouassou, E. H. Fyhn, S. Jacobsen, L. G. Johnsen, L. A. B. Olde Olthof, F. Aliev, J. Shabani, T. Zhou, W. Han, J. E. Han, A. Matos-Abiague, C. Shen, J. Fabian, R. de Sousa, M. Alidoust, D. Caso, C. Gonzalez-Ruano, V. Risinggård, I. Bobokova, A. Bobkov, and F. Gizotto for useful discussions. J.L. was supported by the Research Council of Norway through Grant No. 323766, and through its Centres of Excellence funding scheme Grant No. 262633 “QuSpin.” J. L. also acknowledges support from the Sigma2 project no. NN9577K. J.W.A.R. acknowledge funding from the EPSRC Programme Grant “Super-spin” (no. EP/N017242/1) and EPSRC International Network Grant “Oxide Superspin” (no. EP/P026311/1). I.Ž. was supported by U.S. DOE, Office of Science BES, Award No. DE-SC0004890, U.S. ONR through Grants No. N000141712793 and MURI No. N000142212764 and U.S. NSF ECCS Grant No. 2130845. N.B. was supported by supported by EPSRC through the New Investigator Grant EP/S016430/1. Nordita is funded in part by NordForsk.

REFERENCES

- Aasen, D., M. Hell, R. V. Mishmash, A. Higginbotham, J. Danon, M. Leijnse, T. S. Jespersen, J. A. Folk, C. M. Marcus, K. Flensberg, and J. Alicea, Milestones toward Majorana-based quantum computing, 2016, *Phys. Rev. X* **6**, 031016.
- Abrikosov, A. A., L. P. Gor'kov, and Dzyaloshinski, 1975, *Methods of Quantum Field Theory in Statistical Physics* (Dover Publications), ISBN 9780486632285.
- Aguado, R., Majorana quasiparticles in condensed matter, 2017, *Riv. Nuovo Cimento* **40**, 523.
- Alicea, J., Majorana fermions in a tunable semiconductor device, 2010, *Phys. Rev. B* **81**, 125318.
- Alicea, J., Y. Oreg, G. Refael, F. Von Oppen, and M. P. Fisher, Non-Abelian statistics and topological quantum information processing in 1D wire networks, 2011, *Nat. Phys.* **7**, 412.
- Alidoust, M., Critical supercurrent and ϕ_0 state for probing a persistent spin helix, 2020, *Phys. Rev. B* **101**, 155123.
- Alidoust, M., and K. Halterman, Long-range spin-triplet correlations and edge spin currents in diffusive spin-orbit coupled SNS hybrids with a single spin-active interface, 2015a, *J. Phys.: Cond. Matt.* **27**, 235301.
- Alidoust, M., and K. Halterman, Spontaneous edge accumulation of spin currents in finite-size two-dimensional diffusive spin-orbit coupled SFS heterostructures, 2015b, *New J. Phys.* **17**, 033001.
- Alidoust, M., C. Shen, and I. Žutić, Cubic spin-orbit coupling and anomalous Josephson effect in planar junctions, 2021, *Phys. Rev. B* **103**, L060503.
- Amundsen, M., and J. Linder, Supercurrent vortex pinball via a triplet Cooper pair inverse Edelstein effect, 2017, *Phys. Rev. B* **96**, 064508.
- Amundsen, M., and J. Linder, Quasiclassical theory for interfaces with spin-orbit coupling, 2019a, *Phys. Rev. B* **100**, 064502.
- Amundsen, M., and J. Linder, Quasiclassical theory for interfaces with spin-orbit coupling, 2019b, *Phys. Rev. B* **100**, 064502.
- Ando, F., Y. Miyasaka, T. Li, J. Ishizuka, T. Arakawa, Y. Shiota, T. Moriyama, Y. Yanase, and T. Ono, Observation of superconducting diode effect, 2020, *Nature* **584**, 373.
- Annunziata, G., H. Enoksen, J. Linder, M. Cuoco, C. Noce, and A. Sudbø, Josephson effect in S/F/S junctions: Spin bandwidth asymmetry versus Stoner exchange, 2011, *Phys. Rev. B* **83**, 144520.
- Aoki, D., F. Hardy, A. Miyake, V. Taufour, T. D. Matsuda, and J. Flouquet, Properties of ferromagnetic superconductors, 2011, *C. R. Physique* **12**, 573.
- Aronov, A. G., Spin injection and polarization of excitations and nuclei in superconductors, 1976, *Zh. Eksp. Teor. Fiz.* **71**, 370, [*Sov. Phys. JETP* **44**, 193-196 (1976)].
- Arute, F., K. Arya, R. Babbush, D. Bacon, J. C. Bardin, R. Barends, R. Biswas, S. Boixo, F. G. Brandao, D. A. Buell, B. Burkett, Y. Chen, *et al.*, Quantum supremacy using a programmable superconducting processor, 2019, *Nature* **574**, 505.
- Ast, C. R., J. Henk, A. Ernst, L. Moreschini, M. C. Falub, D. Pacilé, P. Bruno, K. Kern, and M. Grioni, Giant spin splitting through surface alloying, 2007, *Phys. Rev. Lett.* **98**, 186807.
- Baibich, M. N., J. M. Broto, A. Fert, F. N. Van Dau, F. Petroff, P. Eitenne, G. Creuzet, A. Friederich, and J. Chazelas, Giant magnetoresistance of (001)Fe/(001)Cr magnetic superlattices, 1988, *Phys. Rev. Lett.* **61**, 2472.
- Baladić, I., A. Buzdin, N. Ryzhanova, and A. Vedyayev, Interplay of superconductivity and magnetism in superconductor/ferromagnet structures, 2001, *Phys. Rev. B* **63**, 054518.

- Banerjee, A., O. Lesser, M. A. Rahman, H.-R. Wang, M.-R. Li, A. Kringhøj, A. M. Whiticar, A. C. C. Drachmann, C. Thomas, T. Wang, M. J. Manfra, E. Berg, *et al.*, Signatures of a topological phase transition in a planar Josephson junction, 2022, arXiv:2201.03453.
- Banerjee, N., J. A. Ouassou, Y. Zhu, N. A. Stelmashenko, J. Linder, and M. G. Blamire, Controlling the superconducting transition by spin-orbit coupling, 2018, Phys. Rev. B **97**, 184521.
- Banerjee, N., J. W. A. Robinson, and M. G. Blamire, Reversible control of spin-polarized supercurrents in ferromagnetic Josephson junctions, 2014, Nat. Commun. **5**, 4771.
- Baumgartner, C., L. Fuchs, A. Costa, S. Reinhardt, and et al., Supercurrent rectification and magnetochiral effects in symmetric Josephson junctions, 2022, Nat. Nanotechnol. **17**, 38.
- Bauriedl, L., C. Bäuml, L. Fuchs, C. Baumgartner, N. Paulik, J. M. Bauer, K.-Q. Lin, J. M. Lupton, T. Taniguchi, K. Watanabe, C. Strunk, and N. Paradiso, Supercurrent diode effect and magnetochiral anisotropy in few-layer NbSe₂, 2022, Nat. Commun. **13**, 4266.
- Beenakker, C. W. J., Search for non-Abelian Majorana braiding statistics in superconductors, 2020, SciPost Phys. Lect. Notes **15**, 2.
- Belzig, W., F. K. Wilhelm, C. Bruder, G. Schön, and A. D. Zaikin, Quasiclassical Green's function approach to mesoscopic superconductivity, 1999, Superlattices Microstruct. **25**, 1251.
- Benalcazar, W. A., B. A. Bernevig, and T. L. Hughes, Quantized electric multipole insulators, 2017, Science **357**, 61.
- Berezinskii, V. L., New model of the anisotropic phase of superfluid He₃, 1964, JETP Lett. **20**, 628.
- Bergeret, F. S., and I. V. Tokatly, Singlet-triplet conversion and the long-range proximity effect in superconductor-ferromagnet structures with generic spin dependent fields, 2013, Phys. Rev. Lett. **110**, 117003.
- Bergeret, F. S., and I. V. Tokatly, Spin-orbit coupling as a source of long-range triplet proximity effect in superconductor-ferromagnet hybrid structures, 2014, Phys. Rev. B **89**, 134517.
- Bergeret, F. S., and I. V. Tokatly, Manifestation of extrinsic spin Hall effect in superconducting structures: Nondissipative magnetoelectric effects, 2016, Phys. Rev. B **94**, 180502.
- Bergeret, F. S., A. F. Volkov, and K. B. Efetov, Odd triplet superconductivity and related phenomena in superconductor-ferromagnet structures, 2005, Rev. Mod. Phys. **77**, 1321.
- Bhatti, S., R. Sbiaa, A. Hirohata, H. Ohno, S. Fukami, and S. N. Piramanayagam, Spintronics based random access memory: a review, 2017, Mater. Today **20**, 530.
- Binasch, G., P. Grünberg, F. Saurenbach, and W. Zinn, Enhanced magnetoresistance in layered magnetic structures with antiferromagnetic interlayer exchange, 1989, Phys. Rev. B **39**, 4828.
- Birge, N. O., and M. Houzet, Spin-singlet and spin-triplet Josephson junctions for cryogenic memory, 2019, IEEE Magn. Lett. **9**, 4509605.
- Blamire, M. G., A. Aziz, and J. W. A. Robinson, Nanopillar junctions, 2011, Philos. Trans. R. Soc. A **369**, 3198.
- Blonder, G. E., M. Tinkham, and T. M. Klapwijk, Transition from metallic to tunneling regimes in superconducting microconstrictions: Excess current, charge imbalance, and supercurrent conversion, 1982, Phys. Rev. B **25**, 4515.
- Bobkova, I. V., and A. M. Bobkov, Quasiclassical theory of magnetoelectric effects in superconducting heterostructures in the presence of spin-orbit coupling, 2017, Phys. Rev. B **95**, 184518.
- Bobkova, I. V., A. M. Bobkov, and M. A. Silaev, Dynamic spin-triplet order induced by alternating electric fields in superconductor-ferromagnet-superconductor Josephson junctions, 2021, Phys. Rev. Lett. **127**, 147701.
- Boden, K. M., W. P. Pratt, and N. O. Birge, Proximity-induced density-of-states oscillations in a superconductor/strong-ferromagnet system, 2011, Phys. Rev. B **84**, 020510.
- Boutin, S., J. C. Lemyre, and I. Garate, Majorana bound state engineering via efficient real-space parameter optimization, 2018, Phys. Rev. B **98**, 214512.
- Braude, V., and Y. V. Nazarov, Fully developed triplet proximity effect, 2007, Phys. Rev. Lett. **98**, 077003.
- Brouwer, P. W., M. Duckheim, A. Romito, and F. von Oppen, Topological superconducting phases in disordered quantum wires with strong spin-orbit coupling, 2011, Phys. Rev. B **84**, 144526.
- Bujnowski, B., R. Biele, and F. S. Bergeret, Switchable Josephson current in junctions with spin-orbit coupling, 2019, Phys. Rev. B **100**, 224518.
- Bulaevskii, L. N., V. V. Kuzii, and A. A. Sobyenin, Superconducting system with weak coupling to the current in the ground state, 1977, JETP Lett. **25**, 290.
- Buzdin, A., Direct coupling between magnetism and superconducting current in the Josephson ϕ_0 junction, 2008, Phys. Rev. Lett. **101**, 107005.
- Buzdin, A. I., Proximity effects in superconductor-ferromagnet heterostructures, 2005, Rev. Mod. Phys. **77**, 935.
- Buzdin, A. I., L. N. Bulaevskii, and S. V. Panjukov, Critical-current oscillations as a function of the exchange field and thickness of the ferromagnetic metal (F) in an SFS Josephson junction, 1982, JETP Lett. **35**, 178.
- Bychkov E. I., Y. A., and Rashba, Properties of a 2D electron gas with lifted spectral degeneracy, 1984, JETP Lett. **39**.
- Cai, L., and E. M. Chudnovsky, Interaction of a nanomagnet with a weak superconducting link, 2010, Phys. Rev. B **82**, 104429.
- Cai, R., Y. Yao, P. Lv, Y. Ma, W. Xing, B. Li, Y. Ji, H. Zhou, C. Shen, S. Jia, X. C. Xie, I. Žutić, *et al.*, Evidence for anisotropic spin-triplet Andreev reflection at the 2D van der Waals ferromagnet/superconductor interface, 2021, Nat. Commun. **12**, 6725.
- Chandrasekhar, V., 2004, *Proximity Coupled Systems: Quasiclassical Theory of Superconductivity*, volume 2 (Springer-Verlag).
- Chang, C. H., and C. Ortix, Theoretical prediction of a giant anisotropic magnetoresistance in carbon nanoscrolls, 2017, Nano Lett. **17**, 3076.
- Chantis, A. N., K. D. Belashchenko, E. Y. Tsybmal, and M. van Schilfgaarde, Tunneling anisotropic magnetoresistance driven by resonant surface states: First-principles calculations on an Fe(001) surface, 2007, Phys. Rev. Lett. **98**, 046601.
- Chou, P. H., C. H. Chen, S. W. Liu, C. H. Chung, and C. Y. Mou, Geometry-induced topological superconductivity, 2021, Phys. Rev. B **103**, 014508.
- Costa, A., and J. Fabian, Anomalous Josephson Hall effect charge and transverse spin currents in superconductor/ferromagnetic-insulator/superconductor junctions, 2020, Phys. Rev. B **101**, 104508.
- Costa, A., A. Matos-Abiague, and J. Fabian, Skew Andreev reflection in ferromagnet/superconductor junctions, 2019, Phys. Rev. B **100**, 060507.
- Cottier, R. J., B. D. Koehne, J. T. Miracle, D. A. Currie, N. Theodoropoulou, L. Pantelidis, A. Hernandez-Robles, and A. Ponce, Strong spin-orbit interactions in a correlated two-dimensional electron system formed in SrTiO₃(001) films grown epitaxially on p-Si(001), 2020, Phys. Rev. B **102**, 125423.
- Culcer, D., A. C. Keser, Y. Li, and G. Tkachov, Transport in two-dimensional topological materials: recent developments in experiment and theory, 2020, 2D Mater. **7**, 022007.
- Dartiailh, M. C., W. Mayer, J. Yuan, K. S. Wickramasinghe, A. Matos-Abiague, I. Žutić, and J. Shabani, Phase signature of topological transition in Josephson junctions, 2021, Phys. Rev.

- Lett. **126**, 036802, arXiv:1906.01179.
- Das, A., Y. Ronen, Y. Most, Y. Oreg, M. Heiblum, and H. Shtrikman, Zero-bias peaks and splitting in an Al-InAs nanowire topological superconductor as a signature of Majorana fermions, 2012, Nat. Phys. **8**, 887.
- Das, K. S., D. Makarov, P. Gentile, M. Cuoco, B. J. Van Wees, C. Ortix, and I. J. Vera-Marun, Independent geometrical control of spin and charge resistances in curved spintronics, 2019, Nano Lett. **19**, 6839.
- Das Sarma, S., M. Freedman, and C. Nayak, Majorana zero modes and topological quantum computation, 2015, npj Quantum Inf. **1**, 1.
- Davydova, M., S. Prembabu, and L. Fu, Universal Josephson diode effect, 2022, Sci. Adv. **8**, eabo0309.
- de Gennes, P. G., Coupling between ferromagnets through a superconducting layer, 1966, Phys. Lett. **23**, 10.
- de Gennes, P. G., 1999, *Superconductivity of Metals and Alloys* (Perseus Books, Advanced Book Program), 2nd edition.
- de Sousa, R., and S. Das Sarma, Gate control of spin dynamics in III-V semiconductor quantum dots, 2003, Phys. Rev. B **68**, 155330.
- Deng, M. T., C. L. Yu, G. Y. Huang, M. Larsson, P. Caroff, and H. Q. Xu, Anomalous zero-bias conductance peak in a Nb-InSb nanowire-Nb hybrid device, 2012, Nano Lett. **12**, 6414.
- Dery, H., H. Wu, B. Ciftcioglu, M. Huang, Y. Song, R. K. Kawakami, J. Shi, I. Krivorotov, I. Žutić, and L. J. Sham, Nanospintronics based on magnetologic gates, 2012, IEEE Trans. Electron. Dev. **59**, 259.
- Desjardins, M. M., L. C. Contamin, M. R. Delbecq, M. C. Dartiailh, L. E. Bruhat, T. Cubaynes, J. J. Viennot, F. Mallet, S. Rohart, A. Thiaville, A. Cottet, and T. Kontos, Synthetic spin-orbit interaction for Majorana devices, 2019, Nat. Mater. **18**, 1060.
- Deutscher, G., Andreev-Saint-James reflections: A probe of cuprate superconductors, 2005, Rev. Mod. Phys. **77**, 109.
- Di Bernardo, A., S. Diesch, Y. Gu, J. Linder, G. Divitini, C. Ducati, E. Scheer, M. G. Blamire, and J. W. A. Robinson, Signature of magnetic-dependent gapless odd frequency states at superconductor/ferromagnet interfaces, 2015a, Nat. Commun. **6**, 8053.
- Di Bernardo, A., Z. Salman, X. L. Wang, M. Amado, M. Egilmez, M. G. Flokstra, A. Suter, S. L. Lee, J. H. Zhao, T. Prokscha, E. Morenzoni, M. G. Blamire, *et al.*, Intrinsic paramagnetic Meissner effect due to s -wave odd-frequency superconductivity, 2015b, Phys. Rev. X **5**, 041021.
- Dirac, P., The quantum theory of the electron, 1928, Proc. R. Soc. London A **117**, 610.
- Dresselhaus, G., Spin-orbit coupling effects in zinc blende structures, 1955, Phys. Rev. , 580.
- Droghetti, A., I. Rungger, A. Rubio, and I. V. Tokatly, Spin-orbit induced equilibrium spin currents in materials, 2022, Phys. Rev. B **105**, 024409.
- D'yakonov, M. I., and V. I. Perel, Current-induced spin orientation of electrons in semiconductors, 1971, Phys. Lett. A **35**, 459.
- D'yakonov, M. I., and V. I. Perel', Possibility of orienting electron spins with current, 1971, Zh. Eksp. Teor. Fiz. Pisma Red. **13**, 657, [JETP Lett. **13**, 467-469 (1971)].
- Dzyaloshinsky, I., A thermodynamic theory of weak ferromagnetism of antiferromagnetics, 1958, J. Phys. Chem. Solids **4**, 241.
- Edelstein, V. M., Magnetolectric effect in polar superconductors, 1995, Phys. Rev. Lett. **75**, 2004.
- Edelstein, V. M., The Ginzburg–Landau equation for superconductors of polar symmetry, 1996, J. Phys.: Condens. Matter. **8**, 339.
- Edelstein, V. M., Triplet superconductivity and magnetoelectric effect near the s -wave-superconductor–normal-metal interface caused by local breaking of mirror symmetry, 2003, Phys. Rev. B **67**, 020505.
- Eilenberger, G., Transformation of Gorkov's equation for type II superconductors into transport-like equations, 1968, Z. Phys. **214**, 195.
- Elliot, S. R., and M. Franz, Majorana fermions in nuclear, particle, and solid-state physics, 2015, Rev. Mod. Phys. **87**, 137.
- Eschrig, M., Spin-polarized supercurrents for spintronics: A review of current progress, 2015, Rep. Prog. Phys. **78**, 104501.
- Eskilt, J. R., M. Amundsen, N. Banerjee, and J. Linder, Long-ranged triplet supercurrent in a single in-plane ferromagnet with spin-orbit coupled contacts to superconductors, 2019, Phys. Rev. B **100**, 224519.
- Espedal, C., P. Lange, S. Sadjina, A. G. Mal'shukov, and A. Brataas, Spin Hall effect and spin swapping in diffusive superconductors, 2017, Phys. Rev. B **95**, 054509.
- Fabian, J., A. Matos-Abiague, C. Ertler, P. Stano, and I. Žutić, Semiconductor spintronics, 2007, Acta Phys. Slovaca **57**, 565.
- Fatin, G. L., A. Matos-Abiague, B. Scharf, and I. Žutić, Wireless Majorana bound states: From magnetic tunability to braiding, 2016, Phys. Rev. Lett. **117**, 077002.
- Feng, D. C., M. Z. Zheng, Y. Qun, Z. P. Niu, and D. Y. Xing, Origin of the spin-triplet Andreev reflection at ferromagnet/ s -wave superconductor interface, 2008, J. Appl. Phys. **103**, 023921.
- Feofanov, A. K., V. A. Oboznov, V. V. Bol'ginov, J. Lisenfeld, S. Polletto, V. V. Ryazanov, A. N. Rossolenko, M. Khapipov, D. Balashov, A. B. Zorin, P. N. Dmitriev, V. P. Koshelets, *et al.*, Implementation of superconductor/ferromagnet/superconductor π -shifters in superconducting digital and quantum circuits, 2010, Nat. Phys. **6**, 593.
- Fermin, R., v. D. Dyon, M. Hubert, B. Woltjes, M. Silaev, J. Aarts, and K. Lahabi, Superconducting triplet rim currents in a spin-textured ferromagnetic disk, 2022, Nano Lett. **6**, 2209.
- Ferriani, P., K. Von Bergmann, E. Y. Vedmedenko, S. Heinze, M. Bode, M. Heide, G. Bihlmayer, S. Blügel, and R. Wiesendanger, Atomic-scale spin spiral with a unique rotational sense: Mn monolayer on W(001), 2008, Phys. Rev. Lett. **101**, 027201.
- Fittipaldi, R., R. Hartmann, M. T. Mercaldo, S. Komori, A. Bjørlig, W. Kyung, Y. Yasui, T. Miyoshi, L. A. B. Olde Olthof, C. M. Palomares Garcia, V. Granata, I. Keren, *et al.*, Unveiling unconventional magnetism at the surface of Sr₂RuO₄, 2021, Nat. Commun. **12**, 5792.
- Fornieri, A., A. M. Whitarcar, F. Setiawan, E. Portolés, A. C. C. Drachmann, A. Keselman, S. Gronin, C. Thomas, T. Wang, R. Kallaher, G. C. Gardner, E. Berg, *et al.*, Evidence of topological superconductivity in planar Josephson junctions, 2019, Nature **569**, 89.
- Francica, G., M. Cuoco, and P. Gentile, Topological superconducting phases and Josephson effect in curved superconductors with time reversal invariance, 2020, Phys. Rev. B **101**, 094504.
- Francica, G., P. Gentile, and M. Cuoco, Effects of geometry on spin-orbit Kramers states in semiconducting nanorings, 2019, Europhys. Lett. **127**, 30001.
- Fu, L., and C. L. Kane, Superconducting proximity effect and Majorana fermions at the surface of a topological insulator, 2008, Phys. Rev. Lett. **100**, 096407.
- Fulde, P., and R. A. Ferrell, Superconductivity in a strong spin-exchange field, 1964, Phys. Rev. , A550.
- Gentile, P., M. Cuoco, and C. Ortix, Edge states and topological insulating phases generated by curving a nanowire with Rashba spin-orbit coupling, 2015, Phys. Rev. Lett. **115**, 256801.
- Ginzburg, V. L., and L. D. Landau, On the theory of superconductivity, 1950, Zh. Eksp. Teor. Fiz. **20**.
- Gmitra, M., A. Matos-Abiague, C. Draxl, and J. Fabian, Magnetic control of spin-orbit fields: A first-principles study of Fe/GaAs junctions, 2013, Phys. Rev. Lett. **111**, 036603.

- Golubov, A. A., M. Y. Kupriyanov, and E. Il'ichev, The current-phase relation in Josephson junctions, 2004, *Rev. Mod. Phys.* **76**, 411.
- González-Ruano, C., D. Caso, L. G. Johnsen, C. Tiusan, M. Hehn, N. Banerjee, J. Linder, and F. G. Aliev, Superconductivity assisted change of the perpendicular magnetic anisotropy in V/MgO/Fe junctions, 2021, *Sci. Rep.* **11**, 19041.
- González-Ruano, C., L. G. Johnsen, D. Caso, C. Tiusan, M. Hehn, N. Banerjee, J. Linder, and F. G. Aliev, Superconductivity-induced change in magnetic anisotropy in epitaxial ferromagnet-superconductor hybrids with spin-orbit interaction, 2020, *Phys. Rev. B* **102**, 020405.
- Gorini, C., P. Schwab, R. Raimondi, and A. L. Shelankov, Non-abelian gauge fields in the gradient expansion: Generalized Boltzmann and Eilenberger equations, 2010, *Phys. Rev. B* **82**, 195316.
- Gor'kov, L. P., Microscopic derivation of the Ginzburg-Landau equations in the theory of superconductivity, 1959, *Sov. Phys. JETP* **36**, 1364.
- Gor'kov, L. P., and E. I. Rashba, Superconducting 2D system with lifted spin degeneracy: Mixed singlet-triplet state, 2001, *Phys. Rev. Lett.* **87**, 037004.
- Gould, C., C. Rüster, T. Jungwirth, E. Girgis, G. M. Schott, R. Giraud, K. Brunner, G. Schmidt, and L. W. Molenkamp, Tunneling anisotropic magnetoresistance: A spin-valve-like tunnel magnetoresistance using a single magnetic layer, 2004, *Phys. Rev. Lett.* **93**, 117203.
- Grein, R., M. Eschrig, G. Metalidis, and G. Schön, Spin-dependent Cooper pair phase and pure spin supercurrents in strongly polarized ferromagnets, 2009, *Phys. Rev. Lett.* **102**, 227005.
- Griffin, A., and J. Demers, Tunneling in the normal-metal-insulator-superconductor geometry using the Bogoliubov equations of motion, 1971, *Phys. Rev. B* **4**, 2202.
- Gu, J. Y., C.-Y. You, J. S. Jiang, J. Pearson, Y. B. Bazaliy, and S. D. Bader, Magnetization-orientation dependence of the superconducting transition temperature in the ferromagnet-superconductor-ferromagnet system: CuNi/Nb/CuNi, 2002, *Phys. Rev. Lett.* **89**, 267001.
- Güngördü, U., and A. A. Kovalev, Majorana bound states with chiral magnetic textures, 2022, *J. Appl. Phys.* **132**, 041101.
- Güngördü, U., S. Sandhoefner, and A. A. Kovalev, Stabilization and control of Majorana bound states with elongated skyrmions, 2018, *Phys. Rev. B* **97**, 115136.
- Hals, K. M. D., Supercurrent-induced spin-orbit torques, 2016, *Phys. Rev. B* **93**, 115431.
- Halterman, K., and O. T. Valls, Emergence of triplet correlations in superconductor/half-metallic nanojunctions with spin-active interfaces, 2009, *Phys. Rev. B* **80**, 104502.
- Halterman, K., O. T. Valls, and C.-T. Wu, Charge and spin currents in ferromagnetic Josephson junctions, 2015, *Phys. Rev. B* **92**, 174516.
- He, J. J., Y. Tanaka, and N. Nagaosa, A phenomenological theory of superconductor diodes, 2022, *New J. Phys.* **24**, 053014.
- Heinze, S., K. Von Bergmann, M. Menzel, J. Brede, A. Kubetzka, R. Wiesendanger, G. Bihlmayer, and S. Blügel, Spontaneous atomic-scale magnetic skyrmion lattice in two dimensions, 2011, *Nat. Phys.* **7**, 713.
- Hell, M., K. Flensberg, and M. Leijnse, Coupling and braiding Majorana bound states in networks defined in proximate two-dimensional electron gases, 2017a, *Phys. Rev. B* **96**, 035444.
- Hell, M., M. Leijnse, and K. Flensberg, Two-dimensional platform for networks of Majorana bound states, 2017b, *Phys. Rev. Lett.* **118**, 107701.
- Hirohata, A., K. Yamada, Y. Nakatani, L. Prejbeanu, B. Diény, P. Pirro, and B. Hillebrands, Review on spintronics: Principles and device applications, 2020, *J. Magn. Magn. Mater.* **509**, 166711.
- Hirsch, J. E., Spin Hall effect, 1999, *Phys. Rev. Lett.* **83**, 1834.
- Högl, P., A. Matos-Abiague, I. Žutić, and J. Fabian, Magnetoanisotropic Andreev reflection in ferromagnet-superconductor junctions, 2015, *Phys. Rev. Lett.* **115**, 116601.
- Holmes, D. S., A. L. Ripple, and M. A. Manheimer, Energy-efficient superconducting computing - power budgets and requirements, 2013, *IEEE Trans. Appl. Supercond.* **23**, 1701610.
- Hu, J., C. Wu, and X. Dai, Proposed design of a Josephson diode, 2007, *Phys. Rev. Lett.* **99**, 067004.
- Huang, C., I. V. Tokatly, and F. S. Bergeret, Extrinsic spin-charge coupling in diffusive superconducting systems, 2018, *Phys. Rev. B* **98**, 144515.
- Hübler, F., M. J. Wolf, D. Beckmann, and H. v. Löhneysen, Long-range spin-polarized quasiparticle transport in mesoscopic Al superconductors with a Zeeman splitting, 2012, *Phys. Rev. Lett.* **109**, 207001.
- Ikegaya, S., W. B. Rui, D. Manske, and A. P. Schnyder, Tunable Majorana corner modes in noncentrosymmetric superconductors: Tunneling spectroscopy and edge imperfections, 2021, *Phys. Rev. Research* **3**, 023007.
- Ivanov, D. A., Non-Abelian statistics of half-quantum vortices in p -wave superconductors, 2001, *Phys. Rev. Lett.* **86**, 268.
- Jacobsen, S. H., I. Kulagina, and J. Linder, Controlling superconducting spin flow with spin-flip immunity using a single homogeneous ferromagnet, 2016, *Sci. Rep.* **6**, 23926.
- Jacobsen, S. H., J. A. Ouassou, and J. Linder, Critical temperature and tunneling spectroscopy of superconductor-ferromagnet hybrids with intrinsic Rashba-Dresselhaus spin-orbit coupling, 2015, *Phys. Rev. B* **92**, 24510.
- Jeon, K. R., C. Ciccarelli, A. J. Ferguson, H. Kurebayashi, L. F. Cohen, X. Montiel, M. Eschrig, J. W. Robinson, and M. G. Blamire, Enhanced spin pumping into superconductors provides evidence for superconducting pure spin currents, 2018, *Nat. Mater.* **17**, 499.
- Jeon, K.-R., C. Ciccarelli, H. Kurebayashi, L. F. Cohen, S. Komori, J. W. A. Robinson, and M. G. Blamire, Abrikosov vortex nucleation and its detrimental effect on superconducting spin pumping in Pt/Nb/Ni₈₀Fe₂₀/Nb/Pt proximity structures, 2019a, *Phys. Rev. B* **99**, 144503.
- Jeon, K.-R., C. Ciccarelli, H. Kurebayashi, L. F. Cohen, X. Montiel, M. Eschrig, S. Komori, J. W. A. Robinson, and M. G. Blamire, Exchange-field enhancement of superconducting spin pumping, 2019b, *Phys. Rev. B* **99**, 024507.
- Jeon, K.-R., X. Montiel, S. Komori, C. Ciccarelli, J. Haigh, H. Kurebayashi, L. F. Cohen, A. K. Chan, K. D. Stenning, C.-M. Lee, M. Eschrig, M. G. Blamire, *et al.*, Tunable pure spin supercurrents and the demonstration of their gateability in a spin-wave device, 2020, *Phys. Rev. X* **10**, 031020.
- Johnsen, L. G., N. Banerjee, and J. Linder, Magnetization reorientation due to the superconducting transition in heavy-metal heterostructures, 2019, *Phys. Rev. B* **99**, 134516.
- Johnsen, L. G., K. Svalland, and J. Linder, Controlling the superconducting transition by rotation of an inversion symmetry-breaking axis, 2020, *Phys. Rev. Lett.* **125**, 107002.
- Johnson, M., and R. H. Silsbee, Interfacial charge-spin coupling: Injection and detection of spin magnetization in metals, 1985, *Phys. Rev. Lett.* **55**, 1790.
- Jones, N., The information factories, 2018, *Nature* **561**, 163.
- Joynt, R., and L. Taillefer, The superconducting phases of UPt₃, 2002, *Rev. Mod. Phys.* **74**, 235.
- Julliere, M., Tunneling between ferromagnetic films, 1975, *Physics Letters A* **54**, 225.
- Kajiwara, Y., K. Harii, S. Takahashi, J. Ohe, K. Uchida, M. Mizuguchi, H. Umezawa, H. Kawai, K. Ando, K. Takanashi, S. Maekawa, and E. Saitoh, Transmission of electrical signals by

- spin-wave interconversion in a magnetic insulator, 2010, *Nature* **464**, 262.
- Kalcheim, Y., I. Felner, O. Millo, T. Kirzhner, G. Koren, A. Di Bernardo, M. Egilmez, M. G. Blamire, and J. W. A. Robinson, Magnetic field dependence of the proximity-induced triplet superconductivity at ferromagnet/superconductor interfaces, 2014, *Phys. Rev. B* **89**, 180506.
- Kalcheim, Y., O. Millo, A. Di Bernardo, A. Pal, and J. W. A. Robinson, Inverse proximity effect at superconductor-ferromagnet interfaces: Evidence for induced triplet pairing in the superconductor, 2015, *Phys. Rev. B* **92**, 060501.
- Kalcheim, Y., O. Millo, M. Egilmez, J. W. A. Robinson, and M. G. Blamire, Evidence for anisotropic triplet superconductor order parameter in half-metallic ferromagnetic $\text{La}_{0.7}\text{Ca}_{0.3}\text{Mn}_3\text{O}$ proximity coupled to superconducting $\text{Pr}_{1.85}\text{Ce}_{0.15}\text{CuO}_4$, 2012, *Phys. Rev. B* **85**, 104504.
- Kallin, C., Chiral p -wave order in Sr_2RuO_4 , 2012, *Rep. Prog. Phys.* **75**, 42501.
- Kang, K., S. Jiang, H. Berger, K. Watanabe, T. Taniguchi, L. Forró, J. Shan, and K. F. Mak, Giant anisotropic magnetoresistance in Ising superconductor-magnetic insulator tunnel junctions, 2021, arXiv:2101.01327 .
- Kaur, R. P., D. F. Agterberg, and M. Sigrist, Helical vortex phase in the noncentrosymmetric CePt_3Si , 2005, *Phys. Rev. Lett.* **94**, 137002.
- Keizer, R. S., S. T. B. Goennenwein, T. M. Klapwijk, G. Miao, and A. Gupta, A spin triplet supercurrent through the half-metallic ferromagnet CrO_2 , 2006, *Nature* **439**, 825.
- Kent, A. D., and D. C. Worledge, Quantum information processing with superconducting circuits: a review, 2015, *Nat. Nanotechnol.* **10**, 187.
- Khaire, T. S., M. A. Khasawneh, W. P. Pratt, and N. O. Birge, Observation of spin-triplet superconductivity in Co-based Josephson junctions, 2010, *Phys. Rev. Lett.* **104**, 137002.
- Kim, H., A. Palacio-Morales, T. Posske, L. Rózsa, K. Palotás, L. Szunyogh, M. Thorwart, and R. Wiesendanger, Toward tailoring Majorana bound states in artificially constructed magnetic atom chains on elemental superconductors, 2018, *Sci. Adv.* **4**, eaar5251.
- Kim, S. K., S. Tewari, and Y. Tserkovnyak, Control and braiding of Majorana fermions bound to magnetic domain walls, 2015, *Phys. Rev. B* **92**, 020412(R).
- Kitaev, A. Y., Unpaired Majorana fermions in quantum wires, 2001, *Phys.-Usp.* **44**, 131.
- Kitaev, A. Y., Fault-tolerant quantum computation by anyons, 2003, *Ann. Phys.* **303**, 2.
- Kjaergaard, M., F. Nichele, H. J. Suominen, M. P. Nowak, M. Wimmer, A. R. Akhmerov, J. A. Folk, K. Flensberg, J. Shabani, C. J. Palmstrøm, and C. M. Marcus, Quantized conductance doubling and hard gap in a two-dimensional semiconductor-superconductor heterostructure, 2016, *Nat. Commun.* **7**, 1.
- Kjaergaard, M., K. Wölms, and K. Flensberg, Majorana fermions in superconducting nanowires without spin-orbit coupling, 2012, *Phys. Rev. B* **85**, 020503(R).
- Klinovaja, J., P. Stano, and D. Loss, Transition from fractional to Majorana fermions in Rashba nanowires, 2012, *Phys. Rev. Lett.* **109**, 236801.
- Kolesnichenko, Y. A., and A. N. Omelyanchouk, Spontaneous currents in Josephson junctions between unconventional superconductors and d -wave qubits, 2004, *Low. Temp. Phys.* **30**, 535.
- Komori, S., J. Devine-Stoneman, K. Ohnishi, G. Yang, Z. Devizorova, S. Mironov, X. Montiel, L. Olthof, L. F. Cohen, H. Kurebayashi, M. G. Blamire, A. I. Buzdin, *et al.*, Spin-orbit coupling suppression and singlet-state blocking of spin-triplet Cooper pairs, 2020, *Sci. Adv.* **7**, 0128.
- Konschelle, F., I. V. Tokatly, and F. S. Bergeret, Theory of the spin-galvanic effect and the anomalous phase shift ϕ_0 in superconductors and Josephson junctions with intrinsic spin-orbit coupling, 2015, *Phys. Rev. B* **92**, 125443.
- Konschelle, F., I. V. Tokatly, and F. S. Bergeret, Ballistic Josephson junctions in the presence of generic spin dependent fields, 2016, *Phys. Rev. B* **94**, 014515.
- Kontani, H., J. Goryo, and D. S. Hirashima, Intrinsic spin Hall effect in the s -wave superconducting state: Analysis of the Rashba model, 2009, *Phys. Rev. Lett.* **102**, 086602.
- Kontos, T., M. Aprili, J. Lesueur, F. Genêt, B. Stephanidis, and R. Boursier, Josephson junction through a thin ferromagnetic layer: Negative coupling, 2002, *Phys. Rev. Lett.* **89**, 137007.
- Krantz, P., M. Kjaergaard, F. Yan, T. P. Orlando, S. Gustavsson, and W. D. Oliver, A quantum engineer's guide to superconducting qubits, 2019, *Appl. Phys. Rev.* **6**, 021318.
- Krich, J. J., and B. I. Halperin, Cubic Dresselhaus spin-orbit coupling in 2D electron quantum dots, 2007, *Phys. Rev. Lett.* **98**, 226802.
- Kriener, M., K. Segawa, Z. Ren, S. Sasaki, and Y. Ando, Bulk superconducting phase with a full energy gap in the doped topological insulator $\text{Cu}_x\text{Bi}_2\text{Se}_3$, 2011, *Phys. Rev. Lett.* **106**, 127004.
- Kulagina, I., and J. Linder, Spin supercurrent, magnetization dynamics, and ϕ -state in spin-textured Josephson junctions, 2014, *Phys. Rev. B* **90**, 054504.
- Lahtinen, V. T., and J. K. Pachos, A short introduction to topological quantum computation, 2017, *SciPost Phys.* **3**, 021.
- Larkin, Y. N., and A. I. Ovchinnikov, Inhomogeneous state of superconductors, 1965, *Sov. Phys. JETP* **20**, 762.
- Lebrun, R., A. Ross, S. A. Bender, A. Qaiumzadeh, L. Baldrati, J. Cramer, A. Brataas, R. A. Duine, and M. Kläui, Tunable long-distance spin transport in a crystalline antiferromagnetic iron oxide, 2018, *Nature* **561**, 222.
- Leggett, A. J., A theoretical description of the new phases of liquid ^3He , 1975, *Rev. Mod. Phys.* **47**, 331.
- Leksin, P. V., N. N. Garif'yanov, I. A. Garifullin, Y. V. Fominov, J. Schumann, Y. Krupskaya, V. Kataev, O. G. Schmidt, and B. Büchner, Evidence for triplet superconductivity in a superconductor-ferromagnet spin valve, 2012, *Phys. Rev. Lett.* **109**, 057005.
- Lin, J.-X., P. Siriviboon, H. D. Scammell, S. Liu, D. Rhodes, K. Watanabe, T. Taniguchi, J. Hone, M. S. Scheurer, and J. I. A. Li, Zero-field superconducting diode effect in small-twist-angle trilayer graphene, 2021, arXiv:2112.07841 .
- Linder, J., and M. Amundsen, Quasiclassical boundary conditions for spin-orbit coupled interfaces with spin-charge conversion, 2022, *Phys. Rev. B* **105**, 064506.
- Linder, J., M. Amundsen, and V. Risinggård, Intrinsic superspin Hall current, 2017, *Phys. Rev. B* **96**, 094512.
- Linder, J., and A. V. Balatsky, Odd-frequency superconductivity, 2019, *Rev. Mod. Phys.* **91**, 045005.
- Linder, J., and J. W. A. Robinson, Superconducting spintronics, 2015, *Nat. Phys.* **11**, 307.
- Linder, J., T. Yokoyama, and A. Sudbø, Theory of superconducting and magnetic proximity effect in S/F structures with inhomogeneous magnetization textures and spin-active interfaces, 2009, *Phys. Rev. B* **79**, 054523.
- Liu, H., E. Marcellina, A. R. Hamilton, and D. Culcer, Strong spin-orbit contribution to the Hall coefficient of two-dimensional hole systems, 2018, *Phys. Rev. Lett.* **121**, 087701.
- Liu, J.-F., and K. S. Chan, Anomalous Josephson current through a ferromagnetic trilayer junction, 2010, *Phys. Rev. B* **82**, 184533.
- Liu, J.-F., Y. Xu, and J. Wang, Identifying the chiral d -wave superconductivity by Josephson ϕ_0 -states, 2017, *Sci. Rep.* **7**, 43899.

- Luethi, M., K. Laubscher, S. Bosco, D. Loss, and J. Klinovaja, Planar Josephson junctions in germanium: Effect of cubic spin-orbit interaction, 2022, arXiv:2209.12745 .
- Lutchyn, R. M., J. D. Sau, and S. Das Sarma, Majorana fermions and a topological phase transition in semiconductor-superconductor heterostructures, 2010, Phys. Rev. Lett. **105**, 077001.
- Lv, P., Y.-F. Zhou, N.-X. Yang, and Q.-F. Sun, Magnetoanisotropic spin-triplet Andreev reflection in ferromagnet-Ising superconductor junctions, 2018, Phys. Rev. B **97**, 144501.
- Mackenzie, A. P., and Y. Maeno, The superconductivity of Sr_2RuO_4 and the physics of spin-triplet pairing, 2003, Rev. Mod. Phys. **75**, 657.
- Maeno, Y., H. Hashimoto, K. Yoshida, S. Nishizaki, T. Fujita, J. G. Bednorz, and F. Lichtenberg, Superconductivity in a layered perovskite without copper, 1994, Nature **372**, 532.
- Mal'shukov, A. G., and C. S. Chu, Spin Hall effect in a Josephson contact, 2008, Phys. Rev. B **78**, 104503.
- Mal'shukov, A. G., and C. S. Chu, Spin-Hall current and spin polarization in an electrically biased SNS Josephson junction, 2011, Phys. Rev. B **84**, 054520.
- Mal'shukov, A. G., S. Sadjina, and A. Brataas, Inverse spin Hall effect in superconductor/normal-metal/superconductor Josephson junctions, 2010, Phys. Rev. B **81**, 060502.
- Martínez, I., P. Högl, C. González-Ruano, J. P. Cascales, C. Tiusan, Y. Lu, M. Hehn, A. Matos-Abiague, J. Fabian, I. Žutić, and F. G. Aliev, Interfacial spin-orbit coupling: A platform for superconducting spintronics, 2020, Phys. Rev. Applied **13**, 014030.
- Matos-Abiague, A., J. Shabani, A. D. Kent, G. L. Fatin, B. Scharf, and I. Žutić, Tunable magnetic textures: From Majorana bound states to braiding, 2017, Solid State Commun. **262**, 1.
- Mayer, W., M. C. Dartiailh, J. Yuan, K. S. Wickramasinghe, E. Rossi, and J. Shabani, Gate controlled anomalous phase shift in Al/InAs Josephson junctions, 2020, Nat. Commun. **11**, 212.
- Mazanik, A. A., and I. V. Bobkova, Supercurrent-induced long-range triplet correlations and controllable Josephson effect in superconductor/ferromagnet hybrids with extrinsic spin-orbit coupling, 2022, Phys. Rev. B **105**, 144502.
- Mel'Nikov, A. S., A. V. Samokhvalov, S. M. Kuznetsova, and A. I. Buzdin, Interference phenomena and long-range proximity effect in clean superconductor-ferromagnet systems, 2012, Phys. Rev. Lett. **109**, 237006.
- Meservey, R., and P. M. Tedrow, Spin-polarized electron tunneling, 1994, Phys. Rep. **238**, 173.
- Miron, I. M., G. Gaudin, S. Auffret, B. Rodmacq, A. Schuhl, S. Pizzini, J. Vogel, and P. Gambardella, Current-driven spin torque induced by the Rashba effect in a ferromagnetic metal layer, 2010, Nat. Mater. **9**, 230.
- Mironov, S., and A. Buzdin, Spontaneous currents in superconducting systems with strong spin-orbit coupling, 2017, Phys. Rev. Lett. **118**, 077001.
- Miyazaki, T., and N. Tezuka, Giant magnetic tunneling effect in Fe/Al₂O₃/Fe junction, 1995, J. Magn. Magn. Mater. **139**, L231.
- Mohanta, N., T. Zhou, J. Xu, J. E. Han, A. D. Kent, J. Shabani, I. Žutić, and A. Matos-Abiague, Electrical control of Majorana bound states using magnetic stripes, 2019, Phys. Rev. Applied **12**, 034048.
- Monroe, D., M. Alidoust, and I. Žutić, Tunable planar Josephson junctions driven by time-dependent spin-orbit coupling, 2022, Phys. Rev. Applied **18**, L031001.
- Montiel, X., and M. Eschrig, Generation of pure superconducting spin current in magnetic heterostructures via nonlocally induced magnetism due to Landau Fermi liquid effects, 2018, Phys. Rev. B **98**, 104513.
- Moodera, J. S., L. R. Kinder, T. M. Wong, and R. Meservey, Large magnetoresistance at room temperature in ferromagnetic thin film tunnel junctions, 1995, Phys. Rev. Lett. **74**, 3273.
- Moraru, I. C., W. P. Pratt, and N. O. Birge, Observation of standard spin-switch effects in ferromagnet/superconductor/ferromagnet trilayers with a strong ferromagnet, 2006, Phys. Rev. B **74**, 220507.
- Moriya, T., Anisotropic superexchange interaction and weak ferromagnetism, 1960, Phys. Rev. **120**, 91.
- Moser, J., A. Matos-Abiague, D. Schuh, W. Wegscheider, J. Fabian, and D. Weiss, Tunneling anisotropic magnetoresistance and spin-orbit coupling in Fe/GaAs/Au tunnel junctions, 2007, Phys. Rev. Lett. **99**, 056601.
- Mourik, V., K. Zuo, S. M. Frolov, S. R. Plissard, E. P. Bakkers, and L. P. Kouwenhoven, Signatures of Majorana fermions in hybrid superconductor-semiconductor nanowire devices, 2012, Science **336**, 1003.
- Nadj-Perge, S., I. K. Drozdov, J. Li, H. Chen, S. Jeon, J. Seo, A. H. MacDonald, B. A. Bernevig, and A. Yazdani, Observation of Majorana fermions in ferromagnetic atomic chains on a superconductor, 2014, Science **346**, 602.
- Nagasawa, F., D. Frustaglia, H. Saarikoski, K. Richter, and J. Nitta, Control of the spin geometric phase in semiconductor quantum rings, 2013, Nat. Commun. **4**, 1.
- Nakamura, H., T. Koga, and T. Kimura, Experimental evidence of cubic Rashba effect in an inversion-symmetric oxide, 2012, Phys. Rev. Lett. **108**, 206601.
- Nashaat, M., I. V. Bobkova, A. M. Bobkov, Y. M. Shukrinov, I. R. Rahmonov, and K. Sengupta, Electrical control of magnetization in superconductor/ferromagnet/superconductor junctions on a three-dimensional topological insulator, 2019, Phys. Rev. B **100**, 054506.
- Nayak, C., S. H. Simon, A. Stern, M. Freedman, and S. Das Sarma, Non-Abelian anyons and topological quantum computation, 2008, Rev. Mod. Phys. **80**, 1083.
- Ohnishi, K., S. Komori, G. Yang, K.-R. Jeon, L. Olde Olthof, X. Montiel, M. G. Blamire, and J. W. A. Robinson, Spin-transport in superconductors, 2020, Appl. Phys. Lett. **116**, 130501.
- Olde Olthof, L. A., X. Montiel, J. W. A. Robinson, and A. I. Buzdin, Superconducting vortices generated via spin-orbit coupling at superconductor/ferromagnet interfaces, 2019, Phys. Rev. B **100**, 220505.
- Oreg, Y., G. Refael, and F. von Oppen, Helical liquids and Majorana bound states in quantum wires, 2010, Phys. Rev. Lett. **105**, 177002.
- Ouassou, J. A., A. Di Bernardo, J. W. A. Robinson, and J. Linder, Electric control of superconducting transition through a spin-orbit coupled interface, 2016, Sci. Rep. **6**, 29312.
- Pahomi, T. E., M. Sigrist, and A. A. Soluyanov, Braiding Majorana corner modes in a second-order topological superconductor, 2020, Phys. Rev. Research **2**, 032068.
- Pal, B., A. Chakraborty, P. K. Sivakumar, M. Davydova, A. K. Gopi, A. K. Pandeya, J. A. Krieger, Y. Zhang, M. Date, S. Ju, N. Yuan, N. B. M. Schröter, *et al.*, Josephson diode effect from Cooper pair momentum in a topological semimetal, 2022, Nat. Phys. **18**, 1228.
- Park, B. G., J. Wunderlich, D. A. Williams, S. J. Joo, K. Y. Jung, K. H. Shin, K. Olejník, A. B. Shick, and T. Jungwirth, Tunneling anisotropic magnetoresistance in multilayer (Co/Pt)/AlO_x/Pt structures, 2008, Phys. Rev. Lett. **100**, 087204.
- Parkin, S. S. P., C. Kaiser, A. Panchula, P. M. Rice, B. Hughes, M. Samant, and S. Yang, Giant tunneling magnetoresistance at room temperature with MgO (100) tunnel barriers, 2004, Nat. Mater. **3**, 862.

- Paudel, P. P., T. Cole, B. D. Woods, and T. D. Stanescu, Enhanced topological superconductivity in spatially modulated planar Josephson junctions, 2021, *Phys. Rev. B* **104**, 15542.
- Pekerten, B., J. D. Pakizer, B. Hawn, and A. Matos-Abiague, Anisotropic topological superconductivity in Josephson junctions, 2022, *Phys. Rev. B* **105**, 054504.
- Petrashov, V. T., I. A. Sosnin, I. Cox, A. Parsons, and C. Troadec, Giant mutual proximity effects in ferromagnetic/superconducting nanostructures, 1999, *Phys. Rev. Lett.* **83**, 3281.
- Petrzhik, A. M., K. Y. Constantinian, G. A. Ovsyannikov, A. V. Zaitsev, A. V. Shadrin, A. S. Grishin, Y. V. Kisilinski, G. Cristiani, and G. Logvenov, Superconducting current and low-energy states in a mesa-heterostructure interlayered with a strontium iridate film with strong spin-orbit interaction, 2019, *Phys. Rev. B* **100**, 024501.
- Petsch, A. N., M. Zhu, M. Enderle, Z. Q. Mao, Y. Maeno, I. I. Mazin, and S. M. Hayden, Reduction of the spin susceptibility in the superconducting state of Sr_2RuO_4 observed by polarized neutron scattering, 2020, *Phys. Rev. Lett.* **125**, 217004.
- Pientka, F., A. Keselman, E. Berg, A. Yacoby, A. Stern, and B. I. Halperin, Topological superconductivity in a planar Josephson junction, 2017, *Phys. Rev. X* **7**, 021032.
- Quay, C. H. L., D. Chevallier, C. Bena, and M. Aprili, Spin imbalance and spin-charge separation in a mesoscopic superconductor, 2013, *Nat. Phys.* **9**, 84.
- Raimondi, R., P. Schwab, C. Gorini, and G. Vignale, Spin-orbit interaction in a two-dimensional electron gas: A $SU(2)$ formulation, 2012, *Ann. Phys. (Berlin)* **524**, 153.
- Rammer, J., and H. Smith, Quantum field-theoretical methods in transport theory of metals, 1986, *Rev. Mod. Phys.* **58**, 323.
- Rashba, E. I., Spin currents in thermodynamic equilibrium: The challenge of discerning transport currents, 2003, *Phys. Rev. B* **68**, 241315.
- Rasmussen, A., J. Danon, H. Suominen, F. Nichele, M. Kjaergaard, and K. Flensberg, Effects of spin-orbit coupling and spatial symmetries on the Josephson current in SNS junctions, 2016, *Phys. Rev. B* **93**, 155406.
- Read, N., and D. Green, Paired states of fermions in two dimensions with breaking of parity and time-reversal symmetries and the fractional quantum Hall effect, 2000, *Phys. Rev. B* **61**, 10267.
- Reeg, C. R., and D. L. Maslov, Proximity-induced triplet superconductivity in Rashba materials, 2015, *Phys. Rev. B* **92**, 134512.
- Ren, H., F. Pientka, S. Hart, A. T. Pierce, M. Kosowsky, L. Lunczer, R. Schlereth, B. Scharf, E. M. Hankiewicz, L. W. Molenkamp, B. I. Halperin, and A. Yacoby, Topological superconductivity in a phase-controlled Josephson junction, 2019, *Nature* **569**, 93.
- Reynoso, A. A., G. Usaj, C. A. Balseiro, D. Feinberg, and M. Avignon, Anomalous Josephson current in junctions with spin polarizing quantum point contacts, 2008, *Phys. Rev. Lett.* **101**, 107001.
- Risinggård, V., and J. Linder, Direct and inverse superspin Hall effect in two-dimensional systems: Electrical detection of spin supercurrents, 2019, *Phys. Rev. B* **99**, 174505.
- Robinson, J. W. A., F. Chiodi, M. Egilmez, G. B. Halasz, and M. G. Blamire, Supercurrent enhancement in Bloch domain walls, 2012, *Sci. Rep.* **2**, 699.
- Robinson, J. W. A., A. V. Samokhvalov, and A. I. Buzdin, Chirality-controlled spontaneous currents in spin-orbit coupled superconducting rings, 2019, *Phys. Rev. B* **99**, 180501.
- Robinson, J. W. A., J. D. S. Witt, and M. G. Blamire, Controlled injection of spin-triplet supercurrents into a strong ferromagnet, 2010, *Science* **329**, 59.
- Rogers, M., A. Walton, M. G. Flokstra, F. Al Ma'Mari, R. Stewart, S. L. Lee, T. Prokscha, A. J. Caruana, C. J. Kinane, S. Langridge, H. Bradshaw, T. Moorsom, *et al.*, Spin-singlet to triplet Cooper pair converter interface, 2021, *Commun. Phys.* **4**, 69.
- Rokhinson, L. P., X. Liu, and J. K. Furdyna, The fractional a.c. Josephson effect in a semiconductor-superconductor nanowire as a signature of Majorana particles, 2012, *Nat. Phys.* **8**, 795.
- Rosenbach, D., T. W. Schmitt, P. Schüffelgen, M. P. Stehno, C. Li, M. Schleenvoigt, A. R. Jalil, G. Mussler, E. Neumann, S. Trelenkamp, A. A. Golubov, A. Brinkman, *et al.*, Reappearance of first Shapiro step in narrow topological Josephson junctions, 2021, *Sci. Adv.* **7**, eabf1854.
- Rößler, U. K., A. N. Bogdanov, and C. Pfleiderer, Spontaneous skyrmion ground states in magnetic metals, 2006, *Nature* **442**, 797.
- Ryazanov, V. V., V. A. Oboznov, A. Y. Rusanov, A. V. Veretennikov, A. A. Golubov, and J. Aarts, Coupling of two superconductors through a ferromagnet: Evidence for a π junction, 2001, *Phys. Rev. Lett.* **86**, 2427.
- Salamone, T., M. B. Svendsen, M. Amundsen, and S. Jacobsen, Curvature-induced long-range supercurrents in diffusive superconductor-ferromagnet-superconductor Josephson junctions with a dynamic $0-\pi$ transition, 2021, *Phys. Rev. B* **104**, L060505.
- Samokhin, K. V., Magnetic properties of superconductors with strong spin-orbit coupling, 2004, *Phys. Rev. B* **70**, 104521.
- Samokhin, K. V., Spin-orbit coupling and semiclassical electron dynamics in noncentrosymmetric metals, 2009, *Ann. Phys.* **324**, 2385.
- SanGiorgio, P., S. Reymond, M. R. Beasley, J. H. Kwon, and K. Char, Anomalous double peak structure in superconductor/ferromagnet tunneling density of states, 2008, *Phys. Rev. Lett.* **100**, 237002.
- Sasaki, S., M. Kriener, K. Segawa, K. Yada, Y. Tanaka, M. Sato, and Y. Ando, Topological superconductivity in $\text{Cu}_x\text{Bi}_2\text{Se}_3$, 2011, *Phys. Rev. Lett.* **107**, 217001.
- Satchell, N., and N. O. Birge, Supercurrent in ferromagnetic Josephson junctions with heavy metal interlayers, 2018, *Phys. Rev. B* **97**, 214509.
- Satchell, N., R. Loloee, and N. O. Birge, Supercurrent in ferromagnetic Josephson junctions with heavy-metal interlayers. II. Canted magnetization, 2019, *Phys. Rev. B* **99**, 174519.
- Sau, J. D., R. M. Lutchyn, S. Tewari, and S. Das Sarma, Generic new platform for topological quantum computation using semiconductor heterostructures, 2010, *Phys. Rev. Lett.* **104**, 040502.
- Scammell, H. D., J. I. A. Li, and M. S. Scheurer, Theory of zero-field superconducting diode effect in twisted trilayer graphene, 2022, *2D Materials* **9**, 025027.
- Schindler, F., A. M. Cook, M. G. Vergniory, Z. Wang, S. S. Parkin, B. A. Bernevig, and T. Neupert, Higher-order topological insulators, 2018a, *Sci. Adv.* **4**, aa0346.
- Schindler, F., Z. Wang, M. G. Vergniory, A. M. Cook, A. Murani, S. Sengupta, A. Y. Kasumov, R. Deblock, S. Jeon, I. Drozdov, H. Bouchiat, S. Guéron, *et al.*, Higher-order topology in bismuth, 2018b, *Nat. Phys.* **14**, 918.
- Sengupta, K., I. Žutić, H.-J. Kwon, V. M. Yakovenko, and S. Das Sarma, Midgap edge states and pairing symmetry of quasi-one-dimensional organic superconductors, 2001, *Phys. Rev. B* **63**, 144531.
- Serene, J. W., and D. Rainer, The quasiclassical approach to superfluid ^3He , 1983, *Phys. Rep.* **101**, 221.
- Setiawan, F., C.-T. Wu, and K. Levin, Full proximity treatment of topological superconductors in Josephson-junction architectures, 2019, *Phys. Rev. B* **99**, 174511.
- Shabani, J., M. Kjaergaard, H. J. Suominen, Y. Kim, F. Nichele, K. Pakrouski, T. Stankevic, R. M. Lutchyn, P. Krogstrup, R. Feidenhans'l, S. Kraemer, C. Nayak, *et al.*, Two-dimensional epitaxial superconductor-semiconductor heterostructures: A platform for topological superconducting networks, 2016, *Phys. Rev. B* **93**,

- 155402.
- Shelankov, A. L., On the derivation of quasiclassical equations for superconductors, 1985, *J. Low Temp. Phys.* **60**, 29.
- Shen, S.-Q., 2012, *Topological Insulators: Dirac Equation in Condensed Matters* (Springer, Berlin).
- Shockley, W., The theory of p-n junctions in semiconductors and p-n junction transistors, 1949, *Bell Syst. Tech. J.* **28**, 435.
- Silaev, M. A., I. V. Bobkova, and A. M. Bobkov, Odd triplet superconductivity induced by a moving condensate, 2020, *Phys. Rev. B* **102**, 100507.
- Singh, A., S. Voltan, K. Lahabi, and J. Aarts, Colossal proximity effect in a superconducting triplet spin valve based on the half-metallic ferromagnet CrO₂, 2015, *Phys. Rev. X* **5**, 021019.
- Sinova, J., S. O. Valenzuela, J. Wunderlich, C. H. Back, and T. Jungwirth, Spin Hall effects, 2015, *Rev. Mod. Phys.* **87**, 1213.
- Smidman, M., M. B. Salamon, H. Q. Yuan, and D. F. Agterberg, Superconductivity and spin-orbit coupling in non-centrosymmetric materials: A review, 2017, *Rep. Prog. Phys.* **80**, 036501.
- Sosnin, I., H. Cho, V. T. Petrashov, and A. F. Volkov, Superconducting phase coherent electron transport in proximity conical ferromagnets, 2006, *Phys. Rev. Lett.* **96**, 157002.
- Soulen Jr., R. J., J. M. Byers, M. S. Osofsky, B. Nadgorny, T. Ambrose, S. F. Cheng, P. R. Broussard, C. T. Tanaka, J. Nowak, J. S. Moodera, A. Barry, and J. M. D. Coey, Measuring the spin polarization of a metal with a superconducting point contact, 1998, *Science* **282**, 85.
- Stern, A., and E. Berg, Fractional Josephson vortices and braiding of Majorana zero modes in planar superconductor-semiconductor heterostructures, 2019, *Phys. Rev. Lett.* **122**, 107701.
- Szombati, D. B., S. Nadj-Perge, D. Car, S. R. Plissard, E. P. A. M. Bakkers, and L. P. Kouwenhoven, Josephson ϕ_0 -junction in nanowire quantum dots, 2016, *Nat. Phys.* **12**, 568.
- Tafari, F. (ed.), 2019, *Fundamentals and Frontiers of the Josephson Effect* (Springer Nature, Cham).
- Tagirov, L. R., Low-field superconducting spin switch based on a superconductor/ferromagnet multilayer, 1999, *Phys. Rev. Lett.* **83**, 2058.
- Takahima, R., S. Fujimoto, and T. Yokoyama, Adiabatic and non-adiabatic spin torques induced by a spin-triplet supercurrent, 2017, *Phys. Rev. B* **96**, 121203(R).
- Takayanagi, H., and T. Kawakami, Superconducting proximity effect in the native inversion layer on InAs, 1985, *Phys. Rev. Lett.* **54**, 2449.
- Tanaka, Y., T. Yokoyama, A. V. Balatsky, and N. Nagaosa, Theory of topological spin current in noncentrosymmetric superconductors, 2009, *Phys. Rev. B* **79**, 060505.
- Tedrow, P. M., and R. Meservey, Spin-dependent tunneling into ferromagnetic nickel, 1971, *Phys. Rev. Lett.* **26**, 192.
- Tokatly, I. V., Usadel equation in the presence of intrinsic spin-orbit coupling: A unified theory of magnetoelectric effects in normal and superconducting systems, 2017, *Phys. Rev. B* **96**, 060502.
- Tosato, A. A., V. Levajac, J.-Y. Wang, C. J. Boor, F. Borsoi, M. B. C. N. Borja, S. Marti-Sanchez, J. Arbiol, A. Sammak, M. Veldhorst, and G. Scappucci, Hard superconducting gap in a high-mobility semiconductor, 2022, arXiv:2206.00569.
- Tsymbal, E. Y., and I. Žutić (eds.), 2019, *Spintronics Handbook, 2nd Ed.* (CRC Press, Boca Raton, FL).
- Usman, I. T. M., K. A. Yates, J. D. Moore, K. Morrison, V. K. Pecharsky, K. A. Gschneidner, T. Verhagen, J. Aarts, V. I. Zverev, J. W. A. Robinson, J. D. S. Witt, M. G. Blamire, *et al.*, Evidence for spin mixing in holmium thin film and crystal samples, 2011, *Phys. Rev. B* **83**, 144518.
- Vaidya, P., S. A. Morley, J. Van Tol, Y. Liu, R. Cheng, A. Brataas, D. Lederman, and E. Del Barco, Subterahertz spin pumping from an insulating antiferromagnet, 2020, *Science* **368**, 160.
- Valls, O. T., 2022, *Superconductor/Ferromagnet Nanostructures* (World Scientific, Hackensack, NJ).
- Vezin, T., C. Shen, J. E. Han, and I. Žutić, Enhanced spin-triplet pairing in magnetic junctions with s-wave superconductors, 2020, *Phys. Rev. B* **101**, 014515.
- Virtanen, P., F. S. Bergeret, and I. V. Tokatly, Magnetoelectric effects in superconductors due to spin-orbit scattering: Nonlinear σ -model description, 2021, *Phys. Rev. B* **104**, 064515.
- Waintal, X., and P. W. Brouwer, Magnetic exchange interaction induced by a Josephson current, 2002, *Phys. Rev. B* **65**, 054407.
- Wakamura, T., H. Akaike, Y. Omori, Y. Niimi, S. Takahashi, A. Fujimaki, S. Maekawa, and Y. Otani, Quasiparticle-mediated spin Hall effect in a superconductor, 2015, *Nat. Mater.* **14**, 675.
- Wan, Z., A. Kazakov, M. J. Manfra, L. N. Pfeiffer, K. W. West, and L. P. Rokhinson, Induced superconductivity in high-mobility two-dimensional electron gas in gallium arsenide heterostructures, 2015, *Nat. Commun.* **6**, 7426.
- Wang, S., L. Tang, and K. Xia, Spin transfer torque in the presence of Andreev reflections, 2010, *Phys. Rev. B* **81**, 094404.
- Wang, X. L., A. Di Bernardo, N. Banerjee, A. Wells, F. S. Bergeret, M. G. Blamire, and J. W. A. Robinson, Giant triplet proximity effect in superconducting pseudo spin valves with engineered anisotropy, 2014, *Phys. Rev. B* **89**, 140508.
- Wendin, G., Quantum information processing with superconducting circuits: A review, 2017, *Rep. Prog. Phys.* **80**, 106001.
- Winkler, R., H. Noh, E. Tutuc, and M. Shayegan, Anomalous Rashba spin splitting in two-dimensional hole systems, 2002, *Phys. Rev. B* **65**, 245417.
- Yang, G., C. Ciccarelli, and J. W. A. Robinson, Boosting spintronics with superconductivity, 2021, *Appl. Phys. Lett.* **9**, 050703.
- Yang, G., P. Stano, J. Klinovaja, and D. Loss, Majorana bound states in magnetic skyrmions, 2016, *Phys. Rev. B* **93**, 224505.
- Yang, H., S.-H. Yang, S. Takahashi, S. Maekawa, and S. S. P. Parkin, Extremely long quasiparticle spin lifetimes in superconducting aluminium using MgO tunnel spin injectors, 2010, *Nat. Mater.* **9**, 586.
- Yang, Z.-H., Y.-H. Yang, and W. J., Interfacial spin Hall current in a Josephson junction with Rashba spin-orbit coupling, 2012, *Chin. Phys. B* **21**, 057402.
- Yao, Y., R. Cai, T. Yu, Y. Ma, W. Xing, Y. Ji, X.-C. Xie, S.-H. Yang, and W. Han, Giant oscillatory Gilbert damping in superconductor/ferromagnet/superconductor junctions, 2021, *Sci. Adv.* **7**, eabh3686.
- Yates, K. A., L. A. B. Olde Olthof, M. E. Vickers, D. Prabhakaran, M. Egilmez, J. W. A. Robinson, and L. F. Cohen, Andreev bound states in superconductor/ferromagnet point contact Andreev reflection spectra, 2017, *Phys. Rev. B* **95**, 094516.
- Yazdani, A., Conjuring Majorana with synthetic magnetism, 2019, *Nat. Mater.* **18**, 1036.
- Ying, Z. J., M. Cuoco, C. Ortix, and P. Gentile, Tuning pairing amplitude and spin-triplet texture by curving superconducting nanostructures, 2017, *Phys. Rev. B* **96**, 100506.
- Ying, Z. J., P. Gentile, C. Ortix, and M. Cuoco, Designing electron spin textures and spin interferometers by shape deformations, 2016, *Phys. Rev. B* **94**, 081406.
- Yokoyama, T., Anomalous Josephson Hall effect in magnet/triplet superconductor junctions, 2015, *Phys. Rev. B* **92**, 174513.
- Yokoyama, T., M. Eto, and Y. V. Nazarov, Anomalous Josephson effect induced by spin-orbit interaction and Zeeman effect in semiconductor nanowires, 2014, *Phys. Rev. B* **89**, 195407.
- Yokoyama, T., Y. Tanaka, and J. Inoue, Charge transport in two-dimensional electron gas/insulator/superconductor junctions with Rashba spin-orbit coupling, 2006, *Phys. Rev. B* **74**, 035318.

- Yuan, N. F. Q., and L. Fu, Supercurrent diode effect and finite-momentum superconductors, 2022, Proc. Natl. Acad. Sci. USA **119**, e2119548119.
- Yuasa, S., T. Nagahama, A. Fukushima, Y. Suzuki, and K. Ando, Giant room-temperature magnetoresistance in single-crystal Fe/MgO/Fe magnetic tunnel junctions, 2004, Nat. Mater. **3**, 868.
- Zazunov, A., R. Egger, T. Jonckheere, and T. Martin, Anomalous Josephson current through a spin-orbit coupled quantum dot, 2009, Phys. Rev. Lett. **103**, 147004.
- Zhou, T., M. C. Dartiailh, W. Mayer, J. E. Han, A. Matos-Abiague, J. Shabani, and I. Žutić, Phase control of Majorana bound states in a topological X junction, 2020, Phys. Rev. Lett. **124**, 137001.
- Zhou, T., M. C. Dartiailh, K. Sardashti, J. E. Han, A. Matos-Abiague, J. Shabani, and I. Žutić, Fusion of Majorana bound states with mini-gate control in two-dimensional systems, 2022, Nat. Commun. **13**, 1738.
- Zhou, T., N. Mohanta, J. E. Han, A. Matos-Abiague, and I. Žutić, Tunable magnetic textures in spin valves: From spintronics to Majorana bound states, 2019, Phys. Rev. B **99**, 134505.
- Zhu, X., Tunable Majorana corner states in a two-dimensional second-order topological superconductor induced by magnetic fields, 2018, Phys. Rev. B **97**, 205134.
- Zhu, Y., A. Pal, M. G. Blamire, and Z. H. Barber, Superconducting exchange coupling between ferromagnets, 2017, Nat. Mater. **16**, 195.
- Žutić, I., and S. Das Sarma, Spin-polarized transport and Andreev reflection in semiconductor/superconductor hybrid structures, 1999, Phys. Rev. B **60**, R16322.
- Žutić, I., J. Fabian, and S. Das Sarma, Spintronics: Fundamentals and applications, 2004, Rev. Mod. Phys. **76**, 323.
- Žutić, I., A. Matos-Abiague, B. Scharf, H. Dery, and K. Belashchenko, Proximitized materials, 2019, Mater. Today **22**, 85.
- Žutić, I., and I. Mazin, Phase-sensitive tests of the pairing state symmetry in Sr₂RuO₄, 2005, Phys. Rev. Lett. **95**, 217004.